308 - - - Q200108020003
Scientific Notebook # 385

21
72
150

CNWRA
CONTROLLED
COPY 385

01402-861

Unsaturated and Saturated Flow Under Isothermal Conditions

E. Pearcy / J. Winterle. (USFIC)

WALTER ILLMAN / SWRI
210-522-6085

The Boorum & Pease® Quality Guarantee

The materials and craftsmanship that went into this product are of the finest quality. The pages are thread sewn, meaning they're bound to stay bound. The inks are moisture resistant and will not smear. And the uniform quality of the paper assures consistent rulings, excellent writing surface and erasability. If, at any time during normal use, this product does not perform to your expectations, we will replace it free of charge. Simply write to us:

Boorum & Pease Company
71 Clinton Road, Garden City, NY 11530
Attn: Marketing Services

Any correspondence should include the code number printed at the bottom of this page as well as the book title stamped at the bottom of the spine.

One Good Book Deserves Many Others.

Look for the complete line of Boorum & Pease® Columnar, Journal, and Record books. Custom-designed books also available by special order. For more information about our Customized Book Program, contact your office products dealer. See back cover for other books in this series.

Made in U.S.A.

Contents | Page

① Notes on Topical Hydrology Report - Hydraulic Conductivity and Permeability at Yucca Mountain

② Topical Hydrology Report - Porosity at Yucca Mountain

③ PTn modeling - Flow through PTn unit

Unsaturated and Saturated Flow Under Isothermal Conditions

Objectives: The spatial and temporal distribution of UZ groundwater flow rates and directions at and below the repository horizon must be evaluated to assess the performance of the repository under current and pluvial climatic conditions. Further, it is important to determine the effect of SZ flow on the concentrations of radionuclides at receptor locations in the event of a release. The DOE Repository Safety Strategy identified repository performance-affecting attributes related to groundwater flow, including limit water contacting WPs and radionuclide concentration reduction during transport. To evaluate the DOE work associated with these attributes, the objectives of the USFIC KTI during FY2000 include (i) revising IRSR on USFIC; (ii) reviewing DOE site characterization data, modeling results, and field studies; (iii) refining hydrologic process abstractions and input data for the TPA code; (iv) using of the TPA code to aid in identifying important hydrologic features and processes; (v) using process modeling, field and laboratory studies, and site data analyses for confirmatory investigations of important UZ and SZ features and processes; (vi) developing of innovative research methods; and (vii) reviewing of DOE submittals, including the working draft LA, PMRs, and AMRs.

→ My contribution to:
Major and intermediate milestones for USFIC

number	type	Milestone	Date	Lead
01402.861.000	Int.	Permeab. rep.	02/18/2000	Winterle
01402.861.020	Int.	Porosity rep.	04/07/2000	Farrell
01402.861.030	Int.	Modeling/Field Sx. for Eval. Future Inf. and Percolation	05/12/2000	Fedors
		Field geophysical investigation		Farrell

1-10-2000

Topical Hydrology Report - Hydraulic Conductivity and Permeability at Yucca Mountain.

The purpose of this report is to provide a process-level review of permeability, hydraulic conductivity, and transmissivity of the geologic formations along potential flow paths from the ground surface above the proposed high-level nuclear waste (HLW) repository at Yucca Mountain to a compliance boundary.

The report contains 5 technical sections:

1) Permeability from the surface of YM to the proposed repository horizon.
2) Permeability in the altered zone surrounding excavated drift openings
3) Permeability from below the repository to the water table.
4) Permeability of the saturated volcanic tuff aquifer
5) Permeability of the saturated valley-fill aquifer

My contribution will be on the first technical section. The permeability from the surface of YM to the proposed repository horizon - affects the spatial and temporal distribution of deep percolation reaching the repository horizon. Review of this topic is required under, "Spatial and Temporal Distribution of Flow ISI"

Each technical section will be subdivided into: 1) Background; 2) DOE approach; 3) Review of Available Data; 4) Review of Remaining Uncertainty; 5) Summary of Conclusions.

WI 1/10/00

1-10-2000

Data that we may quote include: [from Automated Technical Data Tracking]

→ near surface alluvium permeabilities (if it exists!?)

→ Matrix permeabilities, saturations, relative permeabilities, and other two-phase flow parameters from core studies. (Flint and Flint, 1990) (Flint et al., 1998)

- those estimates provide us with the low-end of permeability spectrum as measurements and corresponding data are biased toward matrix properties.
- conduct/assess geostatistical analysis on core data(?) to study the spatial distribution of matrix properties. (quote PMR - 11/1999; Integrated Site Model Process Model Report).
  → very important!

→ Raw Data, interpretive methods, and permeability estimates from single- and cross-hole pneumatic tests at Yucca Mountain vertical (surface) boreholes; boreholes in drifts, etc.

→ Gary LeCain (USGS) — Refer to: - USGS - open-file reports
→ J.S.Y. Wang / P. Cook. (LBNL) — - reports
→ Y. Tsang (LBNL) — - journal articles; reports

→ Raw data, interpretive methods, and permeability (or diffusivity) estimates of site-scale pneumatic monitoring tests.

- Rousseau et al., 1997
- Patterson et al., 1996.
- Ahlers et al., 1999

Status:

→ Initial draft of technical Section 1 submitted to J. Winterle on 12/28/1999.

WI 1/10/00

1-11-2000

- List references for pneumatic tests conducted by USGS
- Give some specifics in terms of BH designations, lengths, diameter, total depth, injection interval lengths, etc.

LeCain, 1996 Water-Resources Investigations Report 96-4261
single-hole tests in 4 vertical boreholes
UE-25, UZ-16; USW-SD-12; USW-NRG-6; USW-NRG-7a.

Borehole UZ-16 diameter 0.31m; total depth (t.d.) 514.1m; injection int. length 9.0m except for one test with int. length of 11.3m.

SD-12 diameter 0.31m; t.d 335.4m; int. length 4.9m for tests 1-37; " " 4.6m for tests 38-161.

NRG-6 diameter 0.20m; t.d. 332.3m int. length 4.3m in most tests except for few tests with 11.3m.

NRG-7a diameter 0.20m from the ground surface to 91.5m and 0.15m from 91.5m - 379.9m. test interval lengths of the 0.20- and 0.15m diameter sections were 4.3 and 3.5m, respectively.

- summarize permeability values in tabular form
- provide comparison with barometric pressure data in text.
- comparison with matrix k data in text

WI. 1/11/00

1-13-2000

LeCain (1996)
Total of 194 single-hole tests in 4 vertical boreholes

LeCain (1998) Results from air-injection and tracer testing in the Upper Tiva Canyon, Bow Ridge Fault, and Upper Paintbrush Contact Alcoves of the Exploratory Studies Facility, August 1994 through July 1996, Yucca Mountain, NV.
- Water Resources Investigations Report 98-4058

Single-hole tests in Upper Tiva Canyon Alcove (UTCA)
near horizontal boreholes, 9.6cm diameter → RBT#1, RBT#2, RBT#3
Total depth: RBT#1 30.5m
RBT#2 32.1m
RBT#3 31.3m.

- Rough borehole walls causing cavity
- some tested intervals showed no pressure response under high flow rates.
  possible causes:
  1) packers not properly seated causing leakage around it.
  2) permeability of tested zone may be too high - higher than the maximum range of the equipment.

Total number of tests 27.
range: 0.2×10^{-12} - 85.0×10^{-12} m^2
arithmetic mean: 28.6×10^{-12} m^2
geometric mean: 16.0×10^{-12} m^2

∴ very high values in my opinion from my experience at YMDC

WI 1/13/00

1-13-2000

→ Cross-hole tests showed no measurable response between injection and observation intervals.

→ A stochastic fracture network model developed using ESF fracture mapping data of the UTCA.

→ Implication: There are geologic media that cannot be tested using existing techniques of well hydraulics.

* possible solution → increase measurement scale?

Recommendation: Further investigation of the unit may be required

Pasted my contribution to the Letter Report put together by Jim Winterle. →

Tables included except for the last two due to lack of values at this time.

1/13/00

Contribution to Permeability Report

WI 1/20/00

1.0 PERMEABILITY FROM THE SURFACE OF YUCCA MOUNTAIN TO THE REPOSITORY HORIZON

The U.S. Department of Energy (DOE) is currently assessing the suitability of Yucca Mountain (YM), Nye County, Nevada, located approximately 135 km northwest of Las Vegas, Nevada, as a potential repository for high-level nuclear waste. The current isolation plan advocates a multiple barrier concept with the waste being placed in corrosion resistant canisters prior to emplacement in drifts located within unsaturated fractured tuffs at the site. A key concern that may influence the licensing of the repository is whether the engineered containment system and the natural barrier system will provide effective long-term isolation of the waste from the accessible biosphere. The distribution of permeability from the surface of Yucca Mountain to the proposed repository horizon is important as it can have a large impact on the spatial and temporal distribution of deep percolation reaching the repository horizon. Review of this topic is required under the *Spatial and Temporal Distribution of Flow* Integrated Sub-Issue (ISI). Knowledge of permeability in the UZ at YM is only important insofar as it is closely related to the following three processes demonstrated to be of importance to repository performance:

- The spatial and temporal distribution of percolation flux that might reach the repository drift horizon
- The ability of a capillary barrier imposed by an underground opening (i.e., drift) to divert water and hence reduce the potential for dripping
- The pathways by which a dissolved radionuclide may find its way to the saturated zone beneath the repository

The importance of three processes listed above depends largely on spatial heterogeneity or contrasts in permeability. Permeability contrasts can cause localized fast flow paths, perched waters, capillary barriers, and directional effects in fluid and gas flow motion.

A number of methods have been developed to obtain estimates of permeability in geologic media. Those include laboratory core studies that yield properties representative of the rock matrix as opposed to hydraulic and pneumatic injection or pumping tests that allow for the determination of in situ fracture and matrix properties. Field determination of permeability can be accomplished by means of slug tests, single-hole tests, and large scale pumping tests in the saturated and unsaturated zones. Our focus in this section will be primarily on pneumatic monitoring, single- and cross-hole pneumatic injection tests conducted in Tiva Canyon (TCw), Paintbrush (PTn), and Topopah Spring (TSw) units. Results and conclusions attained from the pneumatic monitoring and injection programs are useful but the insight gained through those experiments may not always be applicable to the phenomenon of liquid flow through unsaturated fractured rocks. As the three processes listed above deal with liquid flow and corresponding transport of radionuclides, one would ideally want to quantify the parameters that govern water flow through those rocks by injecting water into boreholes and through infiltration experiments conducted in the UZ. Experiments that involve borehole liquid injection or infiltration in unsaturated fractured rocks are difficult to conduct more than a single test at any location because the injection of liquid modifies the ambient saturation of the rock, and the time required to recover ambient conditions may be exceedingly long (Illman et al., 1998). Those experiments are currently underway at Yucca Mountain. As data and results from borehole liquid injection tests and infiltration experiments become available, we intend to include those findings as they provide information on the ability of those units to transmit water and aid in addressing the

processes that are demonstrated to be of importance to repository performance. The review of field and laboratory tests in hydrogeologic units below and away the repository are discussed in subsequent sections. WI 1/20/00

Pneumatic injection tests and monitoring of ambient pneumatic pressure fluctuations provide in situ estimates of fracture and matrix flow properties in the unsaturated zone (UZ). In this report, permeability estimates obtained at widely varying scales primarily from the pneumatic injection experiments are tabulated. The corresponding interpretive methods employed by the DOE researchers are discussed in some detail as they are directly relevant to the reliability of those parameters. This report not only summarizes DOE field research efforts and parameters obtained from their data but also is written in an attempt to suggest improvements in their testing program and in their interpretation of field data. Our intention is to propose testing alternative conceptual models and modeling strategies as needed. This may involve researchers from the CNWRA to reinterpret some of the field and laboratory data collected by the DOE researchers. We believe that the constructive criticisms of DOE testing methodology and interpretive techniques to be important as estimates of permeabilities obtained from those experiments are employed in the 3D site scale numerical model for Yucca Mountain (Bodvarsson et al., 1997).

The focus of this section is on permeability from the surface of Yucca Mountain to the repository horizon. In section 1.1, we begin by providing the background to the site; section 1.2 discusses the DOE approach to integrating formation permeability into existing DOE models for groundwater flow that are used in TSPA predictions; 1.3 reviews the available data collected through laboratory and field experiments; 1.4 is a review of remaining uncertainty on permeability estimates obtained by DOE researchers; and 1.5 summarizes concerns resulting from reviewing DOE data, concepts, and models.

1.1 BACKGROUND

It is generally accepted that the rate of deep percolation reaching the repository horizon at Yucca Mountain (YM), will occasionally exceed the capacity of the rock matrix to accommodate the downward flow of water. On such occasions, this excess flow must either be stored in a layer of perched water, be diverted horizontally, or continue downward through a network of connected fractures. In prevailing conceptual models of unsaturated zone (UZ) flow at YM, flow in matrix is generally considered favorable for repository performance due to its low permeability and high sorptivity for radionuclides, while water flow in fractures is generally considered harmful for performance. The fraction of water that resides in either the matrix and/or fracture depends on factors such as permeability, porosity, and capillary saturation relationships of each medium. As matrix porosities are much larger than the porosity of fractures, and pore sizes within the matrix are generally much smaller than fracture openings, most of the water resides in the matrix and its water content is much higher than that of the fractures under isothermal conditions. The extent to which this exchange of fluids between the matrix and fracture takes place is a highly uncertain quantity which is difficult or almost impossible to measure in situ, yet is one of the most important parameters in quantifying the Total Systems Performance Assessment (TSPA) that is required for the licensing of the potential repository.

It has become accepted that fracture flow is the dominant flow mechanism in the welded volcanic tuff units (Bodvarsson and Bandurraga, 1996). As the permeability of matrix is sufficiently lower than the infiltration rate (Flint et al., 1997), researchers conceptualize that fractures act as primary conduits or "fast flow paths" for the bomb pulse isotopes to reach the repository level. The notion of fracture flow causing rapid downward migration of infiltrating water is supported by elevated levels of isotopes Cl-36 and Tc-99

observed at the repository level in the Exploratory Studies Facility (ESF) (Fabrika-Martin et al., 1996) and tritium in the Calico Hills unit (Yang et al., 1996). WI 1/20/00

The geologic formation at Yucca Mountain consists of alternating strata of welded and non-welded ash flow and air fall tuffs with overlying alluvium. The hydrogeologic units have been categorized (Montazer and Wilson, 1984) based roughly on the degree of welding. The units from the soil surface include the Tiva Canyon welded (TCw), the Paintbrush non-welded (PTn) consisting primarily of the Yucca Mountain and Pah Canyon members and the interbedded tuffs, the Topopah Spring welded (TSw), the Calico Hills non-welded (CHn), and the Crater Flat undifferentiated (CFu) units. The welded units typically have lower matrix porosities and are highly fractured, while the bedded and non-welded tuffs tend to have higher matrix porosities and low fracture densities (Montazer and Wilson, 1984; Kwicklis et al., 1998). According to Bodvarsson et al. (1999), fracture density is correlated with increasing degree of volcanic rock welding at smaller scales. Zeolites and clays have been found in small portion of those units and are related to the cooling history.

The Tiva Canyon unit consists of crystalized moderately to densely welded tuff. Neutron probe measurements of water content in the overlying alluvium and the TCw caprock shows rather slow movement of infiltrating water near the surface (Flint et al., in preparation, cited in Bodvarsson et al., 1999). Infiltration data from Flint et al. (1997) suggests that significant infiltration of water through the alluvium and into the bedrock occurs every few years. With a large contrast in permeability between the fracture and matrix, infiltrating water is known to enter the well-connected fracture system with very little attenuation in the matrix. Rapid fluctuations of pneumatic pressure and temperature data detected in a sensor near the bottom of borehole NRG-7a completed at the bottom of this unit have shown to support the rapid movement of water through the fractures (Bodvarsson et al., 1999). Long-term records of barometric pressure show very little attenuation of the amplitude and time lag of pressures indicating that the fractures are well-connected (Rousseau et al., 1996, 1997).

The fast migration of infiltrating water appears to become attenuated in the Paintbrush non-welded (PTn) unit. This unit tends to be less fractured with flow taking place predominantly in the matrix. Its thickness varies and is known to thin towards the south. The unit consists of non-welded tuffs that is less fractured compared to the welded units and tends to have much higher porosity on the order of 30% (Flint et al., 1998). The current conceptual model of water flow is that fast-moving water becomes slowed quite significantly upon contact as fracture flow converts to matrix dominated flow. The redistribution of infiltrating water allows for steady-state flow conditions in the underlying units. Whether or not steady-state flow conditions hold beneath the PTn unit is under considerable scrutiny and is much debated. Evidence from the field that support this concept include low fracture density, low fracture connectivity, higher matrix porosity, lower saturation in the matrix, and attenuation and lag observed in barometric signals through the unit. There is also evidence that suggests focused fast-flow paths in the vicinity of major faults at the site but by and large, the PTn is considered to attenuate episodic water fluxes. Yet, the discovery of bomb pulse isotopes within and below the PTn unit suggests that there may be localized fast flow paths allowing water flux through the units. Further collection of site data and corresponding modeling is desirable to quantify and further constrain the percolation flux through the PTn unit.

The potential repository is to be situated within the 300 m thick Topopah Spring welded (TSw) unit. The average fracture spacing in the TCw and TSw is on the order of 0.5 m (Beason, 1996; Sweetkind, et al., 1996). The water flow in this unit in fractures is quite pervasive yet there are studies that suggest that only 30% of fractures contribute to the total flux of water (Liu et al., 1998). The fact that flow

concentrates in several fractures makes it difficult to model the spatial and temporal distribution of infiltrating water that reaches the repository level.

1.2 DOE MODELING APPROACH

WI 1/20/00

There is considerable uncertainty in the rate of percolation flux through YM. In order to study the movement of moisture within the repository area, LBNL modelers have taken the approach to model the percolation flux through Yucca Mountain using the three-dimensional site scale numerical model (Wu et al., 1999; see also Bandarruga and Bodvarsson, 1999) and a drift scale model (Birkholzer et al. 1999). Both numerical simulations are conducted using the multi-component, multi-phase code TOUGH2 (Pruess, 1991) which allows to take into account of multi-phase flow and heat transfer involving liquid water, vapor, and air in a heterogeneous fractured medium. The code allows for the use of various empirical relations to describe two-phase flow properties, most notably the van Genuchten (1980) function which relates the relative permeability and saturation functions. The effective continuum and dual continuum approaches are employed to idealize flow in the fracture-matrix system. The model is intended for use in assessing the system performance of the repository in the UZ. The site-scale numerical model has been calibrated using temperature, water potential, and saturation data collected in the field and has shown to reproduce the overall heat distribution, moisture profiles, and pneumatic pressure variations in different units. Permeability values employed for the numerical model were estimated through model calibrations and inverse modeling of core and field data. Each modeled layer in the 3D site scale model was specified a value of permeability. No attempt to model the heterogeneities in permeability within an individual unit is made with the site scale model. The site scale model, although useful in studying the overall vapor, liquid, gas, and heat transfer through YM, is not able the capture the water flux through the mountain because of the large grid size. The drift scale model on the other hand, is better suited to capture spatial variability in water flux that reaches the drift due to its small grid blocks. Heterogeneity in flow parameters are considered in the drift scale model which provided insight into the rate and spatial distribution of percolation flux. The stochastic modeling of drift seepage using TOUGH2 assumed a statistically homogeneous, random field of fracture permeability (Birkholzer et al., 1999). Both modeling efforts require extensive data sets on flow properties which are not available at large number of locations. Site characterization at the repository horizon is underway but more data should be collected where the repository is to be situated as the geologic properties are highly uncertain within the confines of the repository.

1.3 REVIEW OF AVAILABLE DATA

The primary controls on fluid and gas flow motion and its rates in fractured media are the fracture/matrix permeabilities, porosities, parameters that govern the exchange of fluids between fracture and matrix, and the spatial distribution of those parameters. In the UZ, the coexistence of air and water necessitates the invocation of two-phase flow concepts for purposes of modeling the spatial and temporal distribution of those fluids. The permeability to water of unsaturated zone at Yucca Mountain is important for shallow infiltration at/near the soil surface, deep percolation through the unsaturated zone to the repository horizon and beneath the repository to the regional aquifer. The permeability to air governs gas flux from the repository horizon to the biosphere induced by barometric pumping and thermally driven processes during the decay of radionuclides. The extent to which the relative permeability of one fluid to

WI 1/20/00

another dominates depends on local rock properties, including saturation and capillary pressure. Intrinsic permeability, a parameter independent of fluid properties is a measure of ability of the geologic formation to conduct fluids. Methods have been developed for characterizing two-phase flow properties of fractured media in the laboratory (Reitsma and Kueper, 1994; Persoff and Pruess, 1995) but the properties determined from those experiments are not usually applicable on field scales. In the context of large scale modeling of water flux reaching the repository horizon and gas flux that may reach the biosphere through barometric pumping and convection anticipated through heat generated from radioactive decay of waste, intrinsic permeability is perhaps the parameter which can be only determined with confidence in the field with existing measurement techniques. Air injection tests are one means to provide estimates of air permeability of unsaturated fracture systems. As most fractures systems are considered essentially dry, estimates of air permeabilities should be close to intrinsic permeabilities and permeability to water. In support of this, Rasmussen et al. (1993) strong correlation between permeabilities obtained by water and air injection tests conducted in boreholes completed in unsaturated fractured tuffs. Air injection tests, however do not directly provide a means to assess the water imbibing mechanisms of the rock. To address this issue, DOE researchers have been conducting a series of borehole water injection and infiltration experiments at the site (Wang et al., 1998; see also Progress Report #20, YMP).

Of importance for predicting the distribution of flow through the UZ is to understand the relationship between the relative permeability and the degree of saturation of the formation. In a heterogenous, layered, fractured geologic system such as the one found at Yucca Mountain, this relationship is likely to exhibit considerable spatial variability. It is known though that there is considerable difficulty in measuring relative permeability and saturation (water content) in unsaturated fractured rocks. It has been found that there is some correlation between the degree of welding of tuffs and fracturing at Yucca Mountain. In welded units such as the Topopah Springs and Tiva Canyon units we expect minimal retention of water in the matrix. The low permeability of matrix to water and high entry pressure causes rapid transmittal of infiltrating water to the subsurface. High variability in water content within the fractures and matrix is expected in those units.

Researchers from the DOE (includes LBNL, LANL, LLNL, USGS) have collected copious amounts of field data at YM in UZ. Relevant data sets to this topical report include spatially varying infiltration rates (Flint et al., 1996), in situ pneumatic data (Ahlers et al., 1999; Rousseau et al., 1997, 1998), single-hole pneumatic injection test data in surface-based boreholes (LeCain, 1997), single- and cross-hole pneumatic injection tests data in the ESF (LeCain et al. 1998, 1999; Wang et al. 1998; Tsang and Birkholzer, 1999; Huang et al. 1999), matrix permeability and van Genuchten parameters from core samples (Flint, 1998), in situ water potential and temperature measurements (Rousseau et al., 1998), core sample saturation and water potential data (Flint, 1998), geophysical saturation data (Thompson and Rael, 1996), and core sample porosity and rock grain density data (Flint, 1998). Here, we briefly review the pneumatic data of Rousseau et al. (1997, 1998) and single- and cross-hole pneumatic injection tests conducted by various groups primarily from the LBNL and USGS as it pertains to in situ estimates of site-scale to meter scale permeabilities. Estimates of core scale permeabilities, its spatial distribution, and two-phase relations are discussed in Flint et al. (1996). A geostatistical analysis of core data has been summarized in CRWMS M&O (1999). A brief discussion on core estimates of permeability obtained by Flint et al. (1996, 1998 - find ref.) is provided and compared to permeability estimates obtained from pneumatic tests at Yucca Mountain.

Measurements of bulk permeability in the unsaturated zone (e.g., Rousseau et al., 1997), taken alone, are generally of little use for predicting flow rates and flow distributions in unsaturated media.

However, monitoring of ambient pressure fluctuations have provided important insight into bulk, site-scale (Neuman, 1998-personal communication) estimates of intrinsic diffusivity through the UZ. Estimates of permeability at the site-scale may be derived from the site-scale estimate of diffusivity by assuming a value of porosity of the UZ units. In particular, the monitoring data were analyzed to determine gas flow properties and vertical permeability of major hydrogeologic units, properties of faults and fracture zones, flow of gas and water vapor through the deep unsaturated zone, and the effects of the Exploratory Studies Facility construction on the gaseous-phase system (Rousseau et al., 1996). Researchers from the USGS employed the AIRK program (Weeks, 1978), while LBNL modelers employed the UZ site-scale model to simulate the barometric pressure propagation through several lithological units (Ahlers et al., 1999). Results showed that the barometric signal travels without signal lag and attenuation through the Topopah Spring and Tiva Canyon units. Significant amplitude attenuation and phase lag of the barometric signal was seen to occur through the Paintbrush unit, although the degree of attenuation appears to vary across the Yucca Mountain site (Rousseau et al., 1996; Patterson et al., 1996; Ahlers et al., 1999). The primary cause of the lateral variation in barometric signal has been linked to the thickness of the Paintbrush unit but the variability in saturation of matrix and presence of fractures can cause significant variability. Estimates of bulk air permeability obtained in this manner were also found to be comparable to estimates of permeability obtained from cross-hole pneumatic tests in the Ghost Dance Fault (LeCain, 1997).The bulk estimates of permeability are useful but, detailed, spatial information on hydraulic and pneumatic flow/transport parameters and continuity/connectivity of permeable pathways are required for the performance assessment of the repository.

WI 1/20/00

To obtain spatial information on hydraulic and pneumatic flow/transport parameters and continuity/connectivity of permeable pathways, extensive field studies are being conducted by DOE researchers to determine air permeability, porosity and anisotropy of major lithological units by means of pneumatic injection tests at Yucca Mountain. The field tests include a large number of single- and cross-hole pneumatic injection and gaseous tracer tests under isothermal conditions and pneumatic tests during the single-heater and the ongoing drift scale heating experiments (Tsang and Birkholzer, 1999). The tests were interpreted using analytical and numerical methods that yield estimates of intrinsic properties of fracture permeabilities and porosities at the site. Analytical methods using linearized single-phase expressions appear to perform well and allow DOE researchers to obtain estimates of bulk, directional estimates of permeability and porosity from cross-hole pneumatic injection tests. Those properties appear to vary considerably with location and direction, implying that the tested rock mass is highly heterogeneous. Air-injection permeability values in the Tiva Canyon and Topopah Spring welded tuffs show considerable variability, reflecting the heterogeneous distribution of fractures and the low permeability of the intact rock matrix (DOE, 1998). The number of single-hole tests conducted in both the surface-based boreholes (LeCain, 1997) and boreholes in the ESF (LeCain, 1998; LeCain et al., 1999) are not large enough to conduct a meaningful geostatistical analysis of air permeability values at the site. Nevertheless, available data exhibit considerable variability in air permeability along boreholes lending support to the notion of high spatial variability in air permeability at Yucca Mountain. Results from a few air injection tests in the Paintbrush nonwelded unit suggests that permeability in this unit have been found to be less variable than the welded tuffs (LeCain, 1997). It is in our opinion that a much larger number of air injection tests need to be conducted in the Paintbrush unit (particularly in the nonwelded subunits) before statistical properties can be addressed.

The U.S. Geological Survey (USGS) conducted numerous (194) single-hole air injection tests using

WI 1/20/00

a straddle packer assembly in four vertical boreholes (UE-25 UZ#16, USW SD-12, USW NRG-6 and USW NRG-7a) that penetrated the Tiva Canyon tuff, nonwelded tuffs of the Paintbrush Group, Topopah Spring tuff, and the Calico Hills formation (LeCain, 1997). Figure 1 is given to illustrate the location of boreholes relative to the Exploratory Studies Facility (ESF) and alcoves at which extensive site characterization has been conducted. Table 1.1 is provided to give characteristics of surface-based boreholes and lengths of injection interval used to conduct single-hole tests. Estimates of permeability were obtained using a steady-state solution modified for compressible airflow. This solution assumes an elliptic flow in an isotropic, homogeneous medium. Results obtained using the steady-state, analytical solution are summarized for the Tiva Canyon tuff (Table 1.2), Paintbrush group (Table 1.3), and the Topopah Spring tuff (Table 1.4) where we provide the minimum and maximum values of permeability and the corresponding arithmetic and geometric means. Extensive areal variation in permeability was observed and results showed that air permeability values from air injection tests conducted in the Tiva Canyon and Topopah Spring units were 3 to 6 orders of magnitude larger than laboratory estimates of matrix permeabilities (Anderson 1991, 1994) obtained from cores. In contrast, the difference between the laboratory (Flint and Flint, 1990; Anderson, 1994) and air injection permeabilities from the Paintbrush nonwelded unit were much smaller. Comparison of single-hole air permeability values and permeabilities from pneumatic monitoring showed that the pneumatic estimates were larger than the single-hole values (LeCain, 1997). Univariate regression analysis performed between six explanatory variables (total fractures, natural fractures, indeterminate fractures, percentage of lithophysal cavities, core rubble, and core lost) and permeability showed lack of correlation between those variables. This result suggests that fracture properties may not be a good indication of permeability at the site.

Air injection and tracer testing were conducted by USGS researchers with the cooperation of the DOE in the upper Tiva Canyon, Bow Ridge Fault, and upper Paintbrush Contact Alcoves of the ESF (LeCain, 1998). Table 1.5 provides characteristics of near horizontal boreholes (RBT #1 through #3) drilled in the Upper Tiva Canyon alcove (UTCA). The USGS researchers noted the roughness of borehole walls causing caving at some borehole intervals. Single-hole tests were conducted in 3 boreholes penetrating the crystal-poor upper lithophysal zone of the Tiva Canyon tuff. Single-hole tests conducted at this site totaled to 27 at this alcove with calculated permeability values ranging from 0.2×10^{-12} m^2 to 85.0×10^{-12} m^2 with an arithmetic mean of 28.6×10^{-12} m^2 and a geometric mean of 16.0×10^{-12} m^2 (variance of LN k is 2.863). Permeability values obtained in the UTCA is summarized in Table 1.5. Some tested sections of boreholes showed no pressure response which according to LeCain (1998) was due to either: 1) packers not properly seated causing leakage around the interval and/or 2) that the permeability of the tested region was higher than the maximum range of test equipment. The high rugosity and evidence of caving of borehole walls could suggest the presence of high permeable pathways which may require further investigation. Cross-hole tests within the same boreholes showed no pneumatic connection between injection and monitoring intervals. This may also be an indication that the permeability of the rock surrounding the alcove is extremely high, not allowing quantification by means of cross-hole pneumatic injection tests. Due to the highly uncertain nature of permeabilities, further pneumatic testing may be required to arrive at conclusions on permeability of the rock within the UTCA.

Single- and cross-hole pneumatic injection tests were also conducted by USGS researchers in boreholes located in the Bow Ridge Fault alcove. The alcove at this location was excavated to test the hydrologic properties of the fault zone. The 2 horizontal and parallel boreholes (HPF#1 and HPF#2) are 3 m apart and penetrate the crystal-poor middle lithophysal zone of the Tiva Canyon tuff, the Bow Ridge

Fault zone and the pre-Rainier Mesa tuff. Characteristics of the two boreholes are summarized in Table 1.7. The Bow Ridge fault is situated 199 m into the ESF, measured from the North Portal with a strike of 180 degs. and dip of 75 degs. The fault is described as a normal fault that is offset by about 128 m. The fault zone is approximately 2.7 m wide and contains 3 brecciated zones. Eighteen single-hole pneumatic injection tests were conducted in the HPF#1 borehole with air permeability values summarized on Table 1.8. Thirteen cross-hole pneumatic injection tests were conducted with borehole HPF#1 as the injection hole while HPF#2 was used to monitor the pressure responses. Several tests yielded good pneumatic connections while others failed to respond in the monitoring intervals. Pneumatic responses in 2 tests exhibited linear flow behavior which indicates the presence of planar features (i.e., large fractures) connecting the injection and monitoring intervals. The pressure responses were not amenable to type-curve models with spherical geometry based on continuum concepts. Considering the proximity of the boreholes employed to conduct the cross-hole tests, and the fact that high permeability features dominating some of the pressure responses in several intervals raises some questions about the applicability of a spherical flow model to interpret the data. The type-curve matches between the field data and the model are not provided in LeCain (1998) not allowing us to assess the reliability of the parameters that the USGS researchers obtain. In any case, permeability values obtained from cross-hole tests were within a factor of 2 to 3 larger than single-hole values. Values of porosity obtained from cross-hole tests include 0.13 and 0.20 in the Bow Ridge fault zone, and 0.27 in the pre-Rainier Mesa tuff. Table 1.9 summarizes results from cross-hole tests 4 through 6.

WI 1/20/00

Single-hole pneumatic injection tests were also conducted in two, horizontal boreholes (RBT #1 and #4) penetrating the crystal-poor lower nonlithophysal columnar subzone of the Tiva Canyon tuff (Tpcplnc) located in the upper Paintbrush contact alcove. Table 1.10 summarizes the characteristics of boreholes RBT#1 and RBT#4. Both boreholes are collared in the crystal-poor lower nonlithophysal columnar subzone of the Tiva Canyon tuff while intersecting the subunits of Paintbrush unit. Borehole RBT#1 intersects the Tiva Canyon crystal-poor vitric 2 (Tpcpv2) at 4.2 m and the Tiva Canyon crystal-poor vitric 1 (Tpcpv1) at 12.2 m. According to LeCain (1998) the degree of welding decreases and porosity seem to increase with depth. Borehole RBT#4 drilled in the opposite direction to RBT#1 in (UPCA) collared in Tpcplnc shows increased degree of welding with depth and intersect at a depth of 9m the crystal-poor lower nonlithophysal hackly subzone (Tpcplnh) of Tiva Canyon tuff. Single-hole tests were conducted with interval lengths of 1 m, except for the bottom hole tests which had lengths of 3.2 to 5.0 m. Results from the 29 tests are summarized in Table 1.11. The relatively large permeability values of the Tpcpv subzones compared to the Tpcpln subzones indicates the possibility for high peremability pathways in the less welded Tpcpv subzones.

More recently, the USGS conducted several cross-hole pneumatic injection tests across the Ghost Dance Fault (Le Cain et al., 1999) which yielded data that were amenable to interpretation by means of analytically derived type-curves. Three boreholes were drilled horizontally in a triangular pattern within the Northern Ghost Dance Fault Alcove (NGDFA). Characteristics of boreholes MF#1, MF#2, and MF#3 in are given in Table 1.12. The USGS researchers identified three zones (foot wall, fault zone, and hanging wall) which had different values of permeability and porosity through their injection tests. The interpretation assumed three individual zones to be homogeneous and isotropic. According to the authors, the same data sets were numerically interpreted using the U.S. Geological Survey AIR3D computer code yielding results comparable to that obtained from type-curve interpretation. Cross-hole pneumatic pressure data were analyzed additionally using a discrete fracture network model (DFNM). The pressure responses from the

hanging and footwall sections were amenable to analysis. The excessive fracturing in the fault zone precluded the researchers to analyze data from the fault zone due to excessive fracturing. A summary of results is provided in Table 1.12.

WI 1/20/00

LBNL researchers conducted numerous cross-hole pneumatic injection tests in niches 3566 and 3650 located in the ESF. In niche 3650, numerous cross-hole pneumatic injection tests have been conducted to determine air permeability prior to and post-excavation of drift (Wang et al., 1998). Air injection tests were conducted in parallel boreholes drilled horizontally. The boreholes were all 10 m in length with pressure measurements taken in consecutive 1-foot sections along each borehole (31 measurements in each hole). A steady-state formula modified for airflow has been employed to calculate permeability from injection interval pressure, temperature and injection flow rate. The tests were said to run for several minutes until pressure responses reached steady values in the injection and monitoring intervals. The cross-hole tests provided valuable insight into connectivity of fracture systems at this site and locations for potential injection zones for the seepage tests. Air permeability tests before and after niche excavations in the ESF revealed increases in permeability near the excavated surface following excavation of the niche. Cross-hole test results have not been quantitatively interpreted by LBNL researchers as of the publication of Wang et al. (1998). This is attributed to reduced in situ stress surrounding the cavity allowing fractures to open. One plausible explanation of the increase in air permeability following the excavation of the niche is due to the increased connectivity of the fracture system that are being tested due to the presence of the niche. Changes in the boundary condition also may affect flow and transport parameters derived from pneumatic flow and tracer tests although without any deformation in the rock post-excavation, the permeability of the rock should be identical to parameters prior to excavation. The value of porosity estimated from cross-hole tests conducted nearby open cavities may be affected by the large volume of the cavity "seen" which may provide larger estimates of porosity (apparent porosity) than the true porosity of the fracture system. Recent findings that exhibit increases in air permeability values (and porosities) following excavation of drifts led DOE researchers to conclude that the increases in flow parameters can suppress seepage into the drift (Progress Report #20, YMP, 1999). According to DOE researchers, high permeability of rock surrounding the drift promotes lateral diversion, and high porosity values require more water to fill the fracture volume to initiate seepage. To further investigate the flow of water in the unsaturated zone several borehole liquid injection tests and infiltration tests are being conducted in the ESF.

LBNL researchers also conducted cross-hole pneumatic injection tests in 31 boreholes drilled in the thermomechanical alcove situated in the ESF to characterize the rock for the single-heater test (Tsang et al., 1996). Straddle-packer systems were installed to isolate sections of all 31 boreholes to prevent communication of borehole intervals with the drift. A typical test consisted of air injection into a specified borehole at constant mass flow rate maintained by a mass flow controller, while the pneumatic responses were monitored in all 30 neighboring boreholes. Pneumatic pressure within the injection and monitoring boreholes were said to reach steady-state within minutes (Tsang and Birkholzer, 1999). The pressure response from the injection borehole was used to estimate the local permeability surrounding the borehole using an analytical solution, while the pressure responses in all other neighboring boreholes yielded information on pneumatic connectivity between the injection and all other observation boreholes. Packed-off injection zones varied in length from 3 to 7 m (in one borehole 11 m). Local estimates of permeability ranged over three orders of magnitude, from a few milli-darcies to a few darcies. The median value for those local estimates is 5.8×10^{-14} m^2. Pressure responses in the monitored boreholes varied considerably

with direction and location, yet its pressure responses were detected in most boreholes implying that on a scale of few meters, the fracture system is well connected and appear to fit a stochastic continuum model. WI 1/20/00

Huang et al. (1999) interpreted data from multiple cross-hole tests (Tsang et al. 1996) by simultaneous inversion of pressure data obtained from multiple monitoring intervals. The inversion of pressure data was conducted in a trial and error fashion which yielded maps of air permeability distribution of the tested rock mass. The determination of the spatial distribution of permeability and porosity is a critical task, which will aid in quantifying the distribution of percolation flux and its magnitude around the drift. LBNL researchers show that the trial and error approach works well for estimating permeability distributions while keeping air-filled porosity as a fixed parameter. The approach that the authors employ is simple, but may be excruciatingly time consuming in three-dimensions. Adjustments of parameters in a trial and error fashion to achieve heterogeneity patterns is not scientifically desirable as it leaves serious questions about the uniqueness of parameters estimated and also does not provide statistical measures of estimation uncertainty. We feel from a scientific point of view that automatic parameter estimation techniques should be employed to conduct the inversion exercise. Therefore, we highly recommend the reinterpretation of those cross-hole test data by LBNL researchers or by CNWRA staff using well-established automatic parameter estimation schemes. Only after the data have been sufficiently interpreted and reviewed rigorously by well-qualified personnel can we ascertain the reliability of the resulting permeability maps and corresponding interpretation. As for incorporating soft information into pneumatic test data, there are other techniques including co-kriging, which may be more flexible and mathematically sound to define heterogeneity structures from multiple cross-hole tests than intuition.

Air injection tests under controlled conditions provide airflow parameters of unsaturated porous and fractured media. As the effect of gravity is negligible on air, results from air injection tests provide information on rock properties other than vertical. As fractures are predominantly occupied by air, those tests provide invaluable information on fracture permeability, porosity, and fracture connectivity and subsurface pathways. However, one issue that is of utmost concern is how water moves through those rocks. In particular, there is lack of information on how water flow in fractures interact with the matrix. As airflow is predominantly through fractures, air injection tests provide information only of fractures and not of the interaction of fracture/matrix.

To address this shortcoming of air injection tests, borehole fluid injection and large scale infiltration experiments are currently being conducted by DOE researchers to quantify the parameters that govern water flow through Yucca Mountain. A series of liquid-injection tests have been conducted recently by the DOE in a borehole interval intersecting a fault at the Lower Paintbrush Tuff Contact Alcove in the Paintbrush nonwelded hydrogeological unit. This experiment revealed that the matrix absorbs large quantities of water. According to DOE researchers (Progress Report #20, YMP,1999), more than 200 L (53 gal.) of water were injected and no water was observed in a slot 3 m (10 ft) below the injection interval. These preliminary results suggest that the flow pulse through the Paintbrush nonwelded hydrogeologic unit could be significantly attenuated. Additional tests are planned to quantify flow along the fault in this nonwelded tuff unit with strong matrix-imbibition capacity.

1.4 REVIEW OF REMAINING UNCERTAINTY

Given the complexities involved in obtaining estimates of permeability at a variety of scales, including uncertainties involved in the models employed, we believe what DOE researchers can best

provide is a conservative range of permeabilities of each unit that has been subjected to laboratory and field testing. The interpretation of core samples obtained from numerous boreholes from a number of hydrogeologic units at YM provide us with low end of the permeability spectrum biased towards properties of the matrix. Permeability estimates from single- and cross-hole pneumatic tests are representative of fractures and consist of mid- to moderately high estimates of permeability. The tested rock mass of single-hole tests conducted at YM are on the range of 0.3 m to several meters while cross-hole test encompass several meters to several tens of meters of unsaturated fractured tuffs at YM. The site scale analysis of pressure data obtained by means of monitoring of ambient barometric pressure fluctuation have yielded the largest permeability estimates. Recent studies suggest that the interpretation of data based on homogeneous and heterogeneous models provide parameters that are not consistent. For example, the interpretation of single- and cross-hole pneumatic test data at the Apache Leap Research Site near Superior, Arizona using a calibrated numerical model that accounted for heterogeneities to the scale of 1-m (on the order of single-hole tests) revealed the disappearance of a scale effect in permeability and porosity seen in an interpretation using an analytical, homogeneous approach such as the type-curve method (Chen et al., 1999). New studies such as those show that method of interpretation in heterogeneous formation can affect parameters estimated from the data/model. The capacity of the Paintbrush unit to attenuate water flux that might reach the repository horizon may be altered once heterogeneities within the unit are considered. The quantity and its spatial distribution of deep-percolating water that reaches the waste packages may have to be revised once heterogeneities in individual units are considered. WI 1/20/00

The analytical interpretation of single- and cross-hole tests conducted by DOE researchers were conducted using simplifying assumptions which may not fully represent complexities that can be accounted for (e.g., borehole geometry, boundary condition, borehole storage) in field data. We recommend both LBNL and USGS researchers to fully document their data sets, provide a detailed qualitative analysis of the data, and reinterpret their data sets using a variety of models that represent field conditions more accurately. Results obtained by means of analytical expressions may become critical in analyzing the same data sets using numerical inverse procedures, to estimate the spatial distribution of permeabilities from the interpretation of multiple single- and cross-hole tests.

It is unclear to us how the DOE researchers were able to obtain a calibrated model of pneumatic flow in the heater test area using a numerical model through a trial and error approach. Calibration of a model involving 2D data is in itself highly complicated task - we doubt that one can accurately obtain a 3D distribution of permeability using data collecting in 3D from multiple cross-hole tests. If one were to obtain a 3D distribution of permeability from such an ad hoc approach, its reliability and use is highly questionable. Joint inversion of data using an established parameter estimation scheme may be necessary to obtain more reliable and credible estimates of permeability, porosity and information on its spatial distribution. An analytical approach (type-curve methods) does not allow one to do this as the formation is assumed to be homogeneous and isotropic. We suspect that some of the parameter estimates and the spatial distribution of permeabilities and porosities may change significantly with the model use to conduct the inversion exercise.

It is becoming apparent that the interpretive method employed (discrete versus continuum; homogeneous versus heterogeneous interpretation) may have an impact on estimated parameters such as permeability and porosity. The USGS has attempted to interpret their most recent cross-hole pneumatic data (LeCain et al., 1999) using both the continuum and discrete fracture network approaches. LeCain et al. (1999) were apparently able to model the cross-hole pneumatic test data collected across the Ghost

Dance Fault (although they do not provide parameters resulting from their interpretation) using a discrete fracture analysis. Available data collected on the scales of several meters to several tens of meters reveal that the data appear to fit the continuum model on which the scale of the experiment, which implies that the data are incompatible with the discrete fracture analysis.

WI 1/20/00

Information on moisture retention properties of rock and fracture networks are difficult to obtain in situ. The difficulty arises from the intricacies involving fluid interaction between the matrix and fracture system. The DOE researchers combined results of air permeability tests with, fracture-spacing surveys, the Cubic Law, and Poissille's Law to estimate van Genuchten's alpha parameters for use in their site-scale UZ flow model (Bodvarsson et al. 1997). We see incompatibilities in obtaining data that appear to fit a continuum model as opposed to a discrete fracture network model (DFNM), estimating permeability using a model that embraces the continuum concept, then calculating van Genuchten's alpha parameter using the cubic law based on DFNM concepts. Despite those incompatibilities, we believe that DOE researchers may not be able to define two-phase flow parameters and relationships on scales larger than several meters as there are no reliable methods to independently determine fracture capillary-pressure / saturation relationships in the field. Interpretation and results from borehole liquid injection and infiltration tests conducted within the ESF may provide more information on two-phase flow parameters through model calibration and/or inverse modeling.

Finally, the question of whether the flow and transport properties of the UZ fracture/matrix continuum may differ after the end of the heating phase due to the decay of the radioactive waste requires further attention. The single-heater and drift-scale heater tests will provide some insight into permeability of unsaturated fractured tuffs at present site conditions. Interpretation of cross-hole pneumatic tests conducted during the single-heater test (SHT) revealed a decrease in fracture permeabilities (Tsang and Birkholzer, 1999). The long term effects of heating and mechanical displacement of rocks due to prolonged heating due to radioactive decay are highly uncertain quantities which may not be adequately resolved through the heating experiments at Yucca Mountain. Visitation of analog sites that exhibit extensive hydrothermal alteration of unsaturated and saturated tuffs may provide additional information on the combined effect thermal, chemical, and mechanical regimes on material and fluid flow properties.

1.5 SUMMARY OF CONCERNS

The permeability from the surface of Yucca Mountain to the proposed repository horizon is important as it affects the spatial and temporal distribution of deep percolation reaching the repository horizon. Review of this topic is required under the *Spatial and Temporal Distribution of Flow* Integrated Sub-Issue (ISI). Permeability of matrix can be estimated well using laboratory techniques while field tests involving in situ monitoring of ambient fluctuations in barometric pressures and pneumatic injection tests allow us to obtain credible estimates of permeability that reflect more of fractures. Cross-hole pneumatic tests provide additional information on the connectivity of fracture system, flow geometry, directional and spatial dependence of permeability. The data that DOE researchers have collected appear to be sufficient outside the repository area and qualitative examination of those data show that they appear to fit the conceptual model outlined by DOE researchers. One foreseeable concern that we have is the inadequate documentation of pneumatic injection test data and insufficient examples of matches between the data presented and the model employed to do the analysis in some reports that we have reviewed. We suggest the DOE researchers to disclose all data and show results from their analysis. An Appendix 7 meeting in

some of those cases may resolve our concerns regarding this matter.

WI 1/20/00

It is unclear to us how the DOE researchers were able to obtain a calibrated model of pneumatic flow for the heater test using a numerical model through a trial and error approach in Huang et al. (1999). We recommend the use of more established automatic calibration procedures in order to estimate model parameters and to obtain statistical information on estimation uncertainty.

Information on moisture retention properties of rock and fracture networks are difficult to obtain in situ. The difficulty arises from the intricacies involving fluid interaction between the matrix and fracture system. The DOE researchers combined results of air permeability tests with, fracture-spacing surveys, the Cubic Law, and Poissille's Law to estimate van Genuchten's alpha parameters for use in their site-scale UZ flow model (Bodvarsson et al. 1997). It is in our view that DOE researchers may not be able to better define two-phase flow parameters and relationships on scales larger than several meters as there are no reliable methods to independently determine fracture capillary-pressure / saturation relationships in the field. Interpretation and results from a number of infiltration tests conducted within the ESF may provide more information pertaining to this matter.

Joint numerical inversion of cross-hole pneumatic test data may be necessary to obtain spatial distribution of permeability and porosity. Analytical approaches (e.g., using type-curves) do not allow one to do this as the formation is assumed to be homogeneous and isotropic. We suspect that some of the parameter estimates may change significantly with the model (homogeneous versus heterogeneous) employed to conduct the inversion exercise. New studies in the literature suggests that the method of interpretation employed to analyze data collected in heterogeneous formations can affect the parameters estimated from field data.

Lack of air permeability data in the Paintbrush unit, particularly the nonwelded subunits is of great concern. Further testing and detailed modeling of flow through those units may be required before conclusions on the attenuation capacity of the unit is made. There is still considerable uncertainty in the rate and spatial distribution of percolation flux through the PTn unit and throughout YM.

Lack of air permeability data within the Topopah Spring formation within the confines of the proposed repository is of concern. We suggest the conduct of single- and cross-hole pneumatic tests at widely varying scales and corresponding detailed interpretation of pneumatic test data in order to test available conceptual models and to obtain more insight on the spatial distribution of permeability and porosity. We also recommend the DOE researchers to use solution techniques that are more widely available in the scientific literature and actively reinterpret their data using a range of models for better credibility.

The question of whether the flow and transport properties of the UZ fracture/matrix continuum may differ after the end of the heating phase due to the decay of the radioactive waste requires some attention. The single-heater and drift-scale heater tests provide some insight into permeability of unsaturated fractured tuffs at present site conditions. Visitation of analog sites that exhibit extensive hydrothermal alteration may provide additional information on the effect of persistent heat flow on material and fluid flow properties.

WI
1/20/00

References

Ahlers, C. F., S. Finsterle, G. S. Bodvarsson, Characterization and prediction of subsurface pneumatic response at Yucca Mountain, Nevada. J. Contam. Hydrol. 38, 47-68.

Anderson, L. A., Results of rock property measurements made on core samples from Yucca Mountain boreholes, Nevada Test Site, Nevada: U. S. Geological Survey Open-File Report 90-474, 43 p., 1991.

Anderson, L. A., Water permeability and related rock properties measured on core samples from the Yucca Mountain USW GU-3/G-3 and USW G-4 boreholes, Nevada Test Site, Nevada: U.S. Geological Survey Open-File Report 92-201, 36 p., 1994.

Bandurruga, T. M. and G. S. Bodvarsson, Calibrating hydrogeologic parameters for the 3-D site-scale unsaturated zone model of Yucca Mountain, Nevada, Journal of Contaminant Hydrology, 38, 25-46, 1999.

Beason, S., Scientific Notebook, SN-0084, US Bureau of Reclamation, Denver, CO, 1996.

Birkholzer, J. T., G. Li, C. F. Tsang, and Y. W. Tsang, Modeling studies and analysis of seepage into drifts at Yucca Mountain, Journal of Contaminant Hydrology 38, 349-384, 1999.

Bodvarsson, G. S., and T. M. Bandurraga (Eds.), Development and Calibration of the Three-Dimensional Site-Scale Unsaturated Zone Model of Yucca Mountain, Nevada, Yucca Mtn. Site Charact. Proj. Milestone OBO2, Rep. LBNL-39315, Lawrence Berkeley Natl. Lab., Berkeley Calif., 1996.

Bodvarsson, G. S., T. M. Bandurraga, Y. S. Wu, The Site-Scale Unsaturated Zone Model of Yucca Mountain, Nevada, for the Viability Assessment. Yucca Mountain Project Milestone Report SP24UFM4, Lawrence Berkeley National Laboratory Report LBNL-40376, Berkeley, CA.

Bodvarsson, G. S., W. Boyle, R. Patterson, and D. Williams, Overview of scientific investigations at Yucca Mountain-the potential repository for high-level nuclear waste, Journal of Contaminant Hydrology, 38, 3-24, 1999.

Chen, G., W. A. Illman, D. L. Thompson, V. V. Vesselinov, and S. P. Neuman, Geostatistical, Type-Curve and Inverse Analyses of Pneumatic Injection Tests in Unsaturated Fractured Tuffs at the Apache Leap Research Site Near Superior, Arizona, paper to appear in Dynamics of Fluids in Fractured Rocks – Concepts and recent advances, in honor of Paul A. Witherspoon's 80th birthday, in press, 1999.

CRWMS M&O (Civilian Radioactive Waste Management System Management and Operating Contractor), Intetgrated Site Model Process Model Report, TDR-NBS-GS-000002 REV 00, November, 1999.

Fabryka-Martin, J. T., H. J. Turin, A. V. Wolfsberg, D. Brenner, P. R. Dixon, J. A. Musgrave, Summary

WI
1/20/00

Report of Chlorine-36 Studies. LA-CST-TIP-96-003, YMP Milestone Report 3782M, Los Alamos National Laboratory, Los Alamos, NM.

Flint, L. E., and A. L. Flint, Preliminary permeability and water-retention data for nonwelded and bedded tuff samples, Yucca Mountain Area, Nye County, Nevada: U. S. Geological Survey open-File Report 90-569, 57 p.

Flint, A. L. Hevesi, J. A., Flint, L. E., Conceptual and numerical model of infiltration for the Yucca Mountain Area, Nevada. U.S.G.S., Water-Resources Investigation Report-96, Denver, Colorado, 1996.

Flint, L. E., Characterization of hydrogeologic units using matrix properties, Yucca Mountain, Nevada, US Geol. Surv. Water Resour. Invest. 97-4243, US Geological Survey, Denver, CO, 1997.

Huang, K., Y. W. Tsang, and G. S. Bodvarsson, Simultaneous inversion of air-injection tests in fractured unsaturated tuff at Yucca Mountain, Water Resour. Res., 35(8), 2375-2386, 1999.

Hudson, D. B., A. L. Flint, Estimation of Shallow Infiltration and Presence of Potential Fast Pathways for Shallow Infiltration in the Yucca Mountain Area, Nevada. USGS, 1995.

Illman W. A., D. L. Thompson, V. V. Vesselinov, G. Chen, and S. P. Neuman, Single- and Cross-Hole Pneumatic Tests in Unsaturated Fractured Tuffs at the Apache Leap Research Site: Phenomenology, Spatial Variability, Connectivity and Scale, NUREG/CR-5559, U. S. Nucl. Regul. Comm., Washington D.C., 1998.

Kwicklis, E. M., A. Flint, and G. S. Bodvarsson, A conceptual model of unsaturated zone flow and transport, USGS Report, Yucca Mountain, NV, in preparation (cited in Bodvarsson et al., 1999)

LeCain, G. D., Air-injection testing in vertical boreholes in welded and nonwelded tuff, Yucca Mountain, Nevada, U.S. Geological Survey Water-Resources Investigations Report 96-4262, 1997.

Le Cain, G. D., Results from Air-Injection and Tracer Testing in the Upper Tiva Canyon, Bow Ridge Fault, and Upper Paintbrush Contact Alcoves of the Exploratory Studies Facility, August 1994 through July 1996, Yucca Mountain, Nevada, Water-Resources Investigations Report 98-4058, 1998.

LeCain, G. D., L. O. Anna, and M. F. Fahy, Results from Geothermal Logging, Air and Core-Water Chemistry Sampling, Air-Injection Testing and Tracer Testing in the northern Ghost Dance Fault, Yucca Mountain, Nevada, November 1996 to August 1998, U.S. Geological Survey Water-Resources Investigations Report 99-4210, 1999.

Liu, H. H., C. Doughty, and G. S. Bodvarsson, An active fracture model for unsaturated flow and transport in fractured rocks, Water Resour. Res., 34(10) 2633-2646, 1998.

Montazer P. and W. E. Wilson, Conceptual hydrologic model of flow in the unsaturated zone, Yucca

Mountain, Nevada. Water Resources Investigations Report 84-4355, U.S. Geological Survey, Denver, CO.

WI 1/20/00

Persoff, P. and K. Pruess, Two-phase flow visualization and relative permeability measurement in natural rough-walled rock fractures, Water Resour. Res., 31(5), 1175-1186, 1995.

Pruess, K., TOUGH2-A General Purpose Numerical Simulator For Multiphase Fluid And Heat Flow, Lawrence Berkeley Laboratory Report LBL-29400 UC-251, May, 1991.

Rasmussen, T. C., D. D. Evans, P. J. Sheets, and J. H. Blanford, Permeability of Apache Leap Tuff: Borehole and Core Measurements Using Water and Air, Water Resour. Res., 29(7), 1997-2006, 1993.

Reitsma, S. and B. H. Kueper, Laboratory measurement of capillary pressure-saturation relationships in a rock fracture, Water Resour., Res., 30(4), 865-878, 1994.

Rousseau, J. P., E. M. Kwicklis, and D. C. Gillies, Hydrogeology Of The Unsaturated Zone, North Ramp Area Of the Exploratory Studies Facility, Yucca Mountain, Nevada, Water-Resources Investigations Report 96-xxxx, 1996.

Rousseau, J. P., C. L. Loskot, F. Thamir, and N. Lu, Results of Borehole Monitoring in the Unsaturated Zone within the Main Drift Area of the Exploratory Studies Facility, Yucca Mountain, Nevada, U.S. Geological Survey, Administrative Report, Level 3 Milestone, SPH22M3, 1997.

Sweetkind, D. S., E. R. Verbeek, J. K. Geslin, T. C. Moyer, Fracture character of the Paintbrush Tuff nonwelded hydrologic unit, Yucca Mountain, Nevada. USGS Administrative Report. US Geological Survey, Denver, CO, 1996.

Thompson, L. E. and H. P. Rael, Determining porosity, balanced water content, and other rock properties from geophysical logs for the modern borehole set at Yucca Mountain, Nevada. Civilian Radioactive Waste Management System Management and Operating Contractor, BAAA00000-01717-0299-00013 REV00, August 16, 1996.

Tsang, Y. W., J. Wang, B. Freifeld, P. Cook, R. Suarez-Rivera, T. Tokunaga, Letter report on hydrological characterization of the single heater test area in the ESF, Yucca Mountain Site Characterization Project Report, Lawrence Berkeley National Laboratory, Berkeley, CA.

Tsang, Y. W., and J. T. Birkholzer, Predictions and observations of the thermal-hydrological conditions in the Single Heater Test, Journal of Contaminant Hydrology, 38, 385-425, 1999.

U. S. Department of Energy, Viability Assessment of a Repository at Yucca Mountain, Introduction and Site Characteristics, Department of Energy, Office of Civilian Radioactive Waste Management, Yucca Mountain Site Characterization Office, Volume 1, DOE/RW-0508/V1, 1998.

van Genuchten, M. T., A closed-form equation for predicting the hydraulic conductivity of unsaturated soils, Soil Sci. Soc. Am. J., 44(5), 892-898, 1980.

Wang, J. S. Y., P. J. Cook, R. C. Trautz, R. Salve, A. L. James, S. Finsterle, T. K. Tokunaga, R. Solbau, J. Clyde, A. L. Flint, and L. E. Flint, Field Testing And Observation of Flow Paths In Niches: Phase 1 Status Report Of The Drift Seepage Test And Niche Moisture Study, Level 4 milestone SPC314M4 for WBS 1.2.3.3.1.2.4, Yucca Mountain Site Characterization Project, 1998.

Weeks, E. P., Field determination of vertical permeability to air in the unsaturated zone, Geological Survey Professional Paper 1051, 41 p., 1978.

Wu, Y. S., C. Haukwa, G. S. Bodvarsson, A site-scale model for fluid and heat flow in the unsaturated zone of Yucca Mountain, Nevada, Journal of Contaminant Hydrology, 38, 185-215, 1999.

Yang, I. C., G. W. Rattray, P. Yu, Interpretations of chemical and isotopic data from boreholes in the unsaturated zone at Yucca Mountain, Nevada, U.S. Geological Survey Water-Resources Investigation Report 96-4058. U.S. Geological Survey, Denver, CO.

WI 1/20/00

Summary of Air Permeability Data

WI 1/20/00

Table 1.1: Characteristics of surface-based boreholes subjected to single-hole pneumatic injection tests and injection interval lengths (data from LeCain, 1997).

Borehole	Diameter [m]	Total Depth [m]	Injection Interval Length [m]
UZ-16	0.31	514.1	4.0 (11.3)[2]
SD-12	0.31	335.4	4.9 (4.6)[3]
NRG-6	0.20	332.3	4.3 (11.3)[4]
NRG-7a	0.2 (0.15)[1]	379.9	4.3 (3.5)[5]

1. 0.20 m form the ground surface to 91.5 m and 0.15 m from 91.5 m to 379.9 m
2. One test with longer interval length
3. 4.9 m for tests 1 through 37; 4.6 m for tests 38 through 161 m
4. Few tests with longer interval length
5. Test interval lengths of the 0.20- and 0.15 m diameter sections were 4.3 and 3.5 m respectively.

Table 1.2: Air permeability from single-hole tests in Tiva Canyon Tuff (adapted from LeCain, 1997).

Borehole	No. of Test Intervals	Minimum [m^2]	Maximum [m^2]	Arithmetic Mean [m^2]	Geometric Mean [m^2]
UZ-16	4	1.5×10^{-12}	27.0×10^{-12}	12.3×10^{-12}	7.6×10^{-12}
SD-12	11	0.8×10^{-12}	38.0×10^{-12}	7.0×10^{-12}	3.4×10^{-12}
NRG-6	4	0.3×10^{-12}	28.0×10^{-12}	11.2×10^{-12}	4.1×10^{-12}
NRG-7a	4*	0.2×10^{-12}	54.0×10^{-12}	26.6×10^{-12}	8.4×10^{-12}

*Does not include the nonwelded crystal-poor vitric test intervals.

Table 1.3: Air permeability from single-hole tests in Paintbrush Group (adapted from LeCain, 1997).

Borehole	No. of Test Intervals	Minimum [m^2]	Maximum [m^2]	Arithmetic Mean [m^2]	Geometric Mean [m^2]
NRG-7a	18*	0.12×10^{-12}	3.0×10^{-12}	0.5×10^{-12}	0.3×10^{-12}

* Includes two test intervals from the crystal-poor nonwelded vitric zone of the Tiva Canyon Tuff.

WI 1/20/00

Table 1.4: Air permeability from single-hole tests in Topopah Spring Tuff (adapted from LeCain, 1997).

Borehole	No. of Test Intervals	Minimum [m^2]	Maximum [m^2]	Arithmetic Mean [m^2]	Geometric Mean [m^2]
UZ-16	54	0.02×10^{-12}	9.5×10^{-12}	1.8×10^{-12}	0.9×10^{-12}
SD-12	27	0.12×10^{-12}	33.0×10^{-12}	4.7×10^{-12}	1.7×10^{-12}
NRG-6	34	0.08×10^{-12}	24.0×10^{-12}	2.1×10^{-12}	0.8×10^{-12}
NRG-7a	38	0.04×10^{-12}	2.4×10^{-12}	0.4×10^{-12}	0.3×10^{-12}

Table 1.5: Characteristics of boreholes RBT#1, RBT#2, and RBT#3 in Upper Tiva Canyon Alcove (UTCA) (data from LeCain, 1998).

Borehole	Angle from Vertical [deg]	Bearing [deg]	Diameter [m]	Depth [m]
RBT#1	85.8	63.2	0.096	30.5
RBT#2	86.3	76.5	0.096	32.1
RBT#3	98.4	69.9	0.096	31.3

Table 1.6: Single-hole air permeability values from boreholes RBT#1, RBT#2, and RBT#3 in Upper Tiva Canyon Alcove (UTCA) (data adapted from LeCain, 1998).

Borehole	No. of Test Intervals	Minimum [m^2]	Maximum [m^2]	Arithmetic Mean [m^2]	Geometric Mean [m^2]
RBT#1	7 (11)*	2.3×10^{-12}	27.0×10^{-12}	11.0×10^{-12}	7.2×10^{-12}
RBT#2	13 (18)	0.8×10^{-12}	81.0×10^{-12}	38.5×10^{-12}	27.1×10^{-12}
RBT#3	7 (12)	0.2×10^{-12}	85.0×10^{-12}	27.8×10^{-12}	13.3×10^{-12}

* Number in parentheses is total number of tests.

Table 1.7: Characteristics of boreholes HPF#1, and HPF#2 in Upper Tiva Canyon Alcove (UTCA) (data from LeCain, 1998).

Borehole	Angle from Vertical [deg]	Bearing [deg]	Diameter [m]	Depth [m]
HPF#1	0	265	0.096	26.2
HPF#2	0	265	0.096	26.1

WI 1/20/00

Table 1.8: Single-hole air permeability values from borehole HPF#1 located in Bow Ridge Fault alcove (BRFA) (data adapted from LeCain, 1998).

Geologic Zone	No. of Test Intervals	Minimum [m^2]	Maximum [m^2]	Arithmetic Mean [m^2]	Geometric Mean [m^2]
Tpcpmn[1]	8	6.0×10^{-12}	26.4×10^{-12}	13.9×10^{-12}	12.2×10^{-12}
Tpcpll[2]	5	0.6×10^{-12}	2.0×10^{-12}	1.3×10^{-12}	1.2×10^{-12}
Fault zone[3]	3	8.0×10^{-12}	15.8×10^{-12}		
Tmbt1[4]	2	41.3×10^{-12}	22.0×10^{-12}		

1. Tiva Canyon Tuff, crystal-poor middle nonlithophysal
2. Tiva Canyon Tuff, crystal- poor lower lithophysal
3. Bow Ridge Fault Zone
4. Pre-Rainier Mesa bedded tuff 1

Table 1.9: Permeability and porosity estimates from cross-hole pneumatic injection tests in boreholes HPF#1 and HPF#2 in Bow Ridge Fault alcove (BARF) (adapted from LeCain, 1998)

Test number	Injection interval in HPF#1	Monitor interval in HPF#2	Permeability [m^2]	Porosity [m^3/m^3]
4	Bow Ridge Fault zone	Bow Ridge Fault zone	27.8×10^{-12}	0.13
5	Bow Ridge Fault zone	Bow Ridge Fault zone	25.9×10^{-12}	0.20
6	Pre-Rainier Mesa bedded tuff1	Pre-Rainier Mesa bedded tuff1	23.2×10^{-12}	0.27

Table 1.10: Characteristics of boreholes RBT#1, and RBT#4 in Upper Paintbrush Contact Alcove (UPCA) (data from LeCain, 1998).

Borehole	Angle from Vertical [deg]	Bearing [deg]	Diameter [m]	Depth [m]
RBT#1	0	287	0.096	30.7
RBT#2	0	107	0.096	30.5

WI 1/20/00

Table 1.11: Single-hole air permeability values from boreholes RBT#1, and RBT#4 located in the Upper Paintbrush Contact Alcove (UPCA) (data from LeCain, 1998).

Geologic Zone	No. of Test Intervals	Minimum [m^2]	Maximum [m^2]	Arithmetic Mean [m^2]	Geometric Mean [m^2]
Tpcplnc[1]	6	0.02×10^{-12}	2.0×10^{-12}	0.7×10^{-12}	0.3×10^{-12}
Tpcpv1[2] and Tpcpv2[3]	12	0.4×10^{-12}	57.0×10^{-12}	16.5×10^{-12}	7.0×10^{-12}
Tpcplnh[4]	11	0.1×10^{-12}	12.0×10^{-12}	3.7×10^{-12}	2.1×10^{-12}

1. Tiva Canyon Tuff crystal-poor lower nonlithophysal columnar subzone
2. Tiva Canyon Tuff crystal- poor vitric subzone 1
3. Tiva Canyon Tuff crystal- poor vitric subzone 2
4. Tiva Canyon Tuff crystal-poor lower nonlithophysal hackly subzone

Table 1.12: Characteristics of boreholes MF#1, MF#2, and MF#3 in Northern Ghost Dance Fault Alcove (NGDFA) (data from LeCain, 1998).

Borehole	Inclination [deg]	Bearing [deg]	Diameter [m]	Depth [m]
MF#1	+00°39'58"	N 271°14'08"	0.096	30.5
MF#2	+00°27'44"	N 270°49'41"	0.096	30.6
MF#3	+01°42'07"	N 271°29'02"	0.096	34.4

Table 1.13: Permeability and porosity estimates from cross-hole pneumatic injection tests in the Ghost Dance Fault (data from LeCain et al., 1999)

	Type-curve analysis		Numerical inverse analysis	
Geologic Zone	Permeability [m^2]	Porosity [m^3/m^3]	Permeability [m^2]	Porosity [m^3/m^3]
Footwall	8.7×10^{-12}	0.04	10.0×10^{-12}	0.07
Fault zone	18.1×10^{-12}	0.13	20.0×10^{-12}	0.20
Hanging wall	5.0×10^{-12}	0.04	5.0×10^{-12}	0.05

3-1-2000

After writing the report (portions) which allowed me to review DOE data and models pertaining to air permeability / pneumatic tests, the following observations can be made:

1) Additional review of data and interpretive methods will be required

* 2) A new analytical solution which considers injection interval borehole storage and transient skin effect + observation wellbore storage ~~using the~~ WI 3/1/2000 based on the framework of Hsieh and Neuman (1985) will be absolutely necessary for a quick determination of k/ϕ.

3) Corresponding numerical inverse modeling of single- / and cross-hole tests will be necessary using data collected by LBNL / USGS researchers.

* 4) An analytical solution for interpreting tracer tests in 3D media (porous / fractured) is necessary to interpret tracer test data collected by LBNL / USGS groups.

WI
3/1/00

3-1-2000

Contribution to porosity report (letter report) led by David Farrell.

→ Review of DOE estimates of matrix and fracture matrix porosities in the UZ at Yucca Mountain

→ Laboratory analysis of rock cores yield estimates of porosity representative of the matrix pores, microfractures.

→ Estimates of porosities from field scale studies ~~give porosity~~ WI. 3/1/2000 are representative of fractures, matrix.

→ Porosity estimates derived from air injection tests represent porosities (intrinsic) of the dry fracture system which is interconnected. Under wetter conditions, the estimated porosity may be smaller

WI
3/1/00

Contribution to Porosity Report

4.2.1 DISCUSSION OF POROSITY FROM THE SURFACE OF YUCCA MOUNTAIN TO THE PROPOSED REPOSITORY HORIZON

WI 3/15/00

Introduction

It is generally accepted that the rate of deep percolation reaching the repository horizon at Yucca Mountain (YM) depends, among other things, on the water storage capacity of the unsaturated fractured rock. The fraction of water that flows in either the matrix and/or fracture depends on factors such as permeability, porosity, and capillary saturation relationships of each medium. As matrix porosities are much larger than the porosity of fractures, and pore sizes within the matrix are generally much smaller than fracture openings, most of the water is under capillary tension in the matrix and its saturation is much higher than that of the fractures under isothermal conditions. Under those conditions, water flow in fractures is the dominant flow mechanism in the welded volcanic tuffs at YM. As the permeability of matrix is sufficiently lower than the infiltration rate, the current conceptualization supports the role of fractures to act as primary conduits or "fast flow paths" for infiltrating water to reach the repository level. The notion of flow in connected fractures causing rapid downward migration of infiltrating water is supported primarily by geochemical data including elevated levels of isotopes Cl-36 and Tc-99 observed at the repository level in the Exploratory Studies Facility (ESF) (Fabrika-Martin et al., 1996) and tritium in the Calico Hills unit (Yang et al., 1996) beneath the repository.

The fast flow of water through the welded tuffs is due to the large permeability in fractures relative to the matrix. However, contrasts in porosities between the rock matrix and fracture can also significantly impact the flow regime. The high porosity of matrix relative to the porosity of fractures causes water to imbibe into the matrix when the saturation of pores in the matrix is low. In contrast, when the saturation of pores in the matrix is high, there is less tendency for water to flow into the matrix, hence flow takes place predominantly through the fractures. The parameters which control the exchange of fluids between the matrix and fracture takes place are highly uncertain, that is difficult to measure in situ, yet is one of the most important parameters in the Total Systems Performance Assessment (TSPA) calculations required for the licensing of the potential repository. The high permeability, small porosity and negligible storage of water in fractures amounts to the fast flow of water through YM.

The spatial distribution of matrix and fracture porosity at YM is important as it can affect the spatial and temporal distribution of deep percolation that could reach the repository horizon. In order to define such a distribution, sufficient data on porosity (field, laboratory, and/or natural analog data) must be available. This data set is employed to support conceptual models, assumptions, and boundary conditions necessary for developing the TSPA abstraction of percolation flux in the UZ. Therefore, a critical review of porosity data and methodologies employed to estimate porosity becomes a necessary component under the *Spatial and Temporal Distribution of Flow* Integrated Sub-Issue (ISI) (**ref. YMRP-preclosure?**).

Existing methods to determine porosity in geologic media are reviewed in chapter 3. Those include laboratory core studies that yield primarily the porosities of the rock matrix to transient hydraulic and pneumatic injection/pumping tests that allow for the determination of in situ fracture and matrix porosities, and geophysical methods. In order to provide a meaningful discussion on porosity of the unsaturated fractured rocks at YM, descriptions of various field and laboratory studies, corresponding interpretive

methods and results are summarized. The cited data and results in this review were obtained through the collaborative experimental effort by researchers from the United Geological Survey (USGS) and Lawrence Berkeley National Laboratory (LBNL).

WI 3/15/00

Laboratory analyses of rock cores

Numerous researchers have attempted laboratory analyses of rock core samples at YM (Anderson, 1981a,b; Rush et al., 1983; Anderson et al., 1984; Weeks and Wilson, 1984; Peters et al., 1984; Whitfield et al., 1984; Klavetter and Peters., 1987; Flint and Flint, 1990; Kume and Hammermeister, 1990; Anderson, 1991; Nelson et al., 1991; Loskot and Hammermeister, 1992; Loskot, 1993; Anderson, 1994; Rautman et al., 1995; Flint et al., 1996). More recently, the USGS collected 4,892 core samples from 23 shallow and 8 deep boreholes for laboratory analyses to provide a detail description of the rock properties at YM (Flint, 1998). Laboratory tests were performed to obtain physical and flow properties that includes porosity. The core samples were 7 cm in diameter and 10 to 20 cm in length. Analyses of cores led to the classification of 31 hydrogeologic units in the UZ. Porosity ranged from less than 9% in the welded Tiva Canyon (TCw) unit with several subunits exceeding 20%. Porosities in the nonwelded Paintbrush (PTn) unit were mostly greater than 30%, while due to welding of the tuff, porosities in the Topopah Springs (TSw) unit were less than 9%. In general, welded units tend to have the lowest porosities, while the nonwelded and bedded units tend to have the highest porosities. A summary of porosities including the mean and standard deviation from each of the 31 hydrogeologic units are summarized in Table 1. One of the key findings from this study included the recognition of transition zones with pronounced changes in porosities over short vertical distances. Porosity variations can be due to mineral alterations, presence of microfractures, depositional and cooling history. Dramatic but smooth transitions in porosity were seen at the top of the PTn unit, while the transition was more abrupt at the bottom boundary of the PTn unit. Porosity also has been related to the alteration history of the rocks at YM. Clay minerals, zeolites, opal, and calcite form in place or are deposited in pore channels and throats, which significantly alter porosities. Statistical analyses of physical and flow properties showed good correlation of porosity with saturated hydraulic conductivity and the moisture retention curve fit parameter α. A geostatistical analysis of matrix porosity data has been reported in CRWMS M&O (1999).

Cross-hole pneumatic injection and gaseous tracer tests

Extensive field studies are being conducted by USGS and LBNL researchers to determine flow and transport properties of lithological units by means of pneumatic injection and gaseous tracer tests at Yucca Mountain. Field determination of porosity can be accomplished by means of slug tests, single-hole tests, and large-scale pumping tests in both saturated and unsaturated zones, although porosity estimates derived from slug and single-hole tests are considered to be notoriously unreliable when compared to porosities obtained from observation well responses in large-scale cross-hole tests.

Cross-hole pneumatic injection tests were conducted by injecting air into a short section of the borehole isolated by means of inflatable packers at a constant flow rate. The corresponding pressure is monitored within the injection interval and in monitoring intervals located in various sections of neighboring boreholes. Gaseous tracer tests were conducted at several locations using the same equipment where cross-hole pneumatic injection tests revealed good connections between injection and monitoring intervals. As the pressure propagation and tracer arrival are monitored over several meters between boreholes, porosities

along with permeabilities from cross-hole pneumatic tests and gaseous tracer tests represent the bulk intrinsic properties of the fractured rock on the scale of several meters. As most fractures systems in the UZ are filled primarily with air, estimates of porosities obtained through cross-hole pneumatic injection and gaseous tracer tests should be close to the fracture porosity of the rock at the site.

WI 3/8/00

Cross-hole pneumatic injection tests were conducted by USGS researchers in boreholes located in the Bow Ridge Fault Alcove (BRFA) (LeCain, 1998) (**perhaps we can show a figure which shows the location of alcove relative to the ESF**). The alcove at this location was excavated to test the hydrologic properties of the fault zone. The 2 horizontal and parallel boreholes (HPF#1 and HPF#2) are 3 m apart and penetrate the crystal-poor middle lithophysal zone of the Tiva Canyon tuff, the Bow Ridge Fault zone and the pre-Rainier Mesa tuff. Thirteen cross-hole pneumatic injection tests were conducted with borehole HPF#1 as the injection hole while HPF#2 was used to monitor the pressure responses. Several tests yielded good pneumatic connections while in other cross-hole tests, monitoring intervals failed to respond. LeCain (1998) employed the spherical type-curve model to conduct the interpretation of cross-hole data. Values of porosity obtained include 0.13 and 0.20 in the Bow Ridge fault zone, and 0.27 in the pre-Rainier Mesa tuff (Table 2).

Several convergent gaseous tracer tests were conducted using sulfur hexafluoride (SF_6) where cross-hole pneumatic tests were conducted. Porosity estimates resulting from gaseous tracer tests were somewhat larger than porosities obtained through cross-hole pneumatic injection tests. Possible reasons cited in LeCain (1998) for the discrepancies include increased tortuosity and tracer adsorption. A summary of results from the tracer tests is provided in Table 3.

More recently, the USGS conducted several cross-hole pneumatic injection tests across the Ghost Dance Fault (LeCain et al., 1999) which yielded data that appear to be amenable to interpretation by means of analytically derived type-curves. Three boreholes were drilled horizontally in a triangular pattern within the Northern Ghost Dance Fault Alcove (NGDFA). The USGS researchers identified three zones (foot wall, fault zone, and hanging wall) which yielded different values of permeability and porosity (Table 4). The interpretation assumed three individual zones to be homogeneous and isotropic. According to the authors, the same data sets were numerically interpreted using the U.S. Geological Survey AIR3D computer code (Joss and Baehr, 1995) yielding results comparable to that obtained from type-curve interpretation (Table 5). Cross-hole pneumatic pressure data were analyzed additionally using the FRACMAN computer code (Dershowitz et al., 1994), based on the discrete fracture network concept. The pressure responses from the hanging and footwall sections were amenable to analysis. The excessive fracturing in the fault zone precluded the researchers to analyze data from the fault zone due to excessive fracturing.

Convergent gaseous tracer tests were conducted in NGDFA where cross-hole pneumatic injection tests revealed connections between the injection and monitoring intervals. Tracers employed include sulfur hexafluoride (SF_6) and helium (He) injected as a slug after the flow system has reached steady-state. Cross-hole tracer data were interpreted using an analytically derived type-curves developed by Moench (1995). Results from the gaseous tracer tests are summarized in Table 6.

The LBNL pneumatic testing program (Tsang et al., 1996) in connection with the single-heater experiments

and niche studies (Wang et al., 1998) yielded numerous single- and cross-hole pneumatic pressure data in the ESF. Those data have not been interpreted adequately to yield estimates of porosity at the time of this report. The simultaneous inversion of cross-hole pneumatic data in Huang et al. (1999) assumes an effective porosity throughout the modeled region. The transient interpretation of the cross-hole pneumatic pressure data using analytically derived type-curves and/or numerical inverse interpretation may yield information on porosity and its spatial distribution in the future. It appears that more work may be required in interpreting pneumatic test data from YM.

WI 3/6/00

Subsurface monitoring of barometric pressure fluctuations

Measurements of bulk diffusivity in the unsaturated zone (e.g., Rousseau et al., 1997), taken alone, are generally of little use for predicting flow rates and flow distributions in unsaturated media. However, monitoring of ambient pressure fluctuations have provided important insight into bulk, site-scale (Neuman, 1998-personal communication) estimates of intrinsic diffusivity through the UZ. In particular, barometric pressure fluctuation data have been analyzed to study gas flow properties of major hydrogeologic units, properties of faults and fracture zones, and the effects of the ESF construction on the gaseous-phase system (Rousseau et al., 1996). Since permeability and porosity cannot be estimated independently (Ahlers et al., 1999), permeability is estimated from diffusivity by assuming a value of porosity. Similarly, site-scale estimates of porosity may be calculated by assuming a value of permeability of the UZ units. Researchers from the USGS employed the AIRK computer code (Weeks, 1978), while LBNL modelers employed the TOUGH2 (Pruess, 1991) and ITOUGH2 (Finsterle, 1997) computer codes to simulate the barometric pressure propagation through several lithological units. Results showed that the barometric signal travels without signal lag and attenuation through the Tiva Canyon (TCw) and Topopah Spring (TSw) units. Significant amplitude attenuation and phase lag of the barometric signal was seen to occur through the Paintbrush (PTn) unit, although the degree of attenuation appears to vary across the Yucca Mountain site (Rousseau et al., 1996; Patterson et al., 1996; Ahlers et al., 1999). The very little attenuation and time lag of barometric response in the welded units suggests that the storage capacity of those units are very small. The PTn unit, which is largely nonwelded, can be considered to be more porous causing the amplitude attenuation and time lag of barometric responses monitored in boreholes. The primary cause of the lateral variation in barometric signal has been linked to the thickness of the PTn unit but the variability in saturation of matrix and presence of fractures can also cause significant variability. The bulk estimates of permeability (and porosity) can be useful but, detailed, spatial information on hydraulic and pneumatic flow parameters and connectivity of permeable pathways are necessary for the performance assessment of the repository. Information on the spatial distribution of permeability and porosity can only be obtained through additional interpretation of existing single- and cross-hole pneumatic injection tests.

References

Ahlers, C. F., S. Finsterle, G. S. Bodvarsson, 1999, Characterization and prediction of subsurface pneumatic response at Yucca Mountain, Nevada. Journal Contaminant Hydrology 38, 47-68.

Anderson, L. A., 1981a, Rock property analysis of core samples from the Calico Hills UE25a-3 borehole, Nevada test Site, Nevada: U. S. Geological Survey Open File Report 81-1337, 30p.

Anderson, L. A., 1981b, Rock property analysis of core samples from the Yucca Mountain UE25a-1

WI 3/6/00

Table 1: Summary of porosity estimates from laboratory analyses of rock cores (Flint, 1998)

	Hydrogeologic Units	Porosity		
Major	Detailed	No. of samples	Mean	SD
Tiva Canyon Welded (TCw)*	CCR	9	0.062	0.020
	CUC	101	0.253	0.060
	CUL	98	0.164	0.062
	CW	599	0.082	0.030
	CMW	90	0.203	0.054
	CNW	101	0.387	0.070
Paintbrush Nonwelded (PTn)	BT4	33	0.439	0.123
	TPY	43	0.254	0.082
	BT3	85	0.411	0.079
	TPP	164	0.499	0.041
	BT2	171	0.489	0.105
Topopah Spring Welded (TSw)	TC	66	0.054	0.036
	TR	439	0.157	0.030
	TUL	455	0.154	0.031
	TMN	266	0.110	0.020
	TLL	453	0.130	0.031
	TM2	225	0.112	0.031
	TM1	102	0.094	0.019
	PV3	89	0.036	0.039
Calico Hills Nonwelded (CHn)	PV2	39	0.173	0.106
	BTla	36	0.288	0.072
	BT1	43	0.273	0.067
	CHV	69	0.345	0.034

WI 3/6/00

	Hydrogeologic Units	Porosity		
	CHZ	293	0.331	0.039
	BT	69	0.266	0.041
	PP4	47	0.325	0.045
	PP3	166	0.303	0.043
	PP2	140	0.263	0.072
	PP1	245	0.280	0.053
Crater Flat (CFu)	BF3	86	0.115	0.040
	BF2	65	0.259	0.084

*Part of CNW is classified as Paintbrush nonwelded (PTn) in Flint (1998).

Table 2: Permeability and porosity estimates from cross-hole pneumatic injection tests in boreholes HPF#1 and HPF#2 in Bow Ridge Fault alcove (BRFA) (adapted from LeCain, 1998)

Test number	Injection interval in HPF#1	Monitor interval in HPF#2	Permeability [$\times 10^{-12}$ m^2]	Porosity [m^3/m^3]
4	Bow Ridge Fault zone	Bow Ridge Fault zone	27.8	0.13
5	Bow Ridge Fault zone	Bow Ridge Fault zone	25.9	0.20
6	Pre-Rainier Mesa bedded tuff1	Pre-Rainier Mesa bedded tuff1	23.2	0.27

Table 3: Results from cross-hole tracer testing in Bow Ridge Fault alcove (BARF) (adapted from LeCain, 1998)

Test number	Pumped interval in HPF#1	Release interval in HPF#2	First arrival [min.]	Peak arrival [min.]	Tracer velocity [$\times 10^{-4}$ m/s]	Darcy velocity [$\times 10^{-4}$ m/s]	Effective porosity
2	Bow Ridge Fault zone	Bow Ridge Fault zone	16	80	6.5	3.1-3.4	0.48-0.52
3	Bow Ridge Fault zone	Bow Ridge Fault zone	16	36	14.4	3.1-3.4	0.22-0.24

WI 3/6/00

Table 4: Summary of porosity estimates from cross-hole pneumatic injection tests in northern Ghost Dance Fault Alcove (NGDFA) obtained using type-curve interpretation (from LeCain et al., 1999)

	Minimum [m^3/m^3]	Maximum [m^3/m^3]	Arithmetic Mean [m^3/m^3]	Geometric Mean [m^3/m^3]
Hanging Wall	0.01	0.09	0.04	0.03
Fault Zone	0.05	0.27	0.13	0.10
Foot Wall	0.01	0.12	0.04	0.03

Table 5: Summary of porosity estimates from cross-hole pneumatic injection tests in northern Ghost Dance Fault Alcove (NGDFA) obtained using a numerical code AIR3D (from LeCain et al., 1999)

	Porosity [m^3/m^3]
Hanging Wall	0.05
Fault Zone	0.20
Foot Wall	0.07

Table 6: Summary of transport porosity values obtained form cross-hole gaseous tracer tests in northern Ghost Dance Fault Alcove (NGDFA) (from LeCain et al., 1999)

	Minimum [m^3/m^3]	Maximum [m^3/m^3]	Arithmetic Mean [m^3/m^3]
Hanging Wall	0.001	0.070	0.013
Fault Zone	0.004	0.034	0.014
Foot Wall	0.003	0.032	0.013

3/6/00

Difficult to obtain porosities from single-hole air injection tests.

→ lacks of transient data from single-hole tests (S.P. Neuman) – personal comm. conducted in DOE Yucca Mountain site.

→ highly connective fracture system?
no storage in fracture system?
no/little interaction with the matrix?

Cross-hole tests can yield porosities
– need further interpretation using calibrated inverse models
(geostatistical inverse models)

3/6/00
WI

WI 3/6/00

3.2.3 Barometric efficiency **(Dave, I propose: Subsurface monitoring of barometric pressure fluctuations)**

Fluctuations in barometric pressures due to diurnal temperature changes and climatic factors cause the movement of air in the unsaturated zone. The diffusive properties of soils and rocks cause the time lag and amplitude attenuation of the barometric signal. The mathematical description of the phenomena was first proposed by Buckingham (1904). It was Stallman (1967) and Stallman and Weeks (1969), however, whom related barometric pressure fluctuations monitored in the subsurface to the diffusivity of geologic media. Geologic media with high diffusion coefficients (e.g., gravel, coarse sand and highly fractured media) tend to have a minimal effect in attenuating and causing time lag in the barometric signal measured at depths, while significant attenuation and time lag are observed in subsurface materials with small diffusion coefficients. Aside from the diffusivity of the geologic medium, the time lag and amplitude attenuation of barometric signals is controlled by variations in water content of soils and rocks with depth. In well drained soils, the effect of water content on the passage of barometric signals is less compared to fine grained materials with higher water contents. The value of permeability, porosity and diffusivity obtained from well drained soils represent quite closely the intrinsic properties of the medium. The Klinkenberg effect (1941) or gas slippage can be important for fine grained materials with intrinsic permeabilities of 10 millidarcies or less (Weeks, 1978).

Measurements of pneumatic pressures have been made at various depths in isolated piezometers constructed in the unsaturated zone at various sites including playa sediments and basalt flows (Weeks, 1978), shallow soils (Rojstaczer and Tunks, 1995), and in fractured tuffs (Rousseau et al., 1997). The time series of barometric pressure fluctuations have been analyzed using numerical methods (Weeks, 1978; Rousseau et al., 1997; Ahlers et al., 1999) and by means of analytical techniques (Shan, 1995; Shan et al., 1999) to yield the diffusivity of the medium. Vertical permeability is estimated from the calculated diffusivity by assuming a value of porosity determined usually from laboratory analyses of cores. Although the focus has been on estimating permeability from barometric pressure fluctuations, air-filled porosity of the medium can be estimated by assuming a value of air permeability, determined from air injection tests or laboratory core analysis. Porosities and permeabilities obtained in this manner are representative of bulk, air-filled properties of the medium.

3.2.? Transient interpretation of pneumatic injection/pumping tests

Pumping or injection tests in the unsaturated zone using air has become more common recently to determine flow properties of unsaturated soil and fractured rocks. The problem of determining soil and rock properties from such tests requires the understanding of mechanisms governing the flow of air in unsaturated media. In principle, pneumatic tests are very similar to their hydraulic counterparts conducted in fully water-saturated media. Air is either injected or withdrawn from packed off intervals, which causes a corresponding increase or decrease in observation wells and packed off intervals. The pressure response in observation wells can be related to pneumatic flow parameters such as air permeability and air-filled porosity through type-curve analysis or numerical inverse modeling. Determination of air-filled porosity requires the transient interpretation of air injection tests. The interpretation of pneumatic tests can be more complicated particularly for single-hole tests that are more prone to nonlinear effects seen near the well. The nonlinear effects seen near the injection well is less apparent in data from cross-hole pneumatic injection tests. Commonly observed nonlinear effects include two phase flow effects that arise from the capillary interaction of injected air with water and

WI 3/6/00

non-Darcian behavior at high Reynolds numbers. Air which is highly compressible, also cause nonlinearities in the equations to be solved for data analysis. For purposes of data interpretation by means of analytical formulae, air compressibility is assumed to be a constant. A complete description of air-water interaction requires two systems of coupled partial differential equations, one for each phase. The development of corresponding analytical formulae to be used for type-curve interpretation requires that two-phase flow is approximated as single-phase airflow and that water is treated as immobile. The coupled equations can also be solved rigorously by means of finite difference or a finite element techniques. Due to the relatively low importance, enhanced permeability due to slip flow [the Klinkenberg (1941) effect] is usually neglected in the interpretation of well tests. The interpretation pneumatic test data based on groundwater equations according to (Massmann, 1989), is possible, when slip flow can be neglected. Estimates of air-filled porosity obtained by type-curve or numerical inverse interpretation represent the bulk air-filled porosity of the soil or rock. Reports of air-filled porosities obtained from the interpretation of pneumatic tests may be found in the literature [Massmann and Madden (1994); Illman et al., 1998; LeCain 1998; LeCain et al., 1999; Chen et al., 2000; Vesselinov and Neuman, 2000, Illman and Neuman, 2000].

Ahlers, C. F., S. Finsterle, G. S. Bodvarsson, 1999, Characterization and prediction of subsurface pneumatic response at Yucca Mountain, Nevada, *Journal of Contaminant Hydrology* 38: 47-68.

Buckingham, E., 1904, Contributions to our knowledge of the aeration of soil: U.S. Dept. Agriculture Soils Bur. Bull. 25. 52 p.

Chen, G., W. A. Illman, D. L. Thompson, V. V. Vesselinov, and S. P. Neuman, 2000, Geostatistical, Type-Curve and Inverse Analyses of Pneumatic Injection Tests in Unsaturated Fractured Tuffs at the Apache Leap Research Site Near Superior, Arizona, paper to appear in *Dynamics of Fluids in Fractured Rocks – Concepts and recent advances, in honor of Paul A. Witherspoon's 80th birthday*, in press.

Huang, K., Y. W. Tsang, and G. S. Bodvarsson, 1999, Simultaneous inversion of air-injection tests in fractured unsaturated tuff at Yucca Mountain, *Water Resources Research*, 35(8), 2375-2386.

Illman W. A., D. L. Thompson, V. V. Vesselinov, G. Chen, and S. P. Neuman, 1998, *Single- and Cross-Hole Pneumatic Tests in Unsaturated Fractured Tuffs at the Apache Leap Research Site: Phenomenology, Spatial Variability, Connectivity and Scale*, NUREG/CR-5559, U. S. Nuclear Regulatory Commission, Washington D.C.

Illman, W. A. and S. P. Neuman, Type-curve interpretation of a cross-hole pneumatic test in unsaturated fractured tuff, submitted to Water Resources Research, 2000.

Klinkenberg, L. J., 1941, The permeability of porous media to liquids and gases, American Petroleum Institite, *Drilling and Production Practice*, 200-213.

LeCain, G. D., 1998, *Results from Air-Injection and Tracer Testing in the Upper Tiva Canyon,*

WI 3/6/00

Bow Ridge Fault, and Upper Paintbrush Contact Alcoves of the Exploratory Studies Facility, August 1994 through July 1996, Yucca Mountain, Nevada, Water-Resources Investigations Report 98-4058.

LeCain, G. D., L. O. Anna, and M. F. Fahy, 1999, *Results from Geothermal Logging, Air and Core-Water Chemistry Sampling, Air-Injection Testing and Tracer Testing in the northern Ghost Dance Fault, Yucca Mountain, Nevada, November 1996 to August 1998*, U.S. Geological Survey Water-Resources Investigations Report 99-4210.

Massmann, J. W., 1989, Applying Groundwater Flow Models In Vapor Extraction System Design, *Journal of Environmental Engineering*, 115(1): 129–149.

Massmann, J. W. and M. Madden, 1994, Estimating air conductivity and porosity from vadose-zone pumping tests, *Journal of Environmental Engineering*, 120(2): 313-328.

Rojstaczer, S. and J. P. Tunks, 1995, Field-based determination of air diffusivity using soil air and atmospheric pressure time series, *Water Resources Research*, 31(12): 3337-3343.

Rousseau, J. P., C. L. Loskot, F. Thamir, and N. Lu, 1997, Results of Borehole Monitoring in the Unsaturated Zone within the Main Drift Area of the Exploratory Studies Facility, Yucca Mountain, Nevada, U.S. Geological Survey, Administrative Report, Level 3 Milestone, SPH22M3.

Shan, C., 1995, Analytical solutions for determining vertical air permeability in unsaturated soils, *Water Resources Research*, 31(9): 2193-2200.

Shan, C., I. Javandel, and P. A. Witherspoon, 1999, Characterization of leaky faults: Study of air flow in faulted vadose zones, *Water Resources Research,* 35(7): 2007-2013.

Stallman, R. W., 1967, Flow in the zone of aeration, in Ven Te Chow, ed., *Advances in Hydroscience*: New York, Academic Press, 4:151-195.

Stallman, R. W. and E. P. Weeks, 1969, The use of atmospherically induced gas-pressure fluctuations for computing hydraulic conductivity of the unsaturated zone (abs.): Geological Society of America Abstracts with Programs, pt. 7, p.213.

Vesselinov, V. V. and S. P. Neuman, 2000, Numerical inverse interpretation of multistep transient single-hole pneumatic tests in unsaturated fractured tuffs at the Apache Leap Research Site. In: *Theory, Modeling and Field Investigations in Hydrogeology: A Special Volume in honor of Shlomo P. Neuman's 60th birthday*, Geological Society of America.

Weeks, E. P., 1978, *Field determination of vertical permeability to air in the unsaturated zone*, Geological Survey Professional Paper 1051, 41 p.

Paintbrush unit

Numerical modeling study of how effective the PTn unit is for attenuating water flux.

notes 12/28/1999
transcribed 3/13/2000

Evidence suggesting attenuation of water flux through PTn

- attenuation of barometric pressures and its time lag monitored in the subsurface (this differs from one location to another)
- capillary barrier effect
- geological, homogeneous description of units at Yucca Mountain

- DOE conceptual model based on 5mm/yr. infiltration rate suggests little lateral flow near the PTn/TCw bound.
- Bodvarsson and Bandurraga (1996, p.20) suggests a pulse-type infiltration occurring over short time frames and then low, steady infiltration rates over relatively long time periods (consistent with measured saturation and moisture tension data)
- PTn attenuates water flux (episodic) and diverts it away (check the current DOE conceptual model of flow through the UZ)

Evidence ~~suggesting~~ against the PTn attenuation concept. WZ 3-1-2000

- presence of Cl-36 in the ESF where PTn is thickest
- attenuation of barometric pressures and its time lag is quite variable at different monitoring stations suggesting that diffusivity varies spatially in the PTn.
- low saturation of matrix in PTn - drains? compared to other units.

WZ
3/13/00

Concepts.

- localized fast flow paths unknown to DOE researchers (not enough data)
- heterogeneity not built in explicitly into layers causing water flux to not make through the unit.
- episodic nature of water flux at the top of PTn unit.
- channelization of water?
- fingering of water in the matrix?
- film flow through fracture walls?
- very limi

Numerical Simulation layered dual,
Flow Through a heterogeneous Continua

Modeling ISSUES notes from 12/28/1999

- build "realistic" model (3D, multiphase, multilayer, isothermal
- challenge DOE steady-state flow assumption
- homogeneous vs. heterogeneous distribution of k/ϕ
  - various correlation scales; correlation structures.
- spatial variation of water input vs constant ~~source~~ flux WZ at top boundary

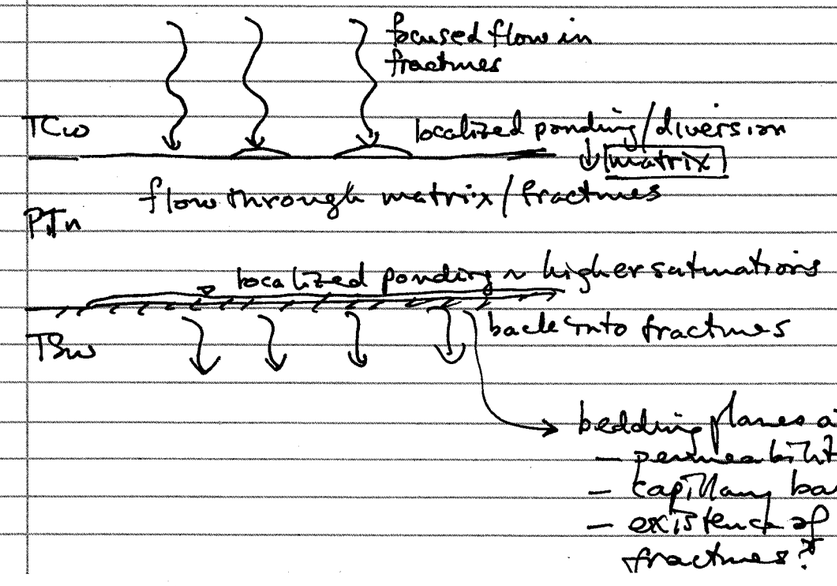

WZ 3/13/00

Test problems #1

Simulation – radial flow (liquid phase) in a confined aquifer

- Attached input file → copied
- problem came from Scott Painter's subdirectory on benchmark problems numerical
- the solution plotted against an analytical solution matches quite well except for the early time.
(p.47)

WI
3/13/00


```
                                        theis
METRA test:  Theis' solution for pumping from infinite aquifer
                  July 21, 1999
:
RSTART 0
:
:grid  geometry  nx  ny  nz ivplwr ipvcal iout gravity pref tref  href
GRID   RADIAL    100   1  1    1      1      3    0      0    0    0
:
LIQUID
:
Pckr                              :relative perm and pc keyword
:   i  type-curv swirm  rpmm(lamda)  alpham  swext  sgc  iecm
:
    1  Van-Gen   0.01   0.63    9.7e-5      0.     0.  0
/
:
Thermal-prop
: no rho        cpr   ckdry  cksat    crp  crt   tau  cdiff    cexp  enb
d
  1  2.510e+3  847.    1.02   1.76     0    0    .5  2.13e-5  1.8  0.
0
:     igrid   rw      re
DXYZ   0      0.0     5000.
: (dx(i),i=1,nx)
0.01
:
: (dy(j),j=1,ny)
360.
:
: (dz(k),k=1,nz)
1.0
:
PhiK
: i1 i2  j1  j2  k1  k2  iist ithrm  vb porm   permx   permy    permz
  1  100   1  1   1  1   1       1   0.  0.2   1.e-11   1.e-11   1.e-1
1
   0   0
:
Init
:
: i1  i2  j1  j2  k1  k2    p         t         sg         xg2
   1   100   1   1   1   1  1.e6   25.0000  0.0  000E+00
   0   0
:
Recurrent-data
Source 1  1. 1.
1 1 1 1 1 1 11
:time[s] T[degC]  qmt[kg/s]
0.        25         -1.00
.
:
```

Page 1

WI
3/13/00

theis

```
Rstart 1 0
Output   A=1
:  isolve newtnmn newtnmx north nitmx level
Solve 4     1    12    2    100   1
:
:AUTO-step  DPMXE    DSMXE  DTMPMXE   DP2MXe
AUTO-step   1.0E+1   0.04    1.        1.e3
:
:TOLR TOLP  TOLS  TOLT  TOLP2  TOLM  TOLA  TOLE rtwotol rmxtol smxtol
Tolr   0.1 1.e-4  1.e-3  1.e-1 1.e-8 1.e-8 1.e-6 1.e-25 1.e-25 1.e-25
:
:Limit dpmx    dsmx dtmpmx dp2mx dtmn dtmx icutmx
LIMIT  5.e3    .1    3.    .5e4  1.e-8  1.e5 .334
Plots 1 1 1
35
Time[y]  0.0001
Time[y]  0.001
Ends
```

WI
3/13/00

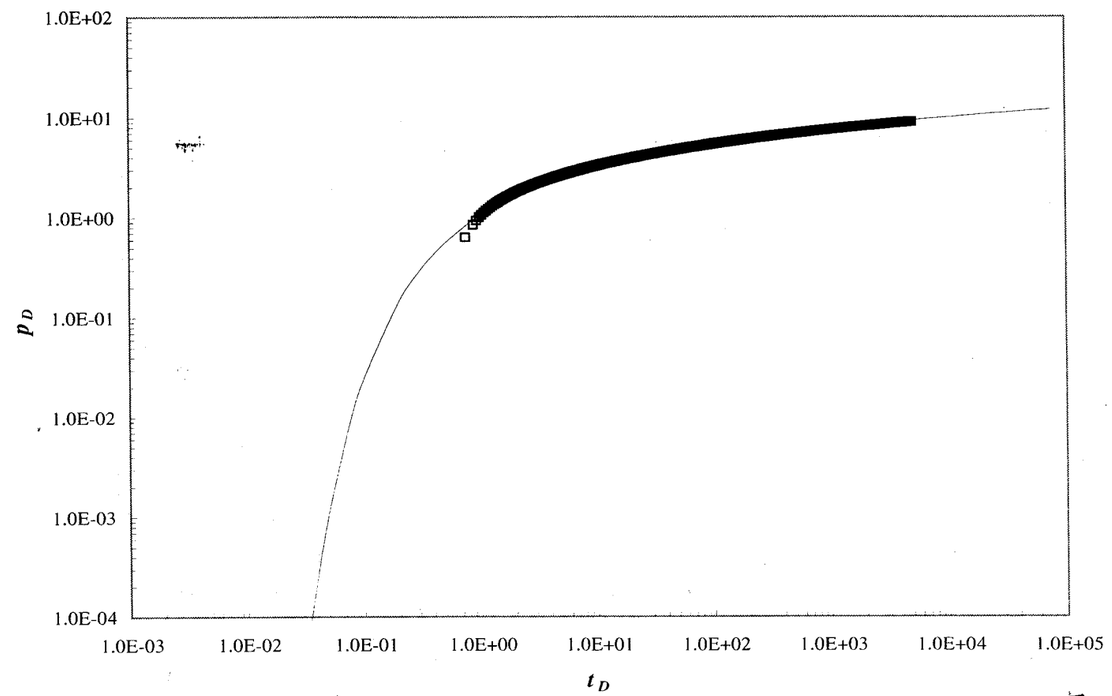

WI
3/13/00

Test Problem #2

- Debra Hughson / Goodluck Ofoegbu.
  Randall Fedors

- Infiltration in DCM in a two phase flow environment; 5 layers.

  1) Tiva Canyon (TCw)
  2) Paintbrush (PTn)
  3) Topopah Springs (TSw)
  4) Calico Hills (CH)
  5) Prow Pass

- 10 mm/yr. at top boundary.
- Type 5 BC. at top (mixed)
- Type 1 BC at bottom. (Dirichlet)
- run simulation until steady-state.

- In general, the program seems to work well but some parameter adjustments are necessary to get acceptable mass, energy balances. WI 3/13/2000

WI
3/13/00


```
                                        trans01
  METRA-DCM, test
  2D structured grid, percolation rate = 10 mm/yr
:
RSTART  0
:
:grid  geometry  nx ny   nz ivplwr ipvcal  iout  gravity  pref tref  h
ref
Grid   DCMXYZ     8  1   80   1       1      1     0         0    0
 0
: ****************************
:  Define size of grid-blocks
: ****************************
DXYZ   0
: (dx(i),i=1,nx)
1.49  1.67  1.8  1.8  1.8  1.8  1.8  1.84
: (dy(j),j=1,ny)
1.
: (dz(k),k=1,nz)
 7.0  8.2  9.0  9.0 10.0 10.0 10.0 10.0 10.0  9.0
 8.0  6.3  4.5  7.0  7.0  4.6  6.9  7.0  7.0  7.5
 7.0  7.0  7.0  8.0 11.0 14.0 16.0 15.0 14.0 13.0
12.0 11.0 10.0  9.0  8.0  7.0  6.0  6.0  5.0  5.0
 5.0  5.0  5.0  5.0  5.0  5.0  3.48 2.08 1.44 1.0
 1.5  2.0  3.0  5.0  6.0  7.0  9.0 10.5 13.0 14.0
14.3 15.0 15.0 16.2 15.0 15.0 11.5  9.0  9.7 12.3
14.0 15.0 15.0 17.0 18.0 16.0 14.0 12.0  8.4  6.5
:
DCMParameters
: i1 i2 j1 j2  k1 k2   volf    areamodf  xlm  ylm  zlm
:
  1   8  1  1  1  13  2.33e-4  5.00e-4  0.5  0.5  0.5  : TCw11
  1   8  1  1  14 21  3.86e-5  5.00e-1  0.5  0.5  0.5  : PTn25
  1   8  1  1  22 63  3.99e-4  5.00e-4  0.5  0.5  0.5  : TSw36
  1   8  1  1  64 71  1.10e-5  9.22e-1  0.5  0.5  0.5  : CH3vc
  1   8  1  1  72 80  7.14e-5  5.00e-4  0.5  0.5  0.5  : PP3vp
0
: ********************************************************************
*
: Hydro parameters
: i = sequential number of material types
: type = the characteristic curves (Van-Gen, Linear, tabular, and core
y)
: swir = irreducible liquid saturation, fraction
: rpm = Van Genuchten parameter
: alpha = Van Genuchten parameter, 1/Pa
: swext = liquid saturation below which the capillary pressure is calc
ulated based on
:         the slope dPcw/dSw evaluated at SWEXT; if <0, cutoff for cap
illary pressure, Pa.
: sgc = residual (immobile) gas saturation, fraction
: iecm = Equivalent Continuum Model (ECM) formulation
```

3/13/00
WI

```
                                    trans01
:          (0 do not invoke, 1 invoke, 2 ECM with tables)
: phi = matrix porosity (fraction)
: perm = intinsic matrix permeability (m^2)
:
Pckr                                : UZ Constitutive Relation Parameters
:   i  type-curv     swir   rpm(lamda)   alpha       swext    sgc    ie
cm
    1  Van-Gen       0.13   0.231        1.15e-6    -1.0e+8   0.0
0 : (TCw11 - matrix)
    2  Van-Gen       0.01   0.667        2.37e-3    -0.0e+8   0.0
0 : (TCw11 - fracture)
    3  Van-Gen       0.10   0.3195       1.81e-4    -0.0e+8   0.0
0 : (PTn25 - matrix)
    4  Van-Gen       0.10   0.320        1.81e-4    -0.0e+8   0.0
0 : (PTn25 - fracture)
    5  Van-Gen       0.18   0.5138       2.272e-6   -0.0e+8   0.0
0 : (TSw36 - matrix)
    6  Van-Gen       0.01   0.667        1.32e-3    -0.0e+8   0.0
0 : (TSw36 - fracture)
    7  Van-Gen       0.20   0.2119       2.16e-5    -1.0e+8   0.0
0 : (CH3zc - matrix)
    8  Van-Gen       0.01   0.654        1.12e-3    -0.0e+8   0.0
0 : (CH3zc - fracture)
    9  Van-Gen       0.07   0.3142       1.66e-5    -0.0e+8   0.0
0 : (PP3vp - matrix)
   10  Van-Gen       0.01   0.667        1.42e-3    -0.0e+8   0.0
0 : (PP3vp - fracture)
0
:
PHIK                          : Permeabilities and Porosities of Fractures
and Matrix
: fracture permeabilities modified by dividing by fracture porosity; m
atrix perm is isotropic
: i1 i2 j1 j2  k1 k2 ist ithrm vb  porf   permxf   permyf   permzf  po
rmm  permm  istm ithrmm
:
  1   8  1  1  1  13   2    1  0. 1.0000 2.59e-08 2.59e-08 9.83e-08 0.
066 5.40e-18   1   1 : TCw11
  1   8  1  1  14 21   4    2  0. 1.0000 2.01e-09 2.01e-09 2.01e-09 0.
464 3.18e-13   3   2 : PTn25
  1   8  1  1  22 63   6    3  0. 1.0000 3.01e-09 3.01e-09 3.01e-09 0.
092 8.70e-18   5   3 : TSw36
  1   8  1  1  64 71   8    4  0. 1.0000 1.06e-09 1.06e-09 2.28e-09 0.
240 2.50e-18   7   4 : CH3zc
  1   8  1  1  72 80  10    5  0. 1.0000 9.69e-09 9.69e-09 9.92e-09 0.
274 1.91e-15   9   5 : PP3vp
0
:
: ***************
:  Debug options
: ***************
```

3/13/00
WI


```
                                    trans01
Debug  1
0
:
: ********************
:  Thermal properties
: ********************
: no = sequential number of data set
: rho = rock density (kg/m^3)
: cpr = rock specific heat (J/kg-K)
: ckdry = thermal conductivity of dry rock (J/s/m-K)
: cksat = thermal conductivity of liquid saturated rock (J/s/m-K)
: crp = pore compressibility with pressure at constant T (1/Pa)
: crt = absolute value of pore compressibility with pressure at consta
nt T (1/Pa)
: tau = tortuosity for binary diffusion
: cdiff = vapor-dir diffusion coefficient, (m^2/s)
: cexp = exponent for binary diffusion
: enbd = enhanced binary diffusion coefficient
:
Thermal-prop
: no rho        cpr     ckdry  cksat    crp  crt    tau  cdiff    cexp  en
bd
  1  2.510e+03 847.     1.02   1.76     0    0     .5  2.13e-5  1.8  0.
  : (TCw11 - matrix)
  2  2.370e+03 1220    0.23   0.67     0    0     .5  2.13e-5  1.8  0.
  : (PTn25 - matrix)
  3  2.560e+03 865     1.42   1.84     0    0     .5  2.13e-5  1.8  0.
  : (TSw36 - matrix)
  4  2.350e+03 1150    0.61   1.20     0    0     .5  2.13e-5  1.8  0.
  : (CH3zc - matrix)
  5  2.580e+03 841     0.66   1.26     0    0     .5  2.13e-5  1.8  0.
  : (PP3vp - matrix)
0
:
Init
:
: i1  i2  j1  j2  k1  k2        p          t          sg          xg2
  pm          tm          sgm        xgm
:
   1   8   1   1   1   1  9.3E+04       20.0        0.99     0.0000E+00 9
.3E+04      20.0         0.75     0.0000E+00
   1   8   1   1   2  79  9.3E+04       25.0        0.99     0.0000E+00 9
.3E+04      25.0         0.75     0.0000E+00
   1   8   1   1  80  80  1.01289E+05  30.0        0.99     0.0000E+00 1
.0129E+05  30.0         0.09     0.0000E+00
   0   0
: ***************
:  Debug options
: ***************
Debug  1
0
```

3/13/00
WI

trans01

```
:
:
Recurrent
:
BCON 2
:
:itype  iface  i1  i2  j1  j2
   5    TOP    1   8   1  1
:timbc  qbcf  pbcf  tbcf  sgbcf  xabcf  emsivtf
:
: Flux equivalent to 10 mm/yr split b/w fracture and matrix
0.0  1.0e-8    93361.  20.  0.95  .0  0.0
0.0  1.316e-3  93361.  20.  0.95  .0  0.0
/
:itype  iface  i1  i2  j1  j2
 1  BOTTOM  1  8  1  1
:timbc  qbcf  pbcf  tbcf  sgbcf  xabcf  emsivtf
0.0  0.0    101325.  30.  0.0  0.0  0.0
0.0  0.0    101325.  30.  0.0  0.0  0.0
/
:
:Output   A=1
Output  P=1 L=1 G=1 T=1 Q=1 B=1 S=-1
:  isolv  newtnmn  newtnmx  north  nitmax  level
Solve 4      1        12      2     100      1
:
:AUTO-step  DPMXE    DSMXE  DTMPMXE  DP2MXe TACCEL   IAUTODT  FAC1
AUTO-step   1.0E+4   0.03    3        1.e4  1.0e-3      0      0
:
:TOLR TOLP  TOLS  TOLT  TOLP2  TOLM  TOLA  TOLE rtwotol  rmxtol   smxt
ol
Tolr   1.0e1 1.e-4 1.e-3 1.0e1 1.e-3 1.e-5 1.e-3
:
:Limit dpmx    dsmx dtmpmx dpamx    dtmn    dtmx   dtfac
LIMIT  1.e+5    .08    6.  1.e+5    1.e-8  1.e5   .334
:
RSTArt 1
:
:Plots 1 1 4
:377 385  386 393
Plots 1 1
:
STEADY[y] 1.0E-7 1.0E-07 1.0E-10
:
Ends
```

3/13/00
WI

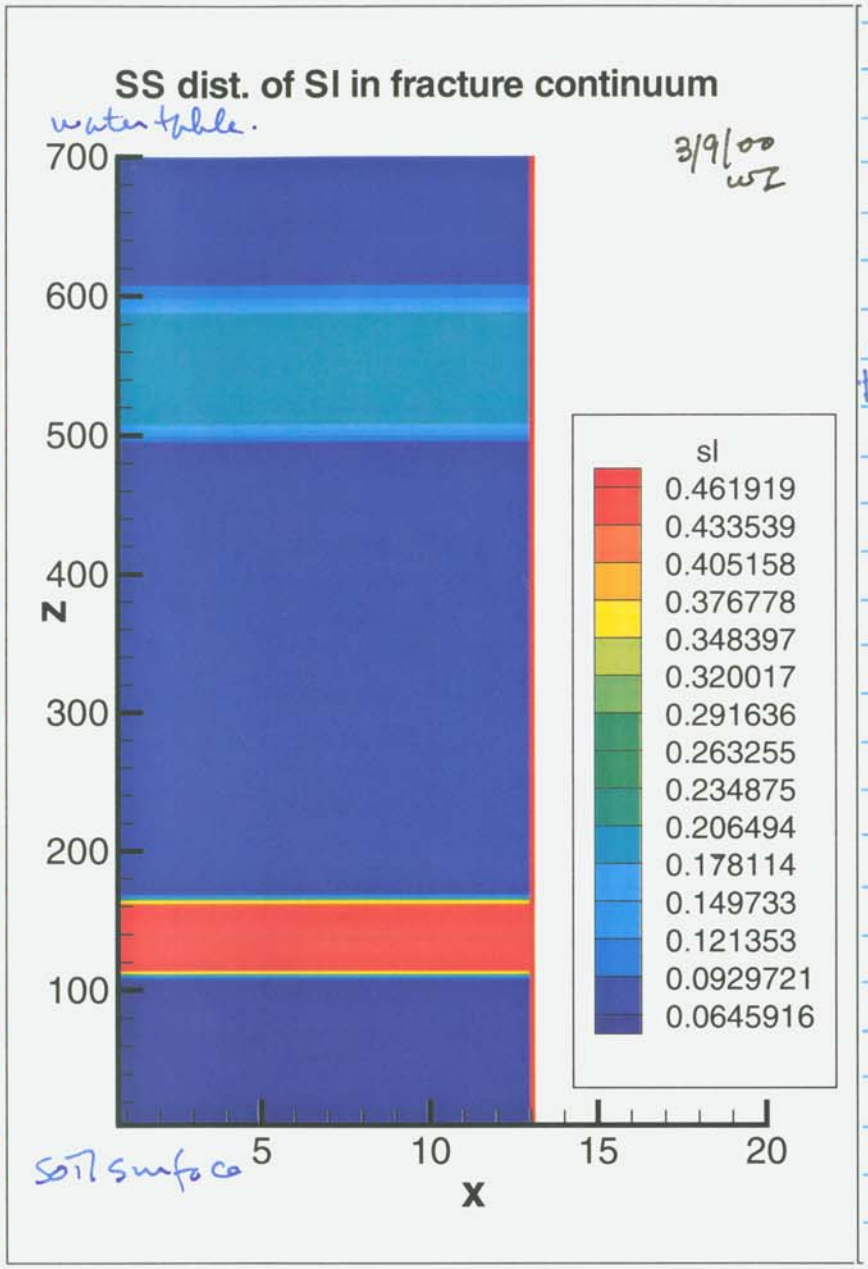

slightly higher S_l in fracture in the Ptn. WI

~~Ao~~ WI 3/9/2000

3-9-2000
note: contour interval differ from fracture & matrix!

TECPLOT – flipped over.

3/13/00
WI

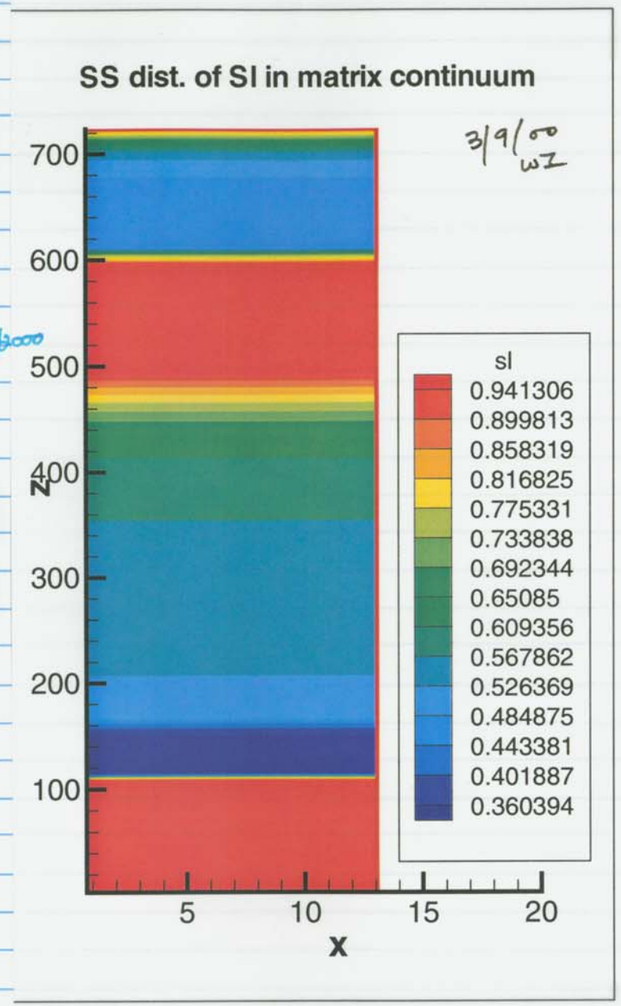

high matrix saturation ~~PTm~~ WI 3/13/2000

relatively low matrix saturation

TECPLOT – flipped over.

3/13/00
WI

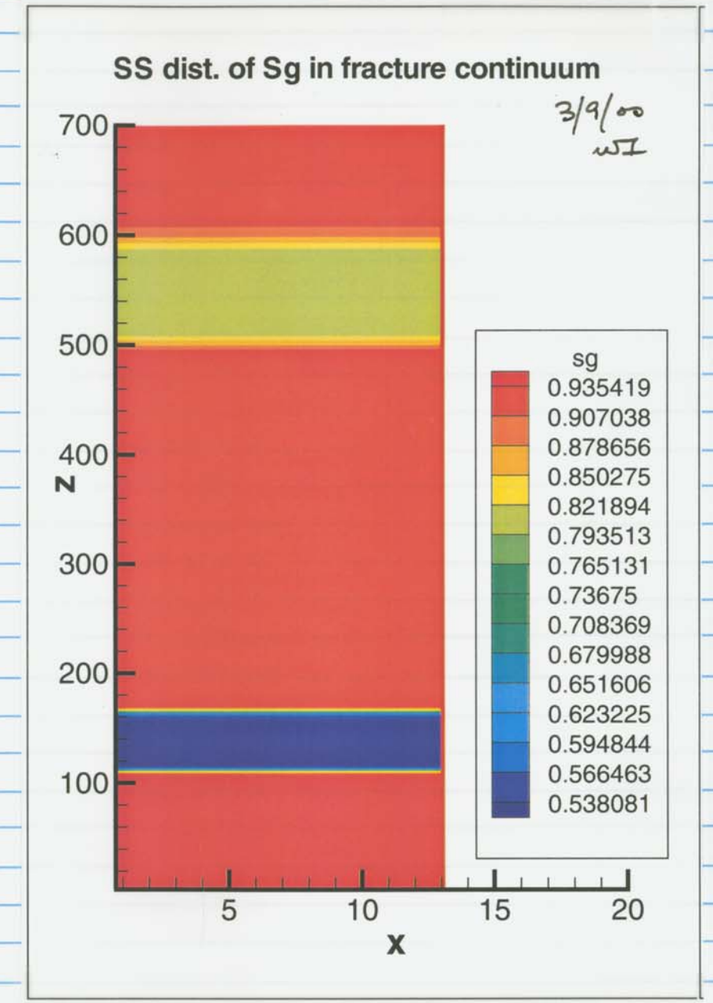

TECPLOT – flipped over

3/13/00
WI

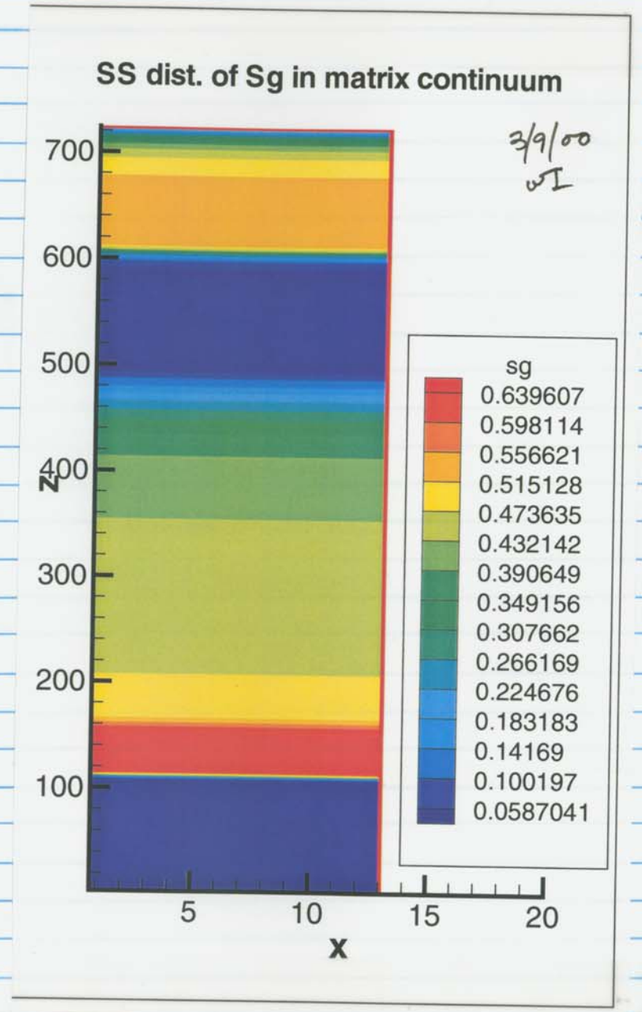

TECPLOT - flipped over

3/13/00
WI

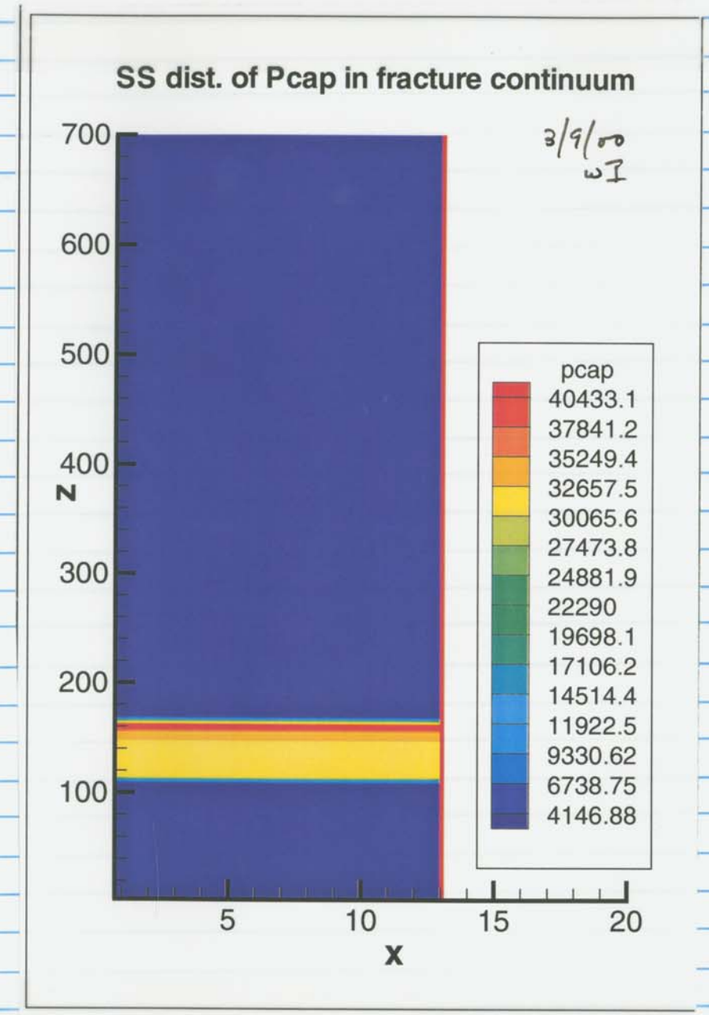

TECPLOT - flipped over

3/13/00
WI

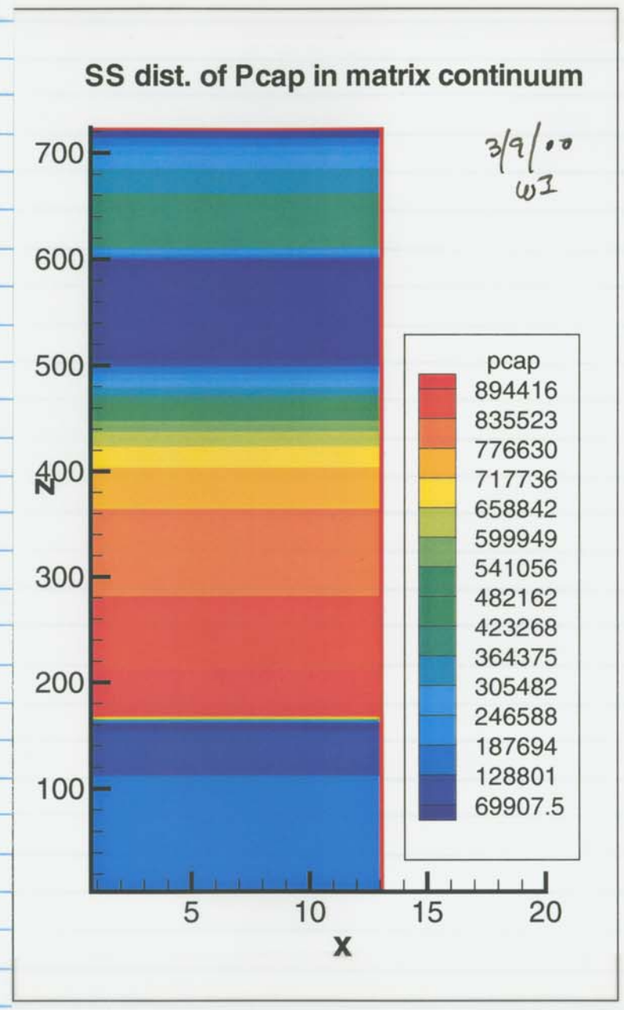

TECPLOT - flipped over

3/13/00
WI

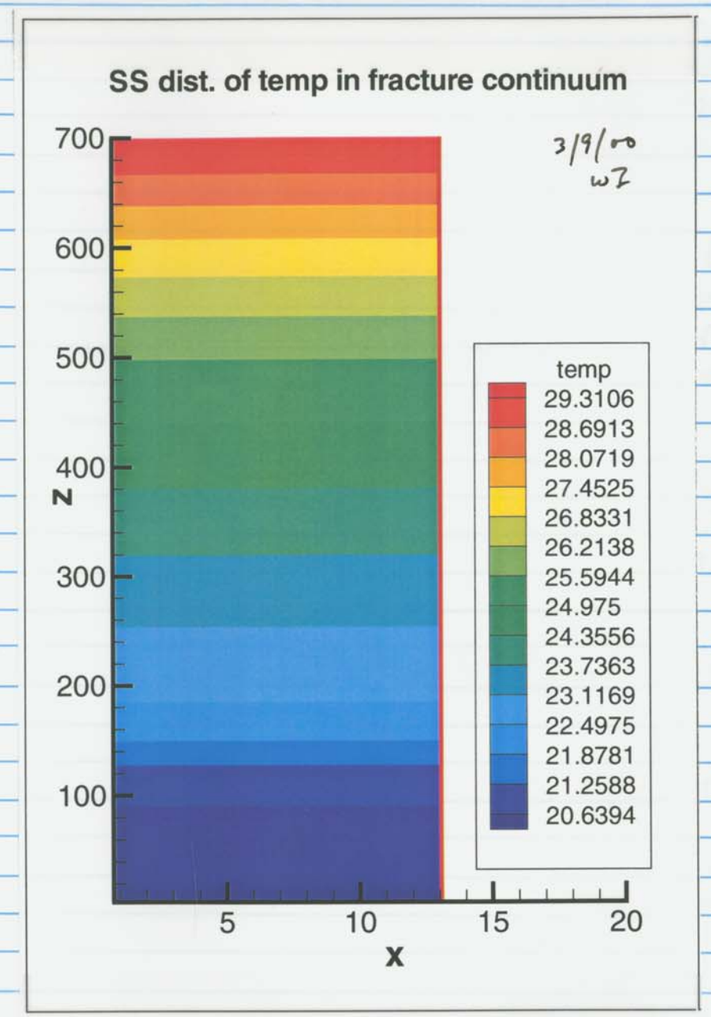

TECPLOT - flipped over

3/13/00
WI

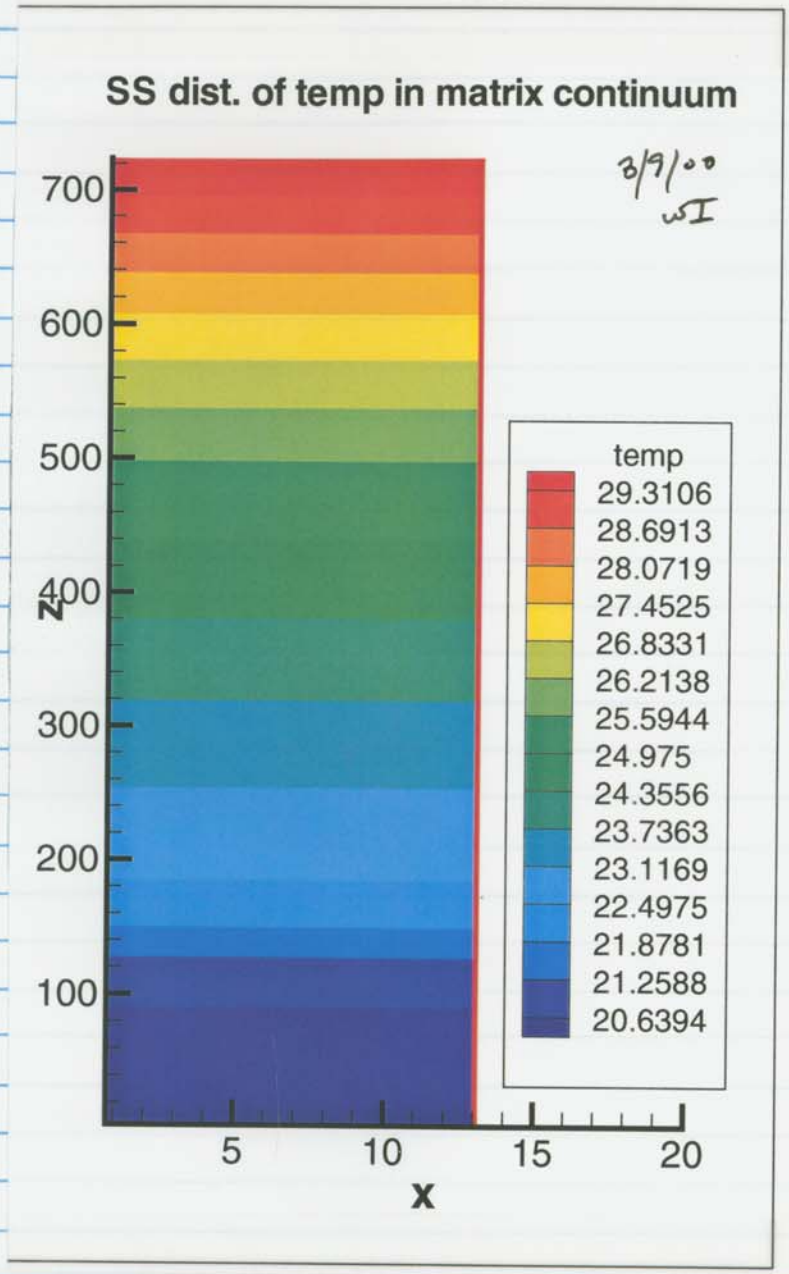

TECPLOT – flipped over

3/13/00
WI

PTn modeling · transcribed 3/13/00 WI

- infiltration is spatially variable
- higher than previously believed >10mm/yr.
- isotopes confirm rapid movement of water through the PTn — unsaturated zone in general to the repository level.

- water in PTn.
  - matrix/fracture saturations are lower
  - simulations using bounding values of various parameters (k, ϕ, α, q, etc.) to gain insight into flow behavior through the PTn.

- what data can help w/ model calibration?
  - estimates of permeability/porosity (single-hole / cross-hole tests)
  - pore water chemistry
  - infiltration tests in Alcove 4.
  - matrix parameters - lab core studies.

- Conceptual model of Montazer/Wilson (1984) for water flow in the unsat. zone
  - very little vertical flow (percolation) in the TSw
  - geochemical data contradicts this conceptual model

- lateral flow in the PTn may be an artifact of the numerical grid and choice of matrix/fracture props. used in modeling (Bodvarsson and Bandarrya, 1996 p.8)

DOE
- current preferred conceptual model is that while the PTn attenuates the spatial/temporal variability in infiltration, water moves through relatively rapidly through the PTn to the highly fractured TSw units through faults and associated fractured system (Bodvarsson et al 1997 p.29

DOE
→ evidence against PTn water attenuation
perched water at TSw/CHn contact dated by C-14 method at about 2,200 to 6,200 yrs. (Yang, Yu et al., p.78) are much younger than that could be accounted for by flow through the matrix porosity, lending credence to fast flow through fractures.

DOE
→ rapid flow may be occuring but the quantity of percolation flux is presumed to be small under current climatic conditions

notes from 12/29/1999
→ PTn unit characteristics.
Summary of USGS findings (circa 1996)
overlying
TCw – welded tuff
$k_a = 1.0\times10^{-12}\ m^2 \leftrightarrow 10.0\times10^{-12}\ m^2$ (1-D barometric press. analysis)
$= 0.3\times10^{-12}\ m^2 \leftrightarrow 50.0\times10^{-12}\ m^2$ (SH data)
↳ larger variance, lower min, larger max capturing local heterogeneity.

PTn – impeding layer to gas flow
subsurface monitoring of pneumatic pressures

major
Submits 1) nonwelded crystal-rich vitric submits of the Topopah Spring tuff.
2) Yucca Mtn. tuff.
3) Pah Canyon tuff
4) bedded tuff
5) non-welded crystal-poor vitric submit of the Tiva Canyon tuff.

3/13/00 WL

vitric submits
- very high matrix porosities 30-50%; sparsely fractured
- other bedded/nonwelded units 30-60%
  very high matrix porosities
- air filled porosities of PTn 15-35%
  diffusivity analysis (1D) $k_a = 0.1\times10^{-12}\ m^2 - 4.0\times10^{-12}\ m^2$
  air injection tests $k_a = 0.1\times10^{-12}\ m^2 - 3.0\times10^{-12}\ m^2$

α is low because of smaller k_a & larger ϕ

notes from 12/29/2000
Summary – In situ pneumatic pressure monitoring & boreholes in the North Ramp Study area.
UZ#4 } Pagany Wash
UZ#5 }
NRG#4 } crest of Azreal Ridge — drainage divide between Pagany Wash and Drill Hole Wash.
UZ-1
SD-9
NRG-7a
NRG#5
NRG-6
} Drill hole wash.
- thickness of PTn varies from 124 ft. (38m) to 276 ft (84m) in monitored boreholes
- variations in thickness alone do not appear sufficient to account for phase lag/attenuation
- suppression increases from east to west paralleling a trend of increasing saturation w/in the unit; decreasing thickness of TCw beneath Drill Hole Wash.

Notes 12/29/1999
PTn tends to attenuate barometric pressure fluc.
- attenuation greatest in the western portion of the study area (UZ-1); decrease to the south to southeasterly direction across the study area
- attenuation and lagging characteristics of the submits are different from one submit to another and the composite thickness of PTn is insufficient to uniquely account for differences in att./lag charac.

- potential causes of attenuation
  - lack of fracture connectivity (limited extent)
  - higher matrix porosity
  - higher water content

3/13/00 WL

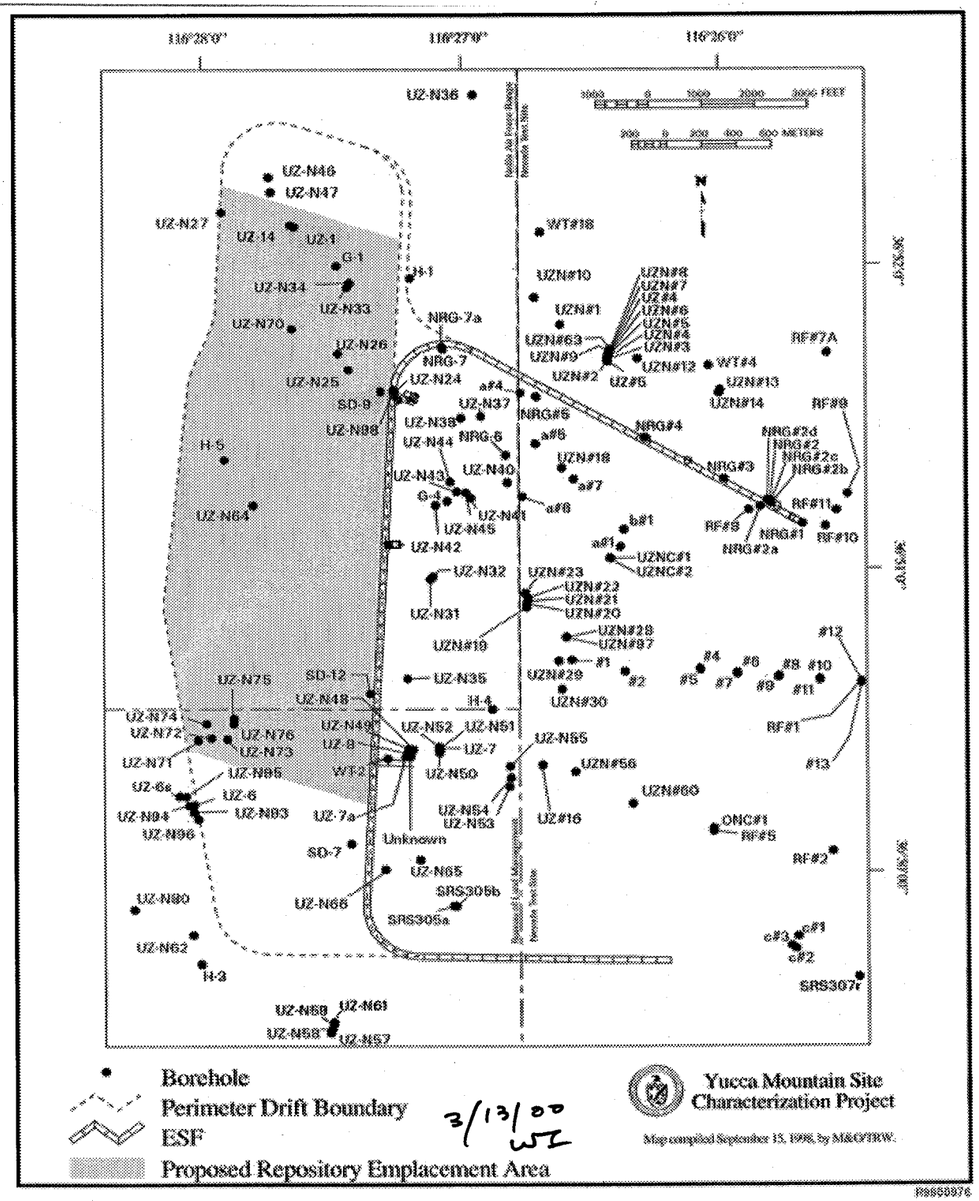

3/13/00
WI

notes from 12/29/2000 PTn unit transcribed 3/13/00 WI
USGS report 1996 LeCain

Single-hole testing in NRG-7a & NRG-6 – vertical holes –
$k_a \sim 3.5 \times 10^{-14} m^2 - 5.4 \times 10^{-11} m^2$ [borehole wall in NRG-7a in good shape

borehole wall in NRG-6 in poor condition through the PTn bedded units and much of the lower Topopah Spring crystal-poor upper lithophysal zone – these units could not be tested

several values of air permeability available in PTn
$0.12 \times 10^{-12} m^2 - 3.0 \times 10^{-12} m^2$
14 intervals mean $0.58 \times 10^{-12} m^2$

12/30/1999
In situ borehole monitoring (water potential/temperature)
5 boreholes UZ#4, #5 ~ Pagany Wash
UZ-1, NRG-7a, NRG-6 ~ Drillhole Wash

In situ water potential – thermocouple psychrometers
① these sensors measure the combined osmotic/matric potential but not the gravitational potential of liquid water contained in pore spaces of the rock matrix and openings of fractures
② psychrometers measure the liquid water potential in vapor phase by sensing the RH, or vapor pressure, of the formation rock gas that is in contact with water-filled pores and fracture openings
③ vapor concentration of rock gas is a function of the capillary tension exerted on a liquid water contained WI 3/13/00 within the largest filled openings of the media. As saturation increases, larger and larger pores become filled, capillary tension is reduced and the vapor concentration of the air in contact with the liquid water increases. (Brown, 1970)

Kelvin eqn. expresses the relationship between the water potential and vapor concentration or relative humidity $\left[\psi_w = \frac{RT}{V_w^o} \ln\left(\frac{e}{e_0}\right)\right]$
ψ_w = water pot.; R = univ. gas const.; T = temp.; V_w^o = molar vol.; e/e0 = RH; V_w

notes 12/20/1999

Modeling exercise 3/13/00 WI

4 cases

- homogeneous
- homogeneous with submits
- heterogeneous (entire unit) - synthetic (isotropic; statistically homogeneous / anisotropic statistically homogeneous)
  $\sigma^2 = 0.5; 1; 2-4$
- heterogeneous (with submits) - synthetic
  → statistics of individual submits are independent?
- multiscale continua? correlation scales that vary with distinct units
- Top BC Type 5 mixed BC
  Bottom BC Type 1 Dirichlet - prefer free drainage condition

notes from 1/24/2000

Questions

- is flow through pTn localized? or through few permeable pathways composed of small/large fractures that vary in its degree of interconnectivity
- Interplay of various size fractures and effect on flow behavior in the pTn → conduit for fast flow; permeability barrier.
- correlation between α and k_s.
- uniform pore size distribution parameter (n) assumes statistical homogeneity of fracture apertures
- is DKM necessary to model flux through pTn?
- what is the effect of lateral diversion (what factors affect diversion capacity?)
- episodicity of fluxes - stress periods
  - dry, wet, dry
  - memory effect?
- concentration of fluxes at a node vs. uniform application

3/13/00 WI

notes from 1/26/2000

Analytical Results - Capillary barrier context 3/13/00 WI

Ross (1990) WRR

- analytically, lateral diversion is a function of sat. hydraulic conductivity (K_s), the angle of incline, the flowrate, and the ambient pressure of the matrix.

→ conditions for capillary barrier with significant diversion capacity:

1. fine textured media must overlie coarse textured media.
2. linear sloping contact
3. low flux rate

Ross (1990)

→ developed analytical model (2D), tilted model

2 main assumptions

- flow is at steady state → is this not? transient episodic fluxes.
- downstream BC can drain infinitely
  ↳ what about at faults in fault gouges.

Factors not considered

- moisture gradients - which are present
- nonlinear phenomena ← finger instabilities
- heterogeneities at the contacts or gradual transitions between rock units
  ↳ heterogeneities can cause localized increases in saturation and thus reducing the diversion length.

→ Oldenburg and Pruess (1993) considered numerical models to simulate results of Ross (1990)

1/26/2000

notes from Flint (1998) on capillary barrier. 4892 rock core samples from 31 boreholes

reverse condition

→ coarser material overlying fine material can result in lateral diversion because the lower layer acts as a capillary barrier

→ occurs in the transition between the coarse grained pTn and the densely welded, fractured, crystal rich vitrophyre of the TSw (Tptrv1) under unsaturated conditions

notes from 1-26-2000

Model location

Data availability
- Alcove #5 (Thermal test facility)
- Alcove #4 (lower Paintbrush Tuff alcove)
- Alcove #3 (upper Paintbrush Tuff alcove)
- Alcove #2 (Bow Ridge Fault alcove)
- Alcove #1 (Upper Tiva Canyon Alcove)

- need data from single- / cross-hole pneumatic tests in various units and corresponding statistics to generate synthetic parameter field.

⇒ vertical hole (surface based) single-hole tests in NRG-7a & NRG-6
↳ some data from PTn.

⇒ matrix data including retention curves
UZ-14, N33, SD-9, NRG-7, NRG-6, N37/N38

⇒ PTn thickness varies between 30-100m
⇒ would one expect to see more fractures in zones where thickness varies quite significantly
(stress analysis of the unit?)

3/13/00
WI

Map of study site with locations of boreholes used to develop matrix properties data set and hydrogeological units

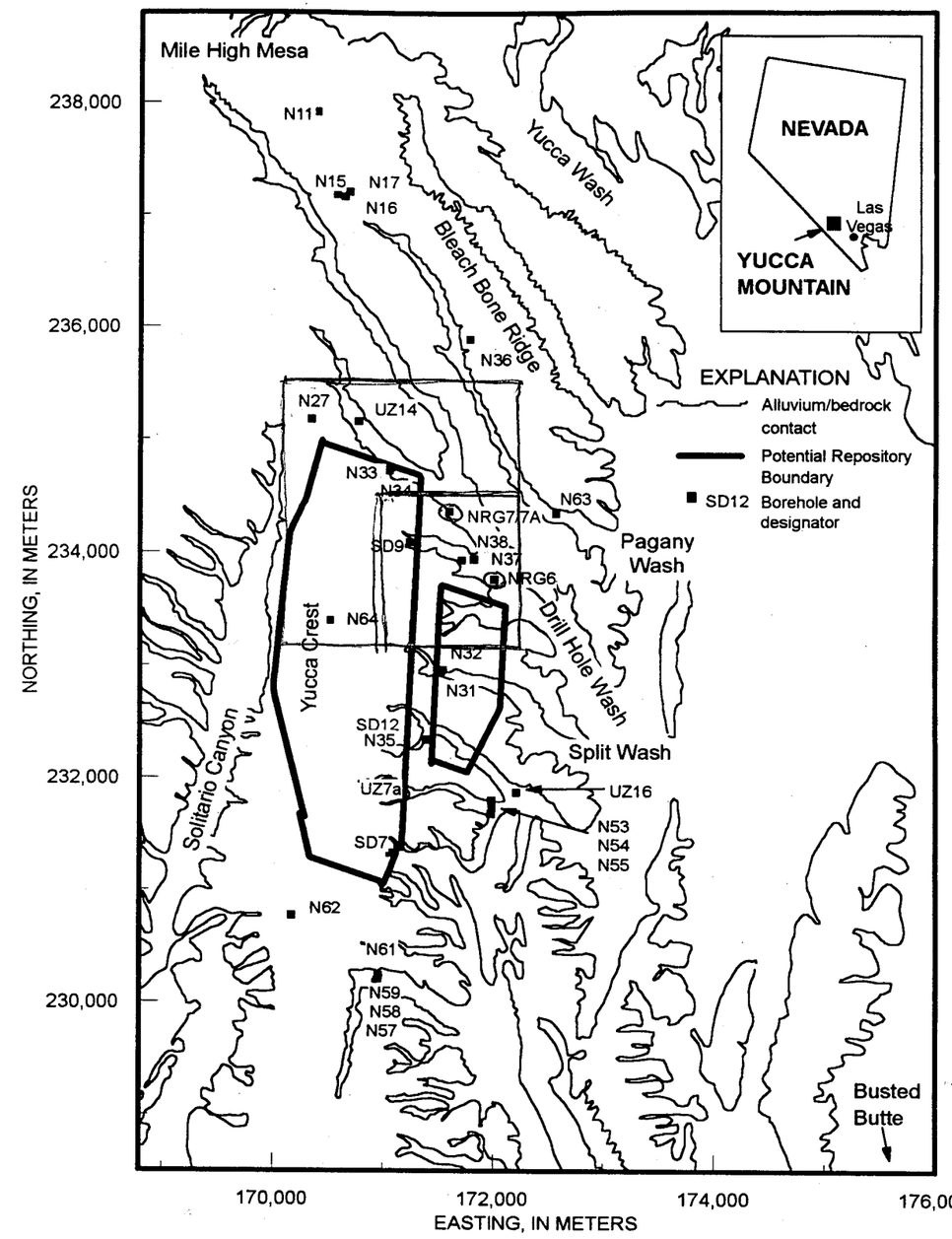

3/13/00
WI

notes from 2/17/2000

PTn modeling

Calculation of mass flux in fractures/matrix applied at top boundary

volumetric flux: $Q = VA$ $\quad Q = \frac{L^3}{T}$ ← velocity

$V = [L][T]^{-1}$

mass flux: $\rho Q \quad \frac{M}{L^3}\frac{L^3}{T} = MT^{-1}$ $\quad A = [L]^2$ - area

$\rho = [M][L^3]^{-1}$ density

mass flux per unit area $\rho q = \frac{\rho Q}{A} = \rho V$

Total flux per unit area $q_T = 10\ mm/yr.$

$\rho = 1000\ kg/m^3$

$$\rho q_T = 1000\frac{kg}{m^3}\cdot 10\frac{mm}{yr}\cdot\frac{1\,yr}{365\,d}\cdot\frac{1\,d}{86400\,s}\cdot\frac{1\,m}{1000\,mm} = 3.17\times10^{-7}\frac{kg}{m^2 s}$$

$\rho q_T = \rho q_m + \rho q_f$ $\quad q_m$ = flux in matrix, q_f = flux in fracture

Define:

k_m = permeability of matrix $\quad g$ = gravitational constant

K = hydraulic conductivity $\quad \mu$ = dynamic viscosity

K_m for Tiva Canyon matrix where $k_m = 5.4\times10^{-18}\ m^2$

$$K_m = \frac{(5.4\times10^{-18}\ m^2)(1000\ kg/m^3)(9.8\ m/s^2)}{(1.005\times10^{-3}\ kg/s\,m)} = 5.266\times10^{-11}\frac{m}{s}$$

under unit gradient conditions near saturation

$q = K(\theta)$ $\quad \theta$ = water content.

* under drier conditions $K(\theta) << K_{sat}$ 3/13/00 WI

$$\rho q_T = \rho(q_m + q_f) = 1000\frac{kg}{m^3}\left(5.266\times10^{-11}\frac{m}{s} + q_f\right)$$
$$= 3.17\times10^{-7}\frac{kg}{m^2 s} = \rho q_T$$
$$q_f = 2.643\times10^{-10}\frac{m}{s}$$

$$\rho q_f = 2.643\times10^{-7}\frac{kg}{m^2 s}$$

For METRA, fluxes applied for fractures must be divided by fracture porosity. (wolf) $\phi \sim [L]^0$

$$\frac{2.643\times10^{-7}\frac{kg}{m^2 s}}{2.33\times10^{-4}} = 1.134\times10^{-3}\frac{kg}{m^2 s}$$

notes from 3/10/2000

Boundary conditions

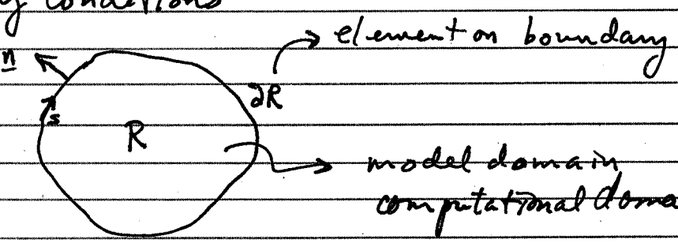

Type 1 i) Dirichlet condition $u = f$ on ∂R

Type 2 ii) Neumann condition $\frac{\partial u}{\partial n} = f$ or $\frac{\partial u}{\partial s} = g$ on ∂R

Type 5 iii) Mixed or Robin condition $\frac{\partial u}{\partial n} + bu = f$ $\quad b > 0$ on ∂R

	Type		
METRA	2,5	QBC ~ liquid flux rate	$[kg/m^2/s]$
Keywords.	5,1	PBC ~ gas phase pressure at designated surface	$[Pa]$
	2,1	TBC ~ temperature at designated surface	$[°C]$
	5,1	SGBC ~ gas phase saturation at designated surface	$[1]$

3/13/00 WI

notes from 3/13/2000

Questions

① How many fractures are active/conducive to flow
1) at the surface – distribution?
2) at some depth – channelization
3) at the repository horizon

② Compare distribution of fractures near the surface (50m) and at depths ↔ is this going to be a useful exercise?

Initially began with a 3D model but had difficult time with mass balances; scaled back to 2D model for now. → 3m x 3m blocks
→ model 25 x 25 = 625 nodes; structured grid
Directories → earlier results are not good
tweak parameters until M.B becomes better.
2dptn – 2 cases Case 1 Type 5 BC top
case 2 Type 2 BC top
mass balance not very good

Test cases

2dptn2 – rerun of 2dptn – not much change
2dptn3 – 2 cases; changed convergence tolerance
2dptn4 – 2 cases; increased flow rate at top boundary from 10 mm/yr – 100 mm/yr.
2dptn5 – low flow rate 10 mm/yr
decoupled problem.
2dptn6 – prescribed flux only at one node at the right boundary
2dptn7 – prescribed flux at node 13 top boundary (coupled) 100 mm/yr.
debra – original file worked on by D. Hughson → & checked
debra2 – changed top boundary prescribed gas saturation from 0.95 → 0.85 to match steady state results from type 2 BC at the top. 3/13/00 WI

notes from 3/16/2000

PTn modeling
directory
2dptn8 – point prescribed flux at node 13 top boundary (coupled)

More realistic case

2dptn9 – uniform prescribed flux at top boundary (type 5)
– fix saturation of gas 0.95
– initial gas saturation 0.98 instead of 0.99
how to enter this? – bottom boundary pressure 1 bar capillary pressure
– top & bottom temperature at 20°C try to maintain isothermal conditions

2dptn10 – similar to 2dptn8 but IC/BC
low flux revised as in 2dptn9

2dptn11 – " " 2dptn7 " "
high flux

2D model

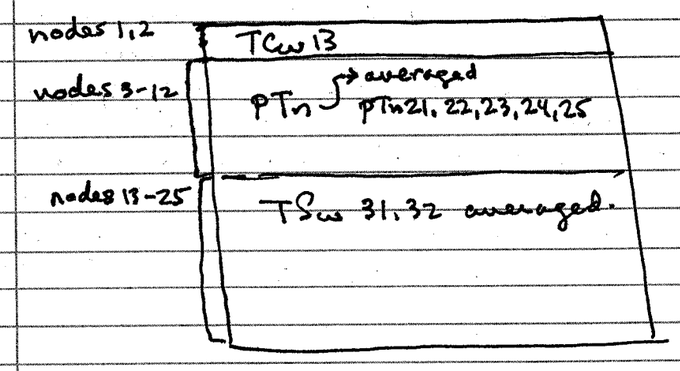

3/16/00 WI

3/16/2000

Model Objectives

① Run 3 layer model with type 5 B.C. at top until steady-state
3 flux rates – 10 mm/yr
– 100 mm/yr
– 250 mm/yr.

② Decrease grid block sizes by factor of 10 and run fine grid simulations (also discretization effects on results.
→ could not accomplish as dimension in sourcecode is too small

③ use steady-state results from 10 mm/yr uniform application case to conduct sim. involving (pulse type?) focused infiltration

④ check results again with fine grid

⑤ Incorporate 5 sublayers in pTn, and 3 sublayers in TSw.

⑥ incorporate heterogeneity in fine grid? coarse grid?

→ plot fluxes – matrix, fracture, between matrix-fracture
– saturation
– capillary pressures

→ compare results with field data – saturation
– capillary pressures?
– temperature
– relative humidity
↳ explain discrepancies (model results)

→ tie into shallow infiltration / seepage into drifts

→ discuss importance of model results (intermediate scale) to large-scale model results.

3/16/00 WI

3/17/2000

Flux calculation for 250 mm/yr case

$$250\ \frac{mm}{yr} \rightarrow 7.927\times10^{-6}\ \frac{kg}{m^2 s}$$

$$\frac{\rho q_f}{\phi} = \frac{7.875\times10^{-6}\ \frac{kg}{m^2 s}}{7.05\times10^{-5}} \approx 1.117\times10^{-1}\ \frac{kg}{m^2 s}$$

this assumes

$$\rho q_T = \rho(q_f + q_m) = 1000\ \frac{kg}{m^3}\left(q_f + 5.266\times10^{-11}\ \frac{m}{s}\right) = 7.927\times10^{-6}\ \frac{kg}{m^2 s}$$

$$\rightarrow q_f = 7.875\times10^{-9}\ \frac{m}{s}$$

and

$$\rho q_T = 1000\ \frac{kg}{m^3} \cdot 250\ \frac{mm}{yr} \cdot \frac{1\,yr}{365\,d} \cdot \frac{1\,d}{86400\,s} \cdot \frac{1\,m}{1000\,mm} = 7.927\times10^{-6}\ \frac{kg}{m^2 s}$$

– Type 5 condition at the top requires
QBC ($kg/m^2/s$) – what we just calculated
PBC (Pa) – air pressure at the elevation 1375 m
TBC (°C) – 20°C
SGBCF – 0.95

3/17/00 WI

PTn modeling
Pressure variation with elevation

At sea level, the standard atmospheric pressure is 101.3 kPa and the temp. is 288 K.

Atmosphere is divided into troposphere and stratosphere
troposphere - layer between sea level and 10,769 m, the temperature decreases linearly with increasing elevation at a lapse rate of 6.50 K/km.
stratosphere - begins at the top of the troposphere and extends to 32.3 km. In the stratosphere the temperature is constant at -55°C.

From Robertson/Crowe p. 41
Engineering Fluid Mechanics

Pressure at 1300 m, assuming sea level absolute press. to be 101.3 kPa and absolute temp. to be 15°C

$$p = p_0 \left[\frac{T_0 - \alpha (z - z_0)}{T_0} \right]^{g/\alpha R}$$

$p_0 = 101{,}300\ N/m^2$, $T_0 = 273 + 15 = 288\ K$
$\alpha = 6.50 \times 10^{-3}\ K/m$
$z - z_0 = 1300\ m$ and $g/\alpha R = 5.259$

at 1300 m $\quad p = 101.3 \left(\frac{288 - 6.50 \times 10^{-3} \times 1300}{288} \right)^{5.259} = 86.6\ kPa$

$\boxed{86615\ Pa}$

at 1375 m $\quad p = 101.3 \left(\frac{288 - 6.50 \times 10^{-3} \times 1375}{288} \right)^{5.259} = 85.8\ kPa$

$\boxed{85829\ Pa}$

3/17/00 WI

notes from 3/17/2000

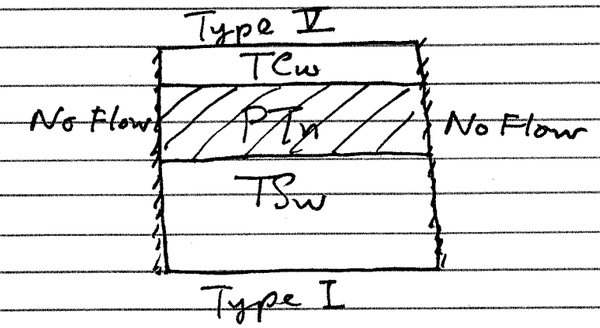

TBC at both top & bottom boundaries kept constant so simulation runs in isothermal mode

notes from 3/22/2000

DOE ~ site scale model with homogeneous units (Wu et al. 1999)
inverse modeling; air injection test data
USGS ~ attempted flow modeling through PTn (Hoyer et al. 1996)
DOE ~ also constructed drift scale numerical model (Birkholzer 1999)

do we know this; have a good handle of this?

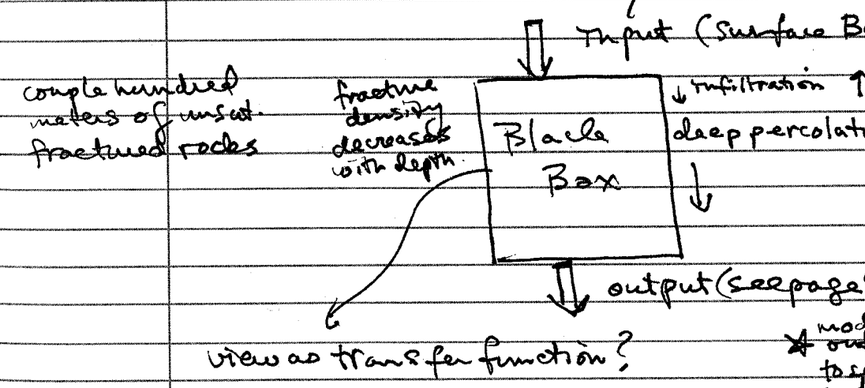

* model output from early time needed to see water movement in fractures and interaction with matrix
* This fracture/matrix interaction is key to understanding pulse water movement from the soil surface to repository horizon.

1) Process level modeling
2) Transfer function approach.

3/17/00 WI

notes from 3/22/2000

cases being run

2dptn12 – use IC from 2dptn10 low flux case
– do point infiltration at larger rate 250mm/yr
– write output at early time

3/22/00 WI

3/23/2000 2dptn13 (250x250) dimension of executable 68500 program not large enough
– talk to Scott Painter about increasing
– recompile program.

2dptn14 repeat of 2dptn9 uniform flux case
75x75 nodes = 5625 nodes

2dptn15 repeat 2dptn10 point flux (38th node) at top boundary 10mm/yr

2dptn16 75x75 repeat of 2dptn11 point flux at top boundary 250mm/yr.

Addition of monitoring points for key variables

	75m x 75m	3m blocks	
layer 1	1–2	(6m)	
layer 2	3–12	(30m)	
layer 3	13–25	(39m)	
		75m.	

	75m x 75m	0.3m block	
layer 1	1–20	(20)	(6m)
layer 2	21–120	(100)	(30m)
layer 3	121–250	(130)	(39m)

3/23/00 WI

Node number:

$$m = i + (j-1)nx + \cancel{(k-1)nxny}$$ only for 3D

for nodes 2, 6, 11, 17 from top boundary in the center $i=13$.

3/23/00 WI

3/24/00 Example calculation monitoring points in MF

$$m = i + (j-1)nx + \cancel{(k-1)nxny}$$

$nx = 25$ $i = 13$ → center node

$j=2$ $m = 13 + (2-1)(25) = 38$

$j=6$ $m = 13 + (6-1)(25) = 138$

$j=11$ $m = 13 + (11-1)(25) = 263$

$j=17$ $m = 13 + (17-1)(25) = 413$

Questions:
– How can large scale model (e.g., site scale model) with its coarse grid resolve phenomena occuring at much finer scale? Subgrid phenomena may be diffused

Issues: Lateral diversion in PTn
comparisons with analytical solution
Ross (1990) – analytical
Oldenburg/Pruess (1993) – numerical
Moyer et al. (1996) – numerical
Yeh et al. – numerical.
Birkholzer and Tsang (1996) – numerical

3/24/00 WI

3/27/00

3 cases
- previous runs - practice runs to test model and to enrich my understanding of the code Metra.

Consider - point infiltration 10 mm/yr
100 mm/yr
250 mm/yr.

2dptn 17 cases
Refine model runs

3/30/00 Fluxes at top boundary

Model Parameter → $q = -K(\theta)\left(\frac{\partial \psi}{\partial z} + 1\right)$

at large time

$q = -K(\theta)$

Set gas saturation to be high ($S_g \cong 0.90$) initially prior to infiltration because of entrapped water (capillary water)

Write-up ~ discussed with R. Fedors
Issues/outline
Flow through the PTn.
Evidence for fast flow
Evidence for flow dimension, capillary barrier
Two phase flow modeling through the PTn.
Model description

3/30/00
WI

Model description
- uniform infiltration at top boundary vs. point - focused infiltration

properties (material)
grid description
Initial/boundary conditions
Run results to steady state

Results 1) uniform flux case
2) Focused infiltration/flux cases
10 mm/yr
100 mm/yr
250 mm/yr.

Discussion

Plots

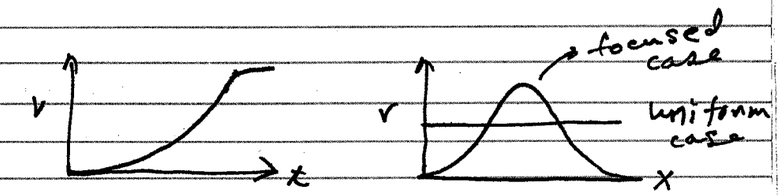

3/30/00
WI

4/4/2000

Problem: What fluxes to assign at top boundary of the model

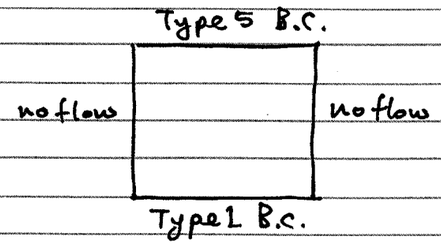

→ no data on boundary condition

→ DOE estimates keep on changing!

→ How do I put in enough mass of water into fracture / matrix?

→ put all flux in fractures as the k is much higher than the matrix k and let the computer code METRA compute fluxes within the matrix

Example ~ 2d ptn 9 run

$\rho q_m \approx 5.266 \times 10^{-8}$ kg/m²/s Insignificant

$\rho q_f \approx 3.749 \times 10^{-3}$ kg/m²/s

$\rho q_T \approx 3.749053 \times 10^{-3}$ kg/m²/s

→ Rerun 2d ptn 9 subdirectories ic-bc

2d ptn 17 c1
c2
c3

adjusted Ic/Bc

$S_{g_{matrix}} = 0.25 \rightarrow 0.75$

4/4/00 WI

4/27/2000 Velocities in METRA

Input into METRA

→ fractures $\frac{\rho q_f}{\phi}$

→ computed velocities $\frac{\rho q_f}{\phi}$ ⇝ vlfz ↗ METRA variable

→ post processed using script $\frac{\rho q_f}{\phi} \cdot \phi = \rho q_f$

Plot ~~Compute~~ velocities
WI 4/27/00

$\vec{v} = v_x \hat{i} + v_z \hat{k}$

$v_m = |\vec{v}| = \sqrt{v_x^2 + v_z^2}$

$v_{xm} = \frac{v_x}{v_m}$ $v_{zm} = \frac{v_z}{v_m}$ normalized vel.

$$|v| = \sqrt{\frac{v_x^2}{v_m^2} + \frac{v_z^2}{v_m^2}} = \frac{\sqrt{v_x^2 + v_z^2}}{\sqrt{v_m^2}} = \frac{v_m}{v_m} = 1$$

---

subdirectories ic-bc.

2d ptn 17 c1 ~ c3 modeling results

3 layers, top 6m: TCw, next 30m: PTn, last 39m: TSw

25x25 nodes 3m x 3m blocks

Model domain: 75m x 75m.

4/27/00 WI

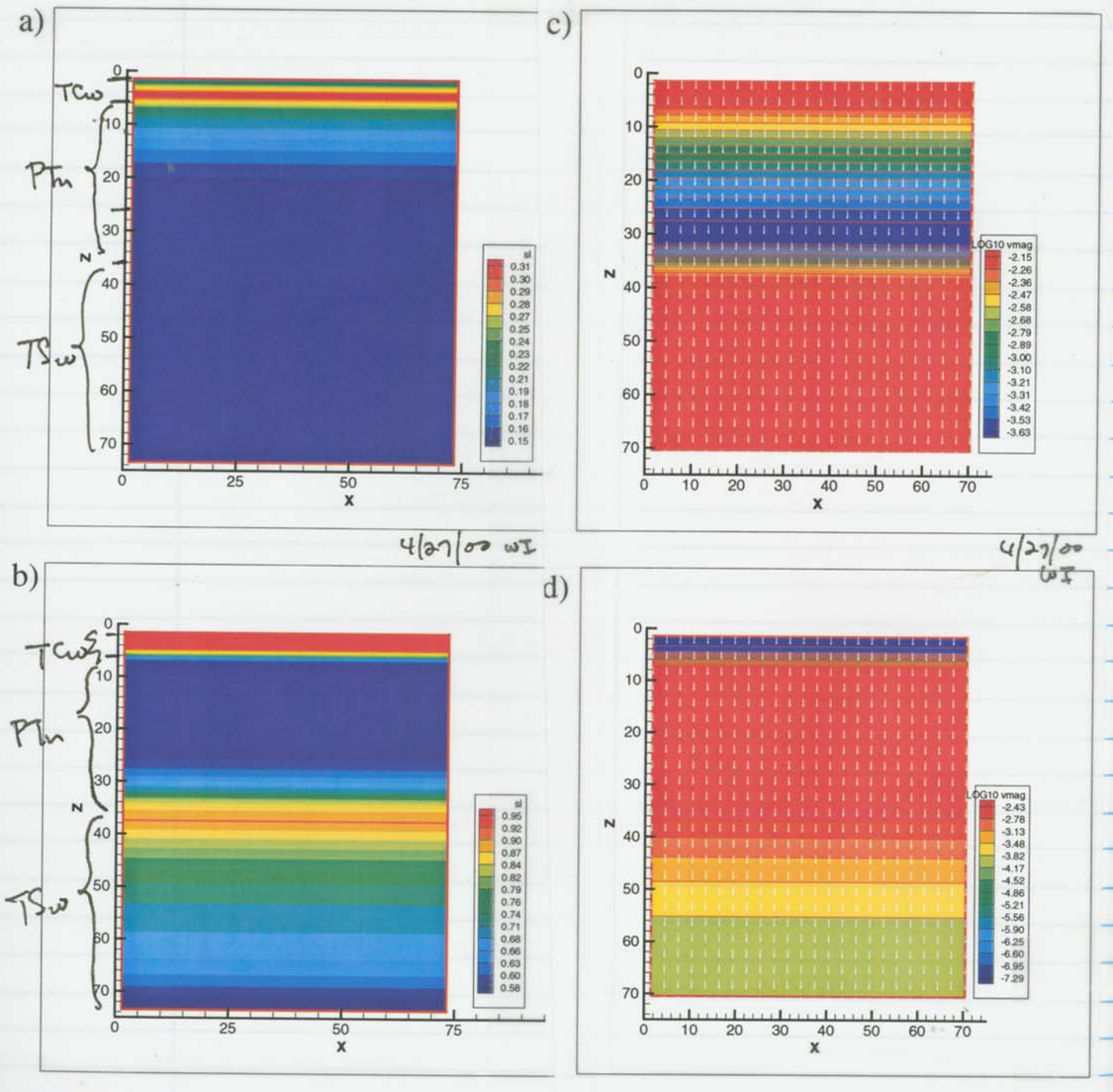

4/27/00 WI

Case 1 DCM modeling results – Steady state distribution of a) saturation in the fracture continuum; b) saturation in the matrix continuum; c) fluxes in fracture continuum; and d) fluxes in matrix continuum

4/27/00 WI

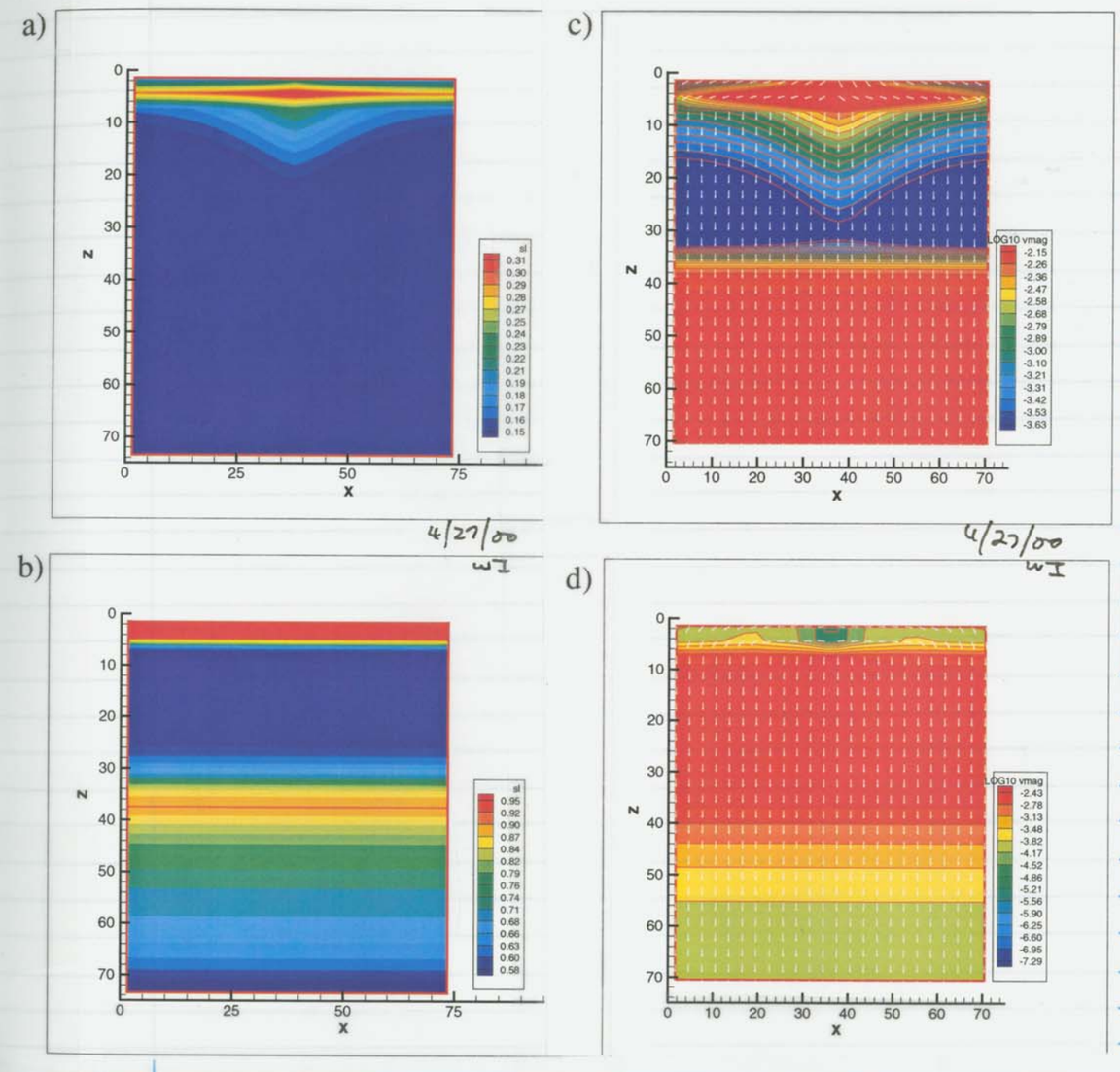

4/27/00 WI

Case 2: Uniform flux at centernode on top boundary. Distribution at 0.5 yr. of a) Fracture Sat.; b) Matrix Sat.; c) Fracture fluxes and d) Matrix fluxes

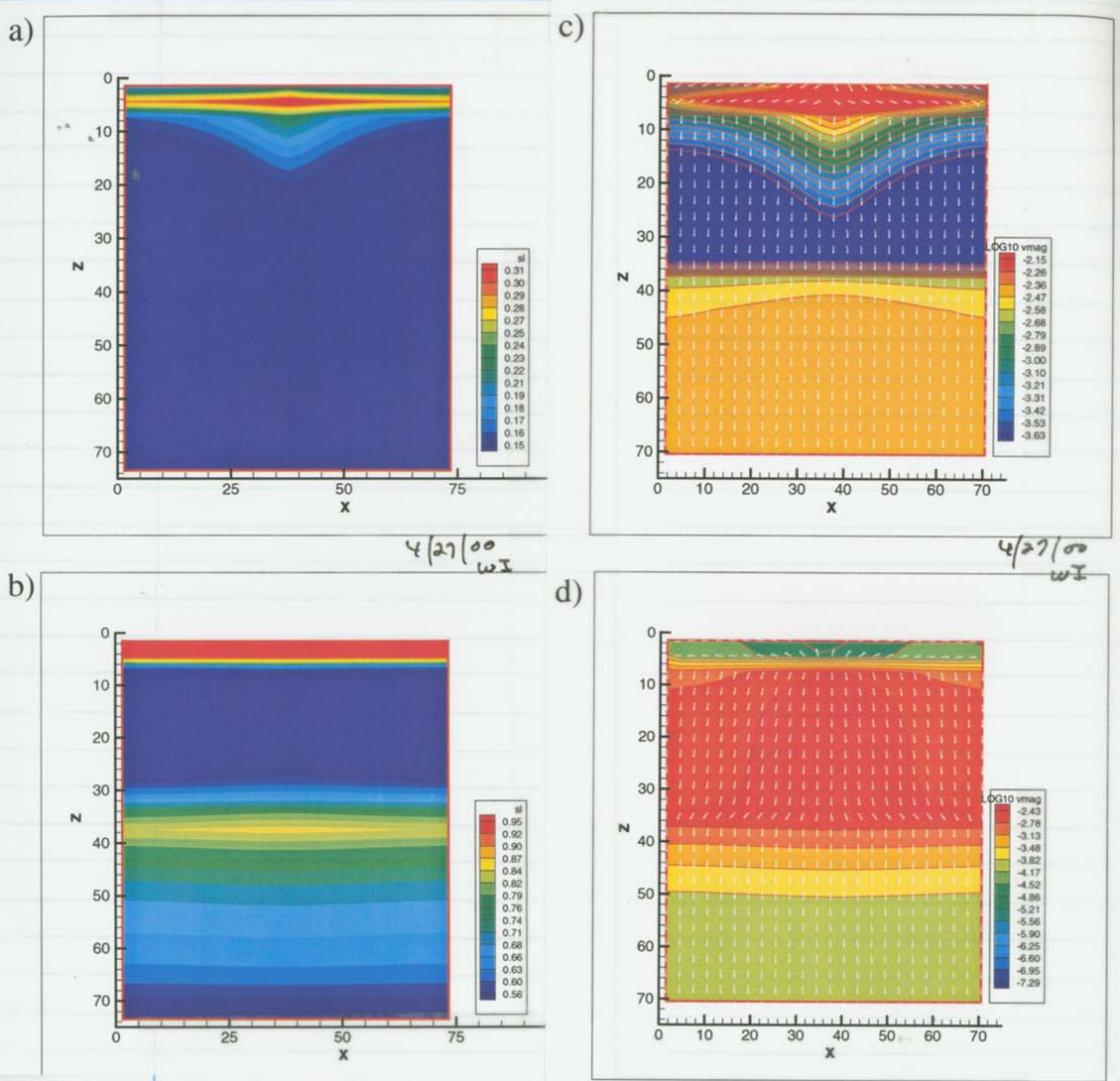

4/27/00 WI

4/27/00 WI

Case 2 results - Steady state distribution

4/27/00 WI

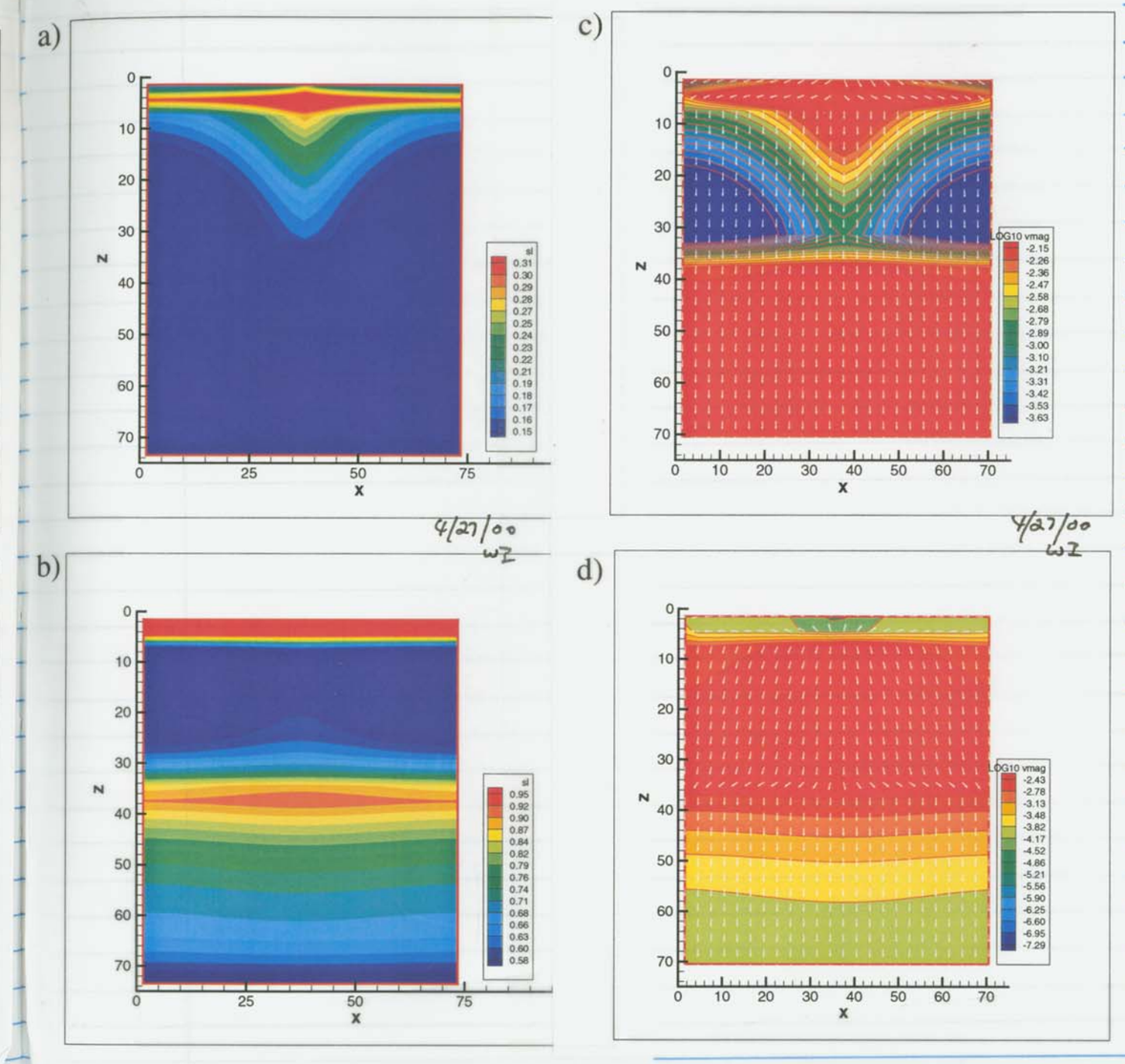

4/27/00 WI

4/27/00 WI

Case 3 : Steady state results

4/27/00 WI

Matrix and Fracture Parameter Sets for the DKM Base Case (Present Infiltration)
DTN: LB971100001254.002

Model Layer	Matrix Perm. k_m [m^2]	Matrix Porosity ϕ_m (-)	Matrix Alpha α_m (Pa^{-1})	Matrix VG m m_m (-)	Matrix Res. Sat. S_{lrm} (-)	Matrix Satia.Sat. S_{lsm} (-)
Tcw13	**4.90E-17**	**0.14**	**6.46E-07**	**0.427**	**0.33**	**1.00**
Ptn21	3.09E-14	0.369	3.80E-05	0.231	0.10	1.00
Ptn22	3.02E-15	0.234	8.71E-06	0.488	0.14	1.00
Ptn23	8.32E-14	0.353	4.57E-05	0.287	0.17	1.00
Ptn24	1.15E-13	0.469	4.27E-05	0.349	0.10	1.00
Ptn25	2.46E-13	0.464	1.95E-04	0.279	0.10	1.00
Ptn	**4.66E-14**	**0.378**	**4.17E-05**	**0.327**	**0.12**	**1.00**
Tsw31	4.90E-17	0.042	1.00E-05	0.237	0.11	1.00
Tsw32	2.75E-16	0.146	2.29E-05	0.273	0.04	1.00
Tsw	**1.16E-16**	**0.094**	**1.51E-05**	**0.255**	**0.08**	**1.00**

Model Layer	Vertical Fracture Perm. k_f (m^2)	Horizontal Fracture Perm. k_f (m^2)	Fracture Porosity ϕ_f (-)	Fracture Alpha α_f (Pa^{-1})	Fracture VG m m_f (-)	Fracture Res. Sat. S_{lrf} (-)	Fracture Satia.Sat. S_{lsf} (-)	Fracture Frequency f (m^{-1})	Frac.-mat. Conn. Area Mod. Fac. X_{fm} (-)
Tcw13	**2.82E-12**	**2.40E-13**	**7.05E-05**	**9.12E-05**	**0.492**	**0.01**	**1.00**	**1.27**	**4.90E-04**
Ptn21	5.25E-13	5.25E-13	4.84E-05	1.10E-03	0.492	0.01	1.00	0.87	1.10E-01
Ptn22	1.95E-13	1.95E-13	4.83E-05	1.82E-03	0.492	0.01	1.00	0.29	7.08E-01
Ptn23	2.57E-13	2.57E-13	1.30E-04	3.39E-03	0.492	0.01	1.00	0.29	6.92E-01
Ptn24	6.17E-14	6.17E-14	6.94E-05	9.33E-04	0.492	0.01	1.00	0.63	4.79E-01
Ptn25	7.76E-14	7.76E-14	3.86E-05	1.95E-04	0.279	0.01	1.00	0.65	4.79E-01
Ptn	**1.66E-13**	**2.23E-13**	**6.06E-05**	**1.04E-03**	**0.449**	**0.01**	**1.00**	**0.55**	**4.94E-01**
Tsw31	1.07E-11	1.00E-12	8.92E-05	3.98E-05	0.481	0.01	1.00	1.10	5.01E-01
Tsw32	1.51E-11	7.08E-13	1.29E-04	9.33E-05	0.488	0.01	1.00	1.01	2.88E-05
Tsw	**1.27E-11**	**8.54E-13**	**1.07E-04**	**6.09E-05**	**0.485**	**0.01**	**1.00**	**1.06**	**2.51E-01**

Model Layer	Fracture Perm. k_f (m^2)	Fracture Porosity ϕ_f (-)	METRA Fracture Perm. k_f/ϕ_f (m^2)
Tcw13	**2.82E-12**	**7.05E-05**	**4.00E-08**
Ptn21	5.25E-13	4.84E-05	1.08E-08
Ptn22	1.95E-13	4.83E-05	4.04E-09
Ptn23	2.57E-13	1.30E-04	1.98E-09
Ptn24	6.17E-14	6.94E-05	8.89E-10
Ptn25	7.76E-14	3.86E-05	2.01E-09
Ptn	**1.66E-13**	**6.06E-05**	**2.74E-09**
Tsw31	1.07E-11	8.92E-05	1.20E-07
Tsw32	1.51E-11	1.29E-04	1.17E-07
Tsw	**1.27E-11**	**1.07E-04**	**1.18E-07**

4/27/00

Model parameters derived from DOE - DKM Base case parameter sets. Numbers in bold used for simulations in cases 1-3.
from CRWMS M&O C 1998 TSPA-VA Technical Basis Ch.2 - Unsaturated Zone Flow

4/27/00

Table 1: Model parameters for cases 1 through 3.

	Geologic Unit		
	TCw	PTn	TSw
DCM Parameters			
SIGMAF	7.05×10^{-5}	6.06×10^{-5}	1.07×10^{-4}
AREAMOD	4.90×10^{-4}	4.94×10^{-1}	2.51×10^{-1}
van Genuchten Parameters			
Residual Saturation (matrix)	0.33	0.12	0.08
Residual Saturation (fracture)	0.01	0.01	0.01
m (matrix)	0.43	0.33	0.26
m (fracture)	0.49	0.45	0.49
α (matrix) (Pa^{-1})	6.46×10^{-7}	4.17×10^{-5}	1.51×10^{-5}
α (fracture) (Pa^{-1})	9.12×10^{-5}	1.04×10^{-3}	6.09×10^{-5}
Flow Parameters			4/27/00 WZ
k (matrix) (m^2)	4.90×10^{-17}	4.66×10^{-14}	1.16×10^{-16}
k (fracture) (m^2)	4.00×10^{-8}	2.74×10^{-9}	1.18×10^{-7}
φ (matrix)	0.14	0.38	0.09
φ (fracture)	1.0	1.0	1.0

4/27/00 WZ

Table 2: Initial conditions for case1.

	Top layer	Model Interior	Bottom layer
For defined region			
P [Pa]	85824	85824	86615
T [°C]	20.0	20	20
SG [fraction]	0.98	0.98	0.98
XG [fraction]	0	0	0
Matrix			4/27/00 WI
PM [Pa]	85824	85824	86615
TM [°C]	20	20	20
SGM [fraction]	0.75	0.75	0.75
XAM [fraction]	0	0	0

4/27/00 WI

Table 3: Boundary conditions for cases 1 through 3.

	case 1	**case 2**	**case 3**
Top boundary			
Type	5	5*	5*
QBC (matrix) [kg/m^2/s]	0	0	0
QBC (fracture) [kg/m^2/s]	3.75×10^{-3}	4.42×10^{-2}	1.12×10^{-1}
PBC (matrix) [Pa]	85824	85824	85824
PBC (fracture) [Pa]	85824	85824	85824
TBC (matrix) [°C]	20	20	20
TBC (fracture) [°C]	20	20	20
SGBC (matrix)	0.95	0.95	0.95
SGBC (fracture)	0.95	0.95	0.95
Bottom boundary			4/27/00 WI
Type	1	1	1
QBC (matrix) [kg/m^2/s]	0	0	0
QBC (fracture) [kg/m^2/s]	0	0	0
PBC (matrix) [Pa]	86615	86615	86615
PBC (fracture) [Pa]	86615	86615	86615
TBC (matrix) [°C]	20	20	20
TBC (fracture) [°C]	20	20	20
SGBC (matrix) [fraction]	0.10	0.10	0.10
SGBC (fracture) [fraction]	0.90	0.90	0.90

*node 13 only; nodes 1 through 12 and 14 through 25 are set to no flow conditions.

Uncertainty in boundary conditions
what values to use?

4/27/00 WI

4/27/00
WI

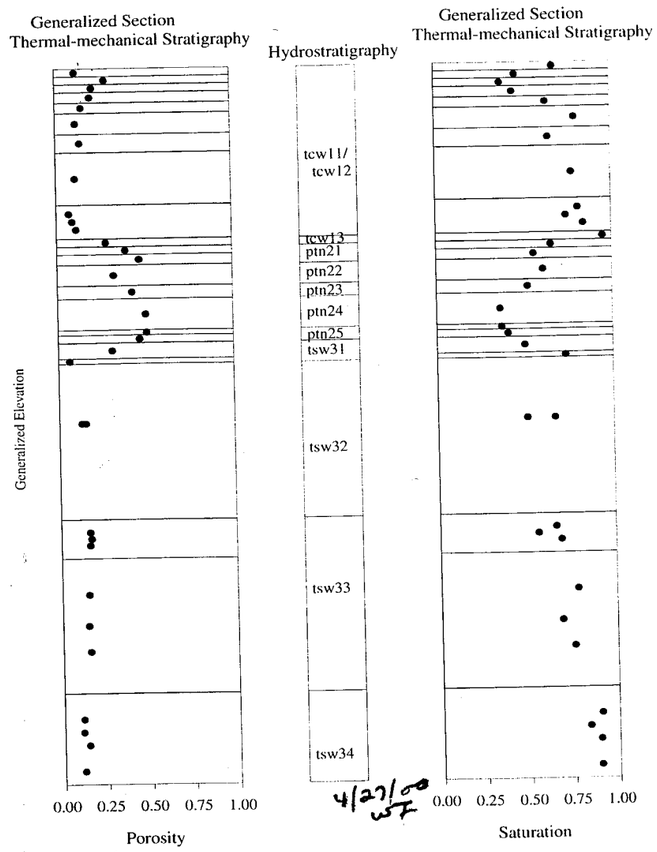

4/27/00
WI

degree of welding controlling retention, distribution of moisture

Observations

→ Saturations agree well with matrix results.

→ Need capillary pressures from units to compare model / field situation

→ Boundary conditions are uncertain (values used in)

→ Physics makes sense

→ Need to length top layer so boundary effects do not affect fluxes at PTn/TCw contact

4/27/00
WI

5/17/2000

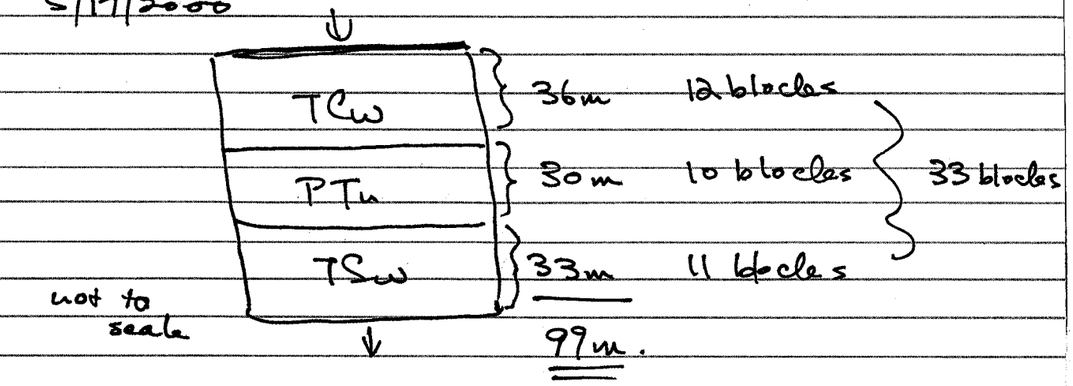

33 × 33 = 1089 nodes.

Consider building in heterogeneities
— Subdividing PTn. and recalculate, run model...

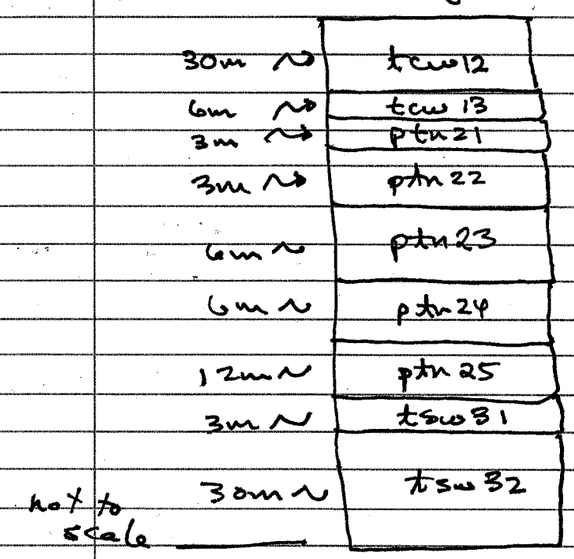

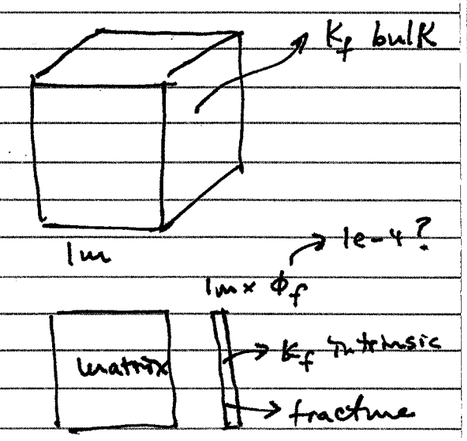

5/17/00 WI

5/17/00

Elevation — Randy Fedors notebook.

top of tsw32 ~ 4188 ft 1276.5 m
bottom of tsw32 ~ 4088 ft $\boxed{1246\,m}$
top of model 1246 m + 99 m = $\boxed{1345\,m}$

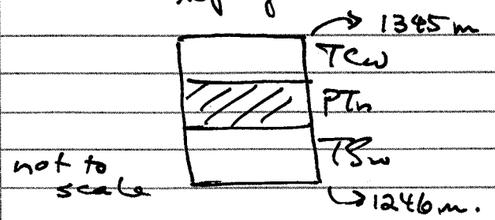

not to scale

Use $p = p_0 \left[\frac{T_0 - \alpha(z - z_0)}{T_0}\right]^{g/\alpha R}$ See p.76 for details of calculation

Barometric pressure at 1246 m $p = 87.189$ kPa

" " " 1345 m $p = 86.140$ kPa.

To calculate permeability for WI 5/17 ⊥ to WI 5/17 flow thru several layers use harmonic mean to get an effective permeability for each layer.
(Is harmonic mean the lower bound of k_{eff} in 2D/3D domain?)

$$k_H = \frac{d}{\sum_{i=1}^{N} \frac{d_i}{k_i}}$$

d ~ total length of flowpath
d_i ~ length of each ind'l flow segment.

5/17/00
WI

5/18/00 Fracture-Matrix Interaction
Mass Balance

Dual Continuum Method

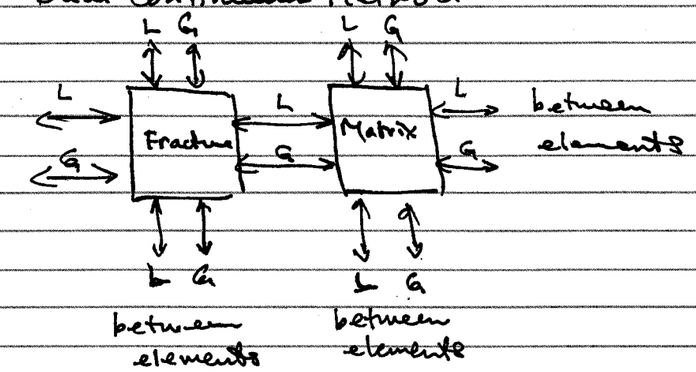

L ~ liquid flux
G ~ gas flux

also energy flux / exchanges between rocks (fracture, matrix) and void space

Need to study in detail the fluxes to fully understand what is going on....

Fluxes 5/18/00

$\boxed{flxlfz}$ ~ ρq → output from METRA; mass flux of liquid ~~divided by fracture porosity~~ per year WI 5/18/00

e.g. $1.1823\times10^5 \times 7.05\times10^{-5}$ volf $= 8.335 \frac{kg}{m^2 yr} \times \frac{1\,yr}{365\,d} \cdot \frac{1\,d}{86400\,s} = 2.643\times10^{-7}\ kg/m^2/s$

unnecessary operation

$2.643\times10^{-7} \frac{kg}{m^2/s} \div 7.05\times10^{-5} = 3.748\times10^{-3} \frac{kg}{m^2 s}$.

→ from output file (velocity file)

$\boxed{vlfz} = 1.1843\times10^2 \frac{m}{yr} \cdot \frac{1\,yr}{365\,d} \cdot \frac{1\,d}{86400\,s} = 3.755\times10^{-6} \frac{m}{s}$

difference is density of water used
$\rho \sim 998\ kg/m^3$ not exactly $1000\ kg/m^3$

5/18/00 WI

5/18/00 Check Mass Balance ~ How?

→ check for velocities in x-direction
→ not only in predominant direction of flow
→ small magnitude but can be important

→ vapor phase movement of water

$$X_a^l + X_L^l = 1$$
$$X_w^g + X_a^g = 1$$

→ Cannot obtain velocities between fracture/matrix
no output from MULTIFLO.

7/11/2000

→ Multiple MF simulations were run
→ Fluxes (input) and computed fluxes of water do not match

→ Error found in volf.dat when computing velocities. When this file was fixed, the fluxes match

→ Fixed volf.dat to print out all rows and columns when fed into volfix3.f; velmix3.f

→ Included D. Hughson's modifications to program where she takes the average of fracture porosities to do the calculation of fluxes at layer boundaries.

7/11/2000
WI

USFIC telecon 7/12/2000
- N. Coleman, S. Winterle, D. Hughson, S. Mayer, W. Illman
- meeting to discuss issue ~~resolution~~ resolution status
WI 7/12/2000

DOE lowers infiltration rate from 7.7 mm/yr → 4.6 mm/yr (mean)
VA estimate
11 mm/yr (upper bound)

look into this rain event

1969 - regional rainfall event
- Amargosa River flooded
- mobile homes displaced
- closure I-95

→ use rain event as extreme case for my simulation

Present day vs. future day infiltrations
- need predictive model to be able to forecast future conditions
- If current model is wrong, then the future model will certainly be wrong.

Infiltration estimates
- from borehole temperature logs
- chloride mass balance?

Infiltration rates of 4.6 mm/yr is an average value over the entire year.
→ this is a parameter resulting from the shallow infiltration model

7/12/2000
WI

7/12/2000 telecon

Deep percolation - flux rates; distribution of fluxes in fracture/matrix
- validity of steady-state assumpt.
- Saturation values (DOE using)

Capillary pressures - Berkeley (LBNL) → very dry 1-5 bars
USGS → 0.5 bars

* what is the cause of the difference

Cross-drift - wetter than they thought

Seepage into drifts - Capillarity
- Film flow

- DOE neglecting film flow (The physical mechanism)
  - controlled by capillarity/saturation of matrix
  - not fractures as water in film flow does not fill up fractures (both sides of fractures)

  - 6×10^{-5} m³/yr/m of drift length.

- When infiltration rate - deep percolation is set at 4.6 mm/yr., the number of waste packages contacted by water using DOE's PA code is zero.

- Film Flow
  - $q = 3 \times 10^{-7}$ m/s
  - thickness of film = 2 μm
  - P_c = 1 kPa in the matrix

- Flux rates inferred from secondary minerals
  - can be uncertain
  - treat as lower bound
  - age dating → based on tiny slices of deposition

7/12/2000 telecon

- Seepage flux (→ very uncertain); uncertain number
- focusing of flow - another mechanism

- tech. exch. 8/16 - 8/17?

7/12/2000 WI

7/13/2000 HF Simulations

- Larger grid simulations
- Cover a range of uncertainties parameters
  vary k_e, ϕ, frac/matrix interaction parameters
  ↓
  calcites; mineral coatings

- Average fluxes 50 mm/yr. (S.P. Neuman's section) expert elicitation

- If deep percolation is considered to be at steady state then it is reasonable to think that the input is 50 mm/yr.

- The fact that the infiltration estimate/deep perc. changes so much (DOE keeps on changing) tells me that those estimates are highly uncertain and that proper experiments need to be conducted at the two boundaries (surface; drift area)

7/13/2000 WI

- Added notes to Seepage resolution note by D. Hughson (not sure if she transmitted/incorporated my comments

→ in D:\4BFid seepage resolution - walter.wpd

"6. The following excerpt (p. SPN-5 of 12) from the 1997 UZ Flow Model Expert Elicitation Project, Yucca Mountain, written by S.P. Neuman, may require some clarification by J.S.Y. Wang (LBNL) ..... "Based on measurements of moisture conditions within the Exploratory Studies Facility (ESF) at Yucca Mountain, J.S.Y. Wang (pers. comm., Feb. 15, 1997) established that, during weekends when the ventilation system is shut off, average moisture flux from the rock into the ESF is about 50 mm/yr"

- My opinion -

Note that the moisture flux is an average, not a maximum. The fact that there is considerable uncertainty in flux rates into the ESF gives me the impression that the DOE experiments in the ESF are of questionable value for determining flow into drifts under ambient conditions. The dry out zone in the ESF changes water flow conditions around the drift significantly and may not allow us to determine boundary conditions accurately, which controls the solution to the flow problem. Without accurate knowledge of the boundary condition at the soil surface and drift horizon, the solution of the flow problem (deep percolation and seepage into drifts) is nonunique. As such, the prediction of seepage into drifts becomes even more so difficult through the use of process based models, that rely on differential calculus and continuum mechanics

9/13/2000 WJ

8/7/2000 MF Simulations

- Examine spatial / temporal variability of deep percolation
  - compare homogeneous vs heterogeneous fields of fracture permeability and its effect on deep percolation
  - build in variability in matrix k_s.
  - build in variability in fracture/matrix α's

- compare distribution of fluxes
  distribution of P_c
  distribution of saturations

- Conduct geostatistical analysis using ISATIS/GSLIB in 3D; take 2D cross-sections of air k data
- Use parameters from variograms to generate synthetic fields

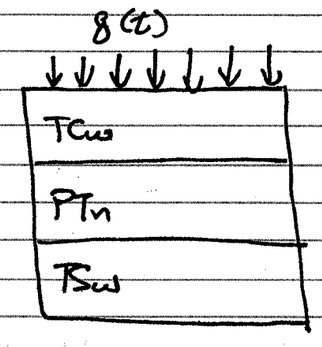

→ vertical correlation length longer than horizontal correlation scale. (for air k. → to simulate vertical fractures)

→ horizontal correlation scale longer than vertical corr. scale (layering; short strata bound fractures)

→ similar properties to TSw compared to TCw.

8/3/2000 WJ

8/7/2000 Geostatistics (Yucca Mountain)

- Approach taken by Birkholzer et al. (1999)
  - Assumed that there is not enough info. to rigorously determine the correlation structure of the fracture permeability fields
  - Employ fracture survey data
    - assign different correlation structures
      - one for small fractures
      - one for larger fractures
    - → build in various fractures as anisotropy in correlation lengths

    or → build in as nested model

    or → employ indicator approach?

8/7/2000 WI.

Birkholzer (1999) model

Topopah Springs – spherical model

$$\gamma(\xi) = \sigma^2_{\ln k}\left[1.5\,\xi/a - 0.5\,(\xi/a)^3\right] \quad \text{for } \xi \le a$$

$$\gamma(\xi) = \sigma^2_{\ln k} \quad \text{for } \xi > a$$

ξ is separation distance; a is correlation parameter

2 populations of fractures with 2 different correlation lengths.

1) a = 2m for k values smaller than $10^{-12.5}\,m^2$
2) a = 14m for k values larger than $10^{-12.5}\,m^2$

Fracture permeability field

Modeled as anisotropic field with one fitted model

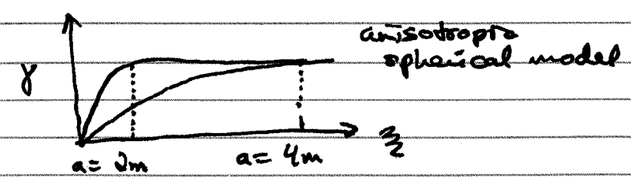

8/7/2000 WI

8/7/2000

(*) Reproduction of major heterogeneities
- → layers with each having different statistical properties

  facies – layer boundaries can be critical in modeling
- → a continuous RF (random fn.) model $Z(\vec{u})$ cannot reproduce severe heterogeneities or discontinuities, as found when crossing a physical boundary such that of lithotype.
- If the phenomenon under study is a mixture of different physical and/or statistical populations (composite data/population), the geometry of the mixture should be modeled and simulated first.

In my case: 1) Fracture properties control the bulk of flow in the units (welded) and also the nonwelded unit (PTn).

(*) 2) Fracture-matrix interaction parameter is also important but there is no data → 1) seepage tests

2) Inverse modeling; single hole tests; cross-hole tests

3) try range of parameters.

3) Heterogeneities in matrix permeability should also be modeled.

8/7/2000 WI.

8/7/2000

Generation of Random Fields

sf3d.f itype=3 spherical model.
.in input file
nx, ny, nz power of 2

Task

(1) Use sf3d.f to calculate/generate a field of perturbations "f" using the Fast fourier transform (spectral method)

→ Program calculates field for a large field (e.g. 128, 128, 128) then samples a smaller field that will be actually used in Multiflow WI 8/7/00 simulations
→ Prints on screen the mean/variance of the large heterogeneous field (not of the smaller field)
→ calculates one realization "srf.out"

(2) Now, have to convert this generated field to a file format readable by Multiflo; also calculate the mean/variance of the smaller field.
→ read in mean log K
→ read in values {i=1,n ; j=1 : i=1,n ; j=2, ...}
→ add the mean F to each entry and convert to k by doing the operation
$k = 2.303 * \exp(f+F)$
→ Calculate mean/variance of smaller field
→ write PHIK keyword file in the format of MF.

→ Phik file
i1 i2 j1 j2 k1 k2 ist ithrm vb porf bx by bz pormm
pormm

8/7/2000 WI

8/9/2000 – notes USFIC

- Discussed with D. Hughson about FFT program
- Need to expand model domain for PTn model
→ 33x33 ~~blocks~~ WI 8/9/2000 to 99x99 ~~blocks~~ 8/9/2000 WI grid
(3m blocks) (1m blocks)
* - new simulations directory km-4mm/finegrid/km-4mm.dat
* - need to also modify bottom BC also
$\frac{dP_c}{dz} = 0$; so $q = k(\theta)$ unit gradient condition

8/9/2000 WI.

8/10/2000 Notes from Fracture Character of the PTn tuff nonwelded hydrologic unit, Yucca Mountain, NV.

purpose: → obtain fracture data; estimates of parameters; structural inform.

p.94: - Majority of fractures (in the PTn) have trace lengths 1.2-2.4m
- relatively few have trace lengths greater than 3m.
- shorter compared to larger fractures documented
(*) → (biased info.)
(*) → bias introduced in data

Fracture data
- Trea canyon (Morgan, 1984; Barton and others, 1993; Throckmorton and Verbeek, 1995)
- Topopah Springs Tuff (Sweetkind and others, 1995)

p.106 Each of the PTn units appear to have its own fracture network – in many cases, they are poorly developed in terms of its characteristic fracture spacing, intensity, and termination style

field characterization
→ - dominantly stratabound fractures
most fractures terminate at welding breaks or litho-
- logic breaks.
- correlation scale on the order of sub unit scales.

8/10/2000 WI

8/10/2000

- large no. of fracture sets identified by authors (seven by this author)
- lack of fracture filling and alteration/mineralization on fracture walls w/in the PTn suggests that flow in fractures is limited.

p.11 - overall fracture intensity of the PTn unit is low and fractures are poorly connected (implying shorter correlation lengths) within and between lithostratigraphic units within the PTn.

p.37. PTn cooling joints - longest fractures - but rarely approached the lengths of 8-15 m. commonly along cooling joints of more densely welded units max. lengths 5-6 m.

p.47. Fracture orientation - measured fractures w/in the PTn unit are dominantly steeply dipping. Fracture orientation data from outcrop stations and the mapped exposure have similar distributions

Notes from G. LeCain's (1996) deliverable. USGS WI Report

p.27 - Fracture analyses of the N. Ramp

- Topopah Springs Tuff is dominated by two near vertical fracture sets 1st set ave. strike 206°; dip of 85°
  2nd set ave. strike 180°; dip of 80°
- fractures with dips less than 45° account for less than 5% of total fractures

- Topopah Springs Tuff - pneumatic monitoring k.
  - order of magnitude larger than air injection k.
  - possible explanation - k is anisotropic estimate of 10:1 vertical

(*) alternative exp.
- wrong fracture porosity used
- wrong model of interpretation used

WI 8/10/2000

8/10/2000 notes from LeCain (1996)

→ Tiva Canyon Tuff also dominated by vertical fractures - yet test results do not indicate anisotropy in k

→ Increase in horizontal k in TCw is supported by higher TCw fracture density and higher TCw air injection k values.

8/10/2000

→ Fracture geometry information not reliable enough to make predictions about flow, permeability, etc.

→ data → highly biased
→ collected based on counting fractures
→ perhaps useful in giving geological information; large-scale estimates; indications of permeability anisotropy; structural controls on flow; delineation of potential pathways, boundaries, heterogeneities.

→ mixed with air injection test data can be highly confusing - mixing different types of data completely unrelated.

8/10/2000 WI.

8/14/2000 Updated PTn modeling strategy

case 1) Homogeneous – simple 99×99 case

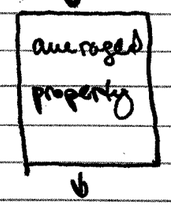

- uniform properties throughout
- take all simple-hole air injection test data to do the averaging.
- base case dual continuum model?

case 2) Homogeneous – simple layer cake model

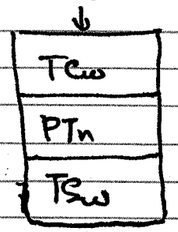

- material properties – base case DKM
- uniform properties throughout each layer
- currently adopted approach by YMP
- recognizes major strata / geological features.

Through averaging flow properties ⊥ to layers

case 3) Statistically Uniform heterogeneous field

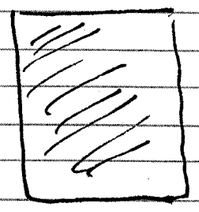

→ statistically uniform throughout the entire field of permeability.
→ does not ~~reg~~ just 8/14/2000 recognize the presence of layers.

how to conduct the averaging formally? literature search

case 4) Statistically nonuniform Heterogeneous field

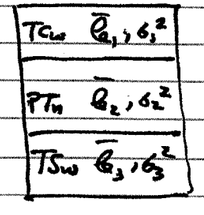

- uniform statistics through each layer
- boundaries are "inferred" from geophysics; borehole logs
- geostatistics/simulation done for each layer.

8/14/2000 WZ

8/14/2000

Averaging done from case 2) → case 1) previous eg.
→ harmonic mean for permeability
theoretical result

→ what about other parameters? ϕ, α, etc.

Averaging from case 4) → case 3)?

Do it by brute force → generate a synthetic field using statistics obtained from geostatistical analysis of tests in each unit
→ Conduct geostatistical analysis of this synthetic field to generate a single field.
→ conduct geostatistical analysis of all data at site?

* Tabulate all data that is available at Yucca Mtn. site
Tabulate all geostatistical model results.

Brute force approach to obtaining upscaled field from 3 smaller random (RF) fields

1) generate RF individually for each layer
   → model 1 TCw → isotropic, spherical $\lambda = 20m$
   → model 2 PTn isotropic, spherical $\lambda = 2m$
   → model 3 TSw anisotropic, spherical $\lambda_1 = 2m$; $\lambda_2 = 14m$
2) conduct geostatistical analysis on entire field
   - generate a variogram
   - fit a global model
   - conduct simulation using this model
   - run MF

8/14/2000 WZ

8/23/2000 PTn modeling runs

→ 99x99 grid ; takes too long to compute ; changed parameters in order to speed up runs

⇒ deterioration of mass balance when limit and tolerances changed to default values listed in the manual. (problem)

Keyword		33x33 grid	99x99 grid (never converged)	hm-4mm (never converged)	hm-4mm2 (never converged)	hm-4mm3
Autostep	dpmxe	10	10	10	10	.10e5
	dsmxe	0.03	0.03	0.03	0.03	0.04
	dtimpmxe	3	3	3	3	5
	dpzmxe	10^4	10^4	10^4	10^4	10^3
	taccel	10^{-3}	10^{-3}	10^{-3}	10^{-3}	10^{-4}
	iautodt	0	0	0	0	0
	facI	0	0	0	0	0
Tolr	tolp	10^{-1}	10	10	10	10
	tols	10^{-4}	10^{-4}	10^{-4}	10^{-4}	10^{-4}
	tolt	10^{-3}	10^{-3}	10^{-3}	10^{-3}	10^{-3}
	tolp2	10	10	10	10	10
	tolm	10^{-7}	10^{-5}	10^{-5}	10^{-5}	10^{-5}
	tola	10^{-5}	10^{-3}	10^{-3}	10^{-3}	10^{-3}
	tola	10^{-3}	10^{-3}	10^{-3}	10^{-3}	10^{-3}
	rtwotol	10^{-15}	10^{-7}	10^{-7}	10^{-7}	10^{-7}
	rmxtol	10^{-15}	10^{-7}	10^{-7}	10^{-7}	10^{-7}
	smxtol	10^{-15}	10^{-7}	10^{-7}	10^{-7}	10^{-7}
	⋮	⋮	⋮	⋮	⋮	⋮

command to execute jobs in background - writes screen output in vscr1/willman directory

↳ gets erased automatically every Sunday

↳ nohup ~spainter/bin/metra hm-4mm3 > /vscr1/willman/screen1.out &

to check job number

ps

ps -e | grep metra

8/23/2000 WI

8/24/2000 Multiflo simulations

→ hm-4mm4.dat started 0737 ; process 27094

changed tolr keyword variables 8/24/2000 WI

8/25/2000

→ hm-4mm5.dat started on 8/25/2000 0740 ; process 27797

8/28/2000 - finished running simulation (hm-4mm5.dat) w/input file

- took 17-18 hrs.
- re run simulation

8/30/2000 - Try out new input file hm-4mm stock.dat

- lack of space on disk to finish simulation
- deleted all earlier simulations in the directory mflo-bmark. and cleaned out the directory.

- Did some research on parameters from LBNL - AMR. → see next pg.
- Developed program which writes Multiflo Phile file from output results WI 8/30/2000 obtained from FFT program. program "tec6.f"

→ Next task:

1. write program that reads velocity at bottom (or near the bottom) of flow domain
   → vel. vs x.
2. Get data set of air & from DOE website together — examine results carefully
3. Test various cases (of Flow through heterog. fields) using Multiflo
   - various bridging methods?
   - correlation lengths
   - variogram models

8/30/2000 WI

8/30/2000 Literature search for Air K. statistics at YM.

Table 6. Comparison of Geometric Means and Standard Deviations of Niches and Alcoves in the Exploratory Studies Facility at Yucca Mountain.

Borehole Cluster	Type of Site	log(k) (m^2) Mean	log(k) (m^2) Standard Deviation
Niche 3566 Pre-Excavation	Intersects brecciated zone	-13.0	0.92
Niche 3566 Radial	Predominantly within brecciated zone	-11.8	0.66
Niche 3650 Pre-Excavation	Moderately fractured welded tuff	-13.4	0.81
Niche 3650 Post-Excavation	Post-excavation welded tuff	-11.8	0.88
Niche 3107 Pre-Excavation	Moderately fractured welded tuff	-13.4	0.70
Niche 3107 Post-Excavation	Post-excavation welded tuff	-12.4	0.82
Niche 3107 Radial	Moderately fractured welded tuff	-13.8	0.92
Niche 4788 Pre-Excavation	Highly fractured welded tuff	-13.0	0.85
Niche 4788 Post-Excavation	Post-excavation welded tuff	-11.9	0.78
Alcove 4	Discretely faulted and fractured non-welded tuff	-13.0	0.93
Alcove 6	Highly Fractured Post-construction welded tuff	-11.9	0.67

WI 8/30/2000

Input:

DTNs: LB980001233124.002, LB980901233124.001, LB990601233124.001, LB980901233124.004, LB980901233124.009, LB980912332245.001

Output:

DTN: LB990901233124.004

In Situ Field Testing of Processes AMR

→ gather data set from DOE website
→ conduct geostatistical analysis of data

WI 8/30/2000

9/1/2000 Multiflo simulations

— purpose: to test Multiflo with Random fracture K.
3 different input files to generate 3 diff. random fracture

sptype 3 spherical ~~flow~~ variogram model WI 9/1/2000
nx, ny, nz 128, 128, 128
spatial steps x, y, z ~~1.0, 1.0, 1.0~~ WI 9/1/2000 1.0, 1.0, 1.0
(4) input variances case 1 = 1.0 case 2 = 3.0 case 3 = 5.0
file names srf0831, srf0831-3, srf0831-5
scales of x, y, z (correlation) 2.0, 2.0, 2.0
random number seed 211111216
actual field dim. 99, 1, 99

→ all other parameters are set constant for this run
→ simulations run to steady-state
→ Notes Figs on pgs. 114–119 with a)–d) are:
a) saturations in fracture stoch. continuum
b) saturations in matrix continuum
c) velocity field ~~fluxes~~ WI 9/1/2000 in fracture stochastic continuum
d) velocity field? in matrix continuum

→ Mass balances all seem to be fine – very good news
→ flow paths appears WI 9/1/2000 very narrow – almost finger like.

9/1/2000 WI

Srf0831 $\sigma^2 = 1.0$

9/5/2000

a)

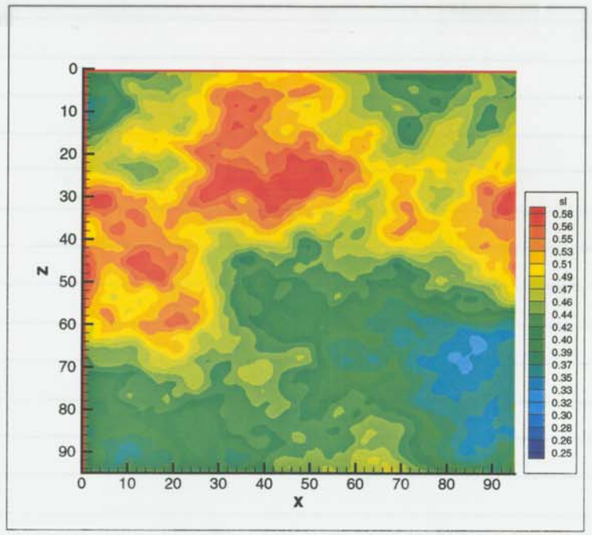

WI 9/5/2000

b)

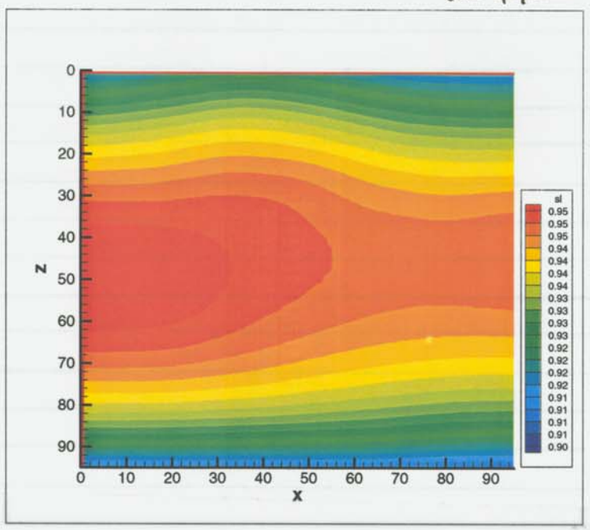

note scale is very narrow range

Srf0831 $\sigma^2 = 1.0$

9/5/2000

c)

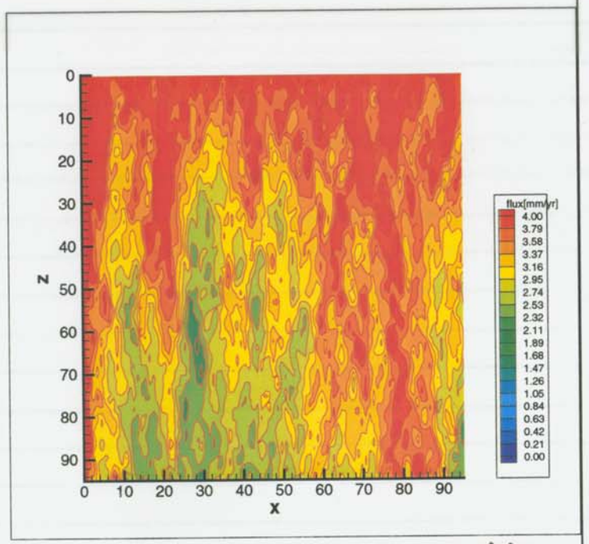

WI 9/5/2000

d)

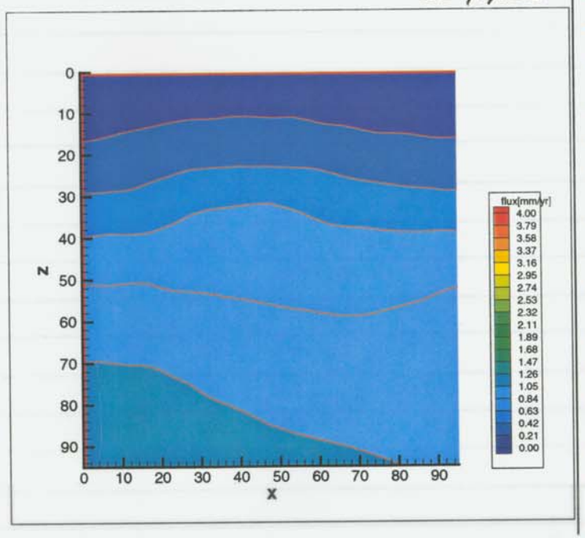

srf 0831-3 $\sigma^2 = 3.0$

9/5/2000

note wider range of saturations

a)

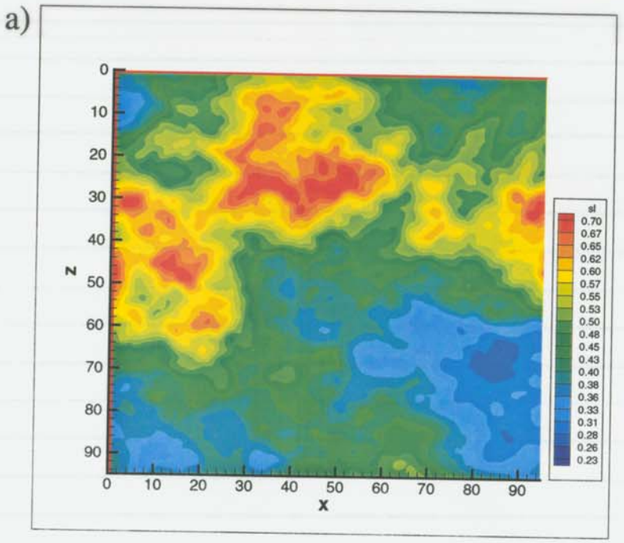

WI 9/5/2000

b)

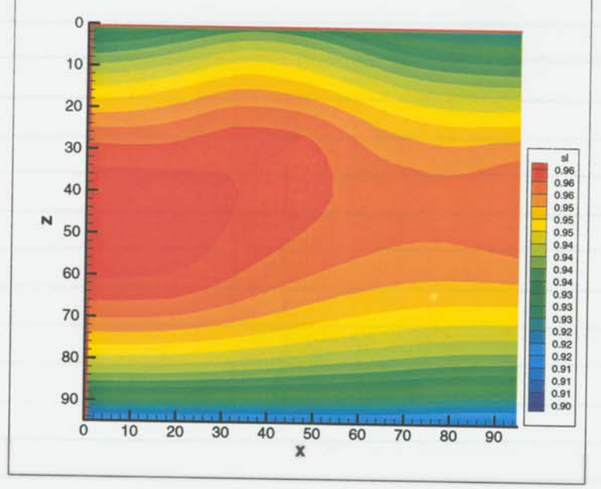

9/5/2000 WI

srf 0831-3 $\sigma^2 = 3.0$

9/5/2000

c)

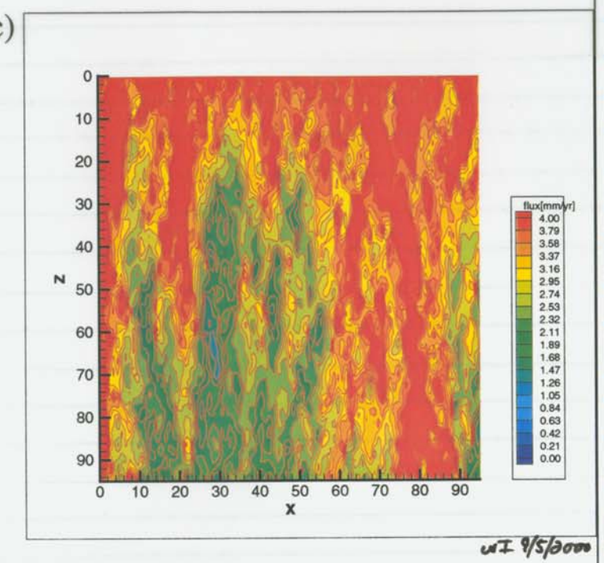

WI 9/5/2000

d)

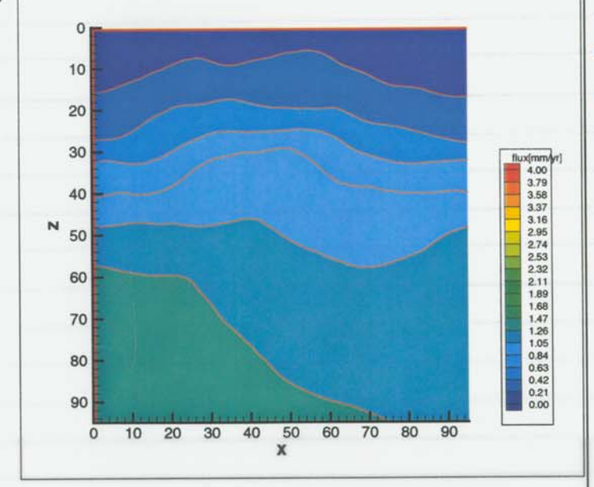

9/5/2000 WI

9/5/2000

Srf 0831-5 $\sigma^2 = 5.0$ extreme case

a)

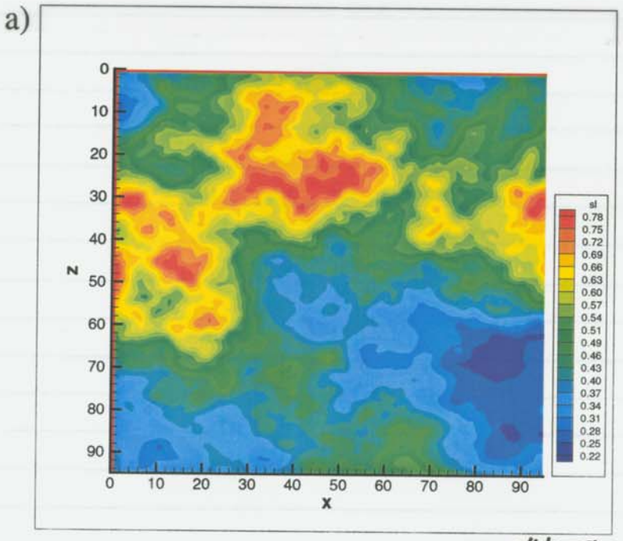

WI 9/5/2000

b)

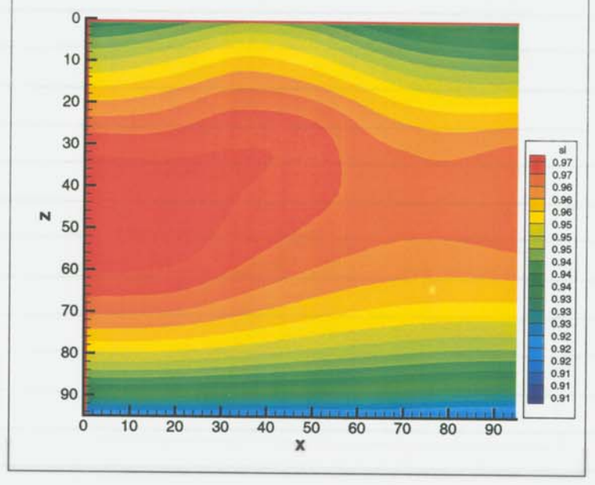

9/5/2000 WI

Srf 0831-5 $\sigma^2 = 5.0$

c)

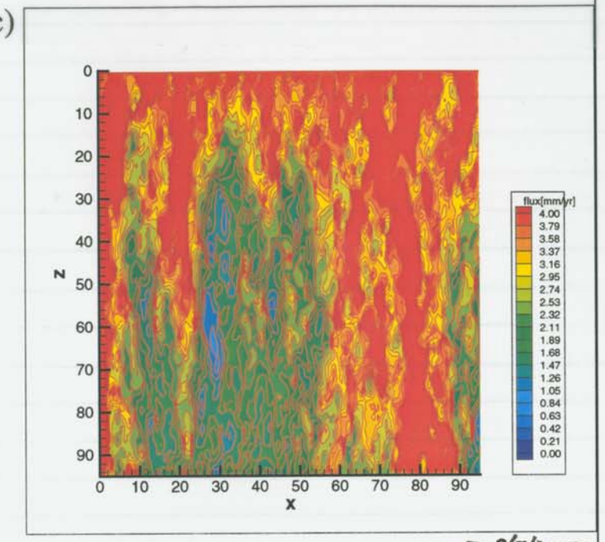

WI 9/5/2000

d)

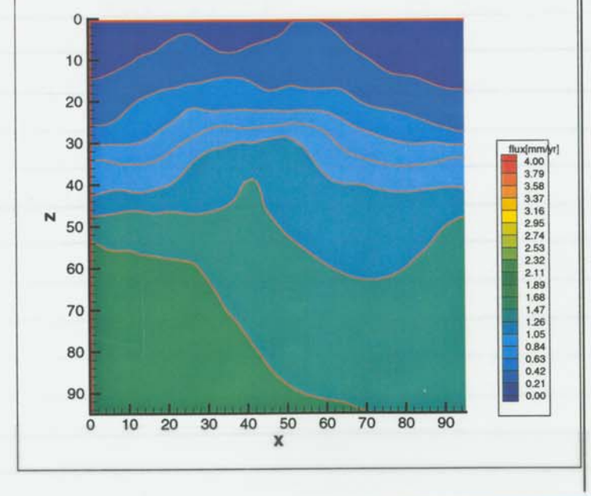

9/5/2000 WI

9/5/2000 USFIC PTn modeling

→ vary matrix k's and φ's for each unit
→ obtain matrix k's from matrix φ's
based on empirical formula

→ obtain matrix α's & fracture α's from Leverett's scaling relationship.

9/5/2000 WI

9/6/2000 USFIC –
Randy Fedors
- introduced me to L. Flint's spreadsheet
- extract data for model domain

Also look at SAND97-1730
- C.A. Rautman, S.A. McKenna, Three dimensional Hydrological and Property Models of Yucca Mountain, Nevada.

- L. Flint, Characterization of Hydrogeologic Units, Matrix Properties, Yucca Mountain, Nevada WR-IR 97-4243.

9/6/2000 WI

9/6/2000

S. Painter examines my input file to increase the speed of convergence.

		old value	new value
Init keyword	sg	0.98	0.88
Auto step	dsmxe	0.03	0.1
	dp2mxe	unchanged	
Limit	dpmx	1e2	5e3
	dsmx	0.08	0.20
	dpamx	1e5	5e4

As a result of these modifications, convergence of the solution has increased by a factor of 20.

9/6/2000 WI

10/27/2000
- Helen calls to find out where I can receive information on borehole data at Yucca Mountain.

- contacted Vince Hattes 702-295-4696 DoE office
referred to Matt Knop 702-295-4808

→ need as built information of boreholes
→ coordinates so that I can reconstruct boreholes using a visualization package.

→ Also called Chad Glenn (NRC-Las Vegas) 702-794-5046

10/27/2000 WI

10/27/2000

→ Test Free drainage (Type 6) boundary condition using old simulation results stored in Report-fedors/case4

→ Created subdirectory in Report-fedors/case4/type6
→ Objective: To test if the boundary condition is indeed working/implemented correctly in version 1.2.2 of MultiFlo.
→ Initial results do not look good.... decide to wait for the next version to come out.

10/27/2000 WI.

10/30/2000 Histograms of velocities near the bottom of
→ Examine previously conducted simulations:
1) srf0831 ; 2) srf0831-3 ; and 3) srf0831-5
↑ $\sigma^2=1$ ↑ $\sigma^2=3$ ↑ $\sigma^2=5$

WI 10/30

In general, as the variance increases, the ~~higher~~ larger the range of fluxes with the highest fluxes in the fracture exceeding the applied flux (channeling causes more water to be concentrated in fractures/discrete features which in turn causes more flow to take place). The average flux decreases with increasing variance as channelization/focusing occurs.
The above is my preliminary observation from a single realization (with different realizations)
A large number of simulations need to be run to test what I say above.

10/30/2000
WI

10/30/2000

→ Spoke to Gary LeCain (USGS) about his air injection testing work at Yucca Mountain

→ Currently, he is monitoring ambient barometric pressure fluctuations in boreholes at YM.
He has seen a large change in barometric pressures and corroborating evidence during the "last" El Nino (precip. 200 mm/3 weeks)
→ still controversial data.

10/30/2000 WI.

10/31/2000 YM alcoves/niches (Mono on boreholes)

- Niche 3566 - 3 boreholes
- Niche 3650, 3107, 4788 — 7 boreholes per niche prior to excavation
- Alcove 4, Alcove 6.

- Single-hole air injection tests done prior to pre excavation and post-excavation.

- In situ AMR footnote on p.43
As-built surveys had not been performed and/or the qualified survey data had not been released for use to determine the final configuration of the niche opening and borehole location.

→ Request data from DOE
* borehole spatial data
* x,y,z coordinates for test locations

10/31/2000

10/31/2000

Conduct detailed sensitivity analysis of parameters to spatial/temporal distribution of fluxes in both the fracture/matrix.

→ if we have difficult time obtaining data from YM, consider using data from ALRS to construct variograms, to obtain statistics to generate random fields.

→ Conduct geostatistical analysis in-house? or cite report to S.P. Neuman of Math 597 term project? for results.

⇒ use only 3-m data sets for now and look at $\log k_a$, $\log k_w$, Φ, θ, $\log \alpha$, $\log k_{a,lab}$, $\log k_{w,lab}$, Thermal properties

⇒ Use fracture permeability, fracture porosity info from cross-hole test interpretation (inverse results)

→ consider correlation between the 2 parameters (fracture permeability / fracture porosity)

→ Independently vary (homogeneous / heterogeneous) based on geostatistical analysis of 3-m data

→ explain why we have heterogeneous field of k_a, k_w for the fractures but not for matrix values.

→ Try to determine which parameters are most important in determining influencing spatial/temporal dist. of fluxes (when using a dual continuum model)

→ consider availability of parameters/data ...

10/31/2000 WI

10/31/2000

- Particular interest in using a complex model.
  → why? when we cannot obtain parameters in situ do we use such a complex model?

→ simpler models cannot capture the water movement behavior in heterogeneous formation (infiltration)
→ refer to publications by Jury, Faybishenko, Pruess, Finsterle.

→ Hard to find the optimal balance in properly accounting for heterogeneities → complexity of model, availability of data, conceptualizations.

→ we see a value in simulation exercises to find out about sensitivities in certain parameters to flow → of water in unsaturated fractured rocks.

Preliminary outline (deliverable ; paper)

→ Statement of problem / Background
→ Evolution of conc. models of UZ flow
→ Results from geostatistical analysis → separate report / paper
→ Mathematical Problem (Model) → Hydrogeology Journal → Mathematical Geol. → Conjoing, co-kriging simulation.
→ Model Results → subtitles → → vary parameters systematically.
→ Discussion.

purpose: Examine the effect of assuming certain variables as homogeneous quantities ~~of~~ on the spatial and temporal distribution of water flow in a dual continuum medium

→ Also examine the issue of 1) data reliability? ; 2) data measurability ; and 3) worth of certain data in two phase flow modeling in unsaturated, fractured/heterogeneous medium.

10/31/2000 WI

10/31/2000

- Proposed approach in modeling – ideas
  2D, 99x99
  → use geometric mean for homogeneous model. (base case – identify as)
  → vary fracture permeability, matrix permeability matrix α, fracture α
  → establish monitoring points and study distribution of fluxes. (away from bottom boundary)
  → Quantify $ amount for the investigation (for each data point)
  → vary initial distribution of water → [neutron probe measurements]
  → base the order of simulation on statistical data; qualitative assessment of which parameters are important for modeling purposes; reliability; measurability; cost.
  → importance of data in characterizing an unsaturated fractured rock site
  ↓
  ⇒ which data is least costly and gives us most information about the rock's ability to conduct water.
  Incorporate reliability of testing method
  Incorporate reliability of analysis.

10/31/2000 WJ

11/30/2000 Random variable generation for the PTn model

Scott Painter's program to generate random fields

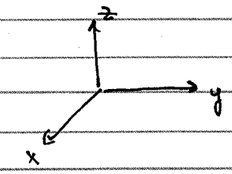

simregion
3, 0, 300, 0, 300, 300, 300, 1, 0, 1.
↓ ↓ ↓ ↓ ↓ ↓ ↓
x_n x_m y_n y_m n_x n_y n_z

$i = 1, n_x$
$j = 1, n_y$
$k = 1, n_z$

Power model
$\gamma(s) = c s^{2\omega}$

s = separation distance
c = constant
ω = Hurst coefficient

from Illman et al. (1998)
Integral scale = 2ω = 0.4475
ω = 0.224
$\sigma^2 = 0.2715$ $\sigma = 0.521$

Random field generator.
seed → rename file if we want to keep this as once code is run, it will rewrite the seed number.

command to start the program
fbmSim Project1 dum1 → variable that will be simulated
↑ executable
↓ subdirectory that contains input files

contains file → [well] GEOEAS format

x dum1
y dum2
z

y → vertical.

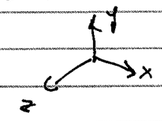

3, 0., 300., 0.
↑ always

11/30/2000 WJ

11/30/2000

Model Parameters

					isotropic	
20	0.25	0.01	-10	10	1	1
			min	max	x	z
not read knob for nonGaussianity	Hurst coeff.	st. dev.	allowable values		factor relative to y correlation scale	

well (file)

synthetic test
5
x
y
z
dum1
dum2
150.5 0.5 150.5 00 0.1

dum1 dum2

x y z

"conditioning point?"

n spainter/field/fBmSim
/seed
/project 1
/well
/modelparms

11/30/2000 WI

12/1/2000

→ Simulate ALRS le data

Sim region 0 – 63 m x
0 – 54 m y
0 – 45 m z

12/1/2000 WI

12/1/2000 USFIC telecon. Neil Coleman, Debra Hughson
Bo Bodvarsson, Joe Wang, T. Wintle

discussion on field tests in ESF
3 m long slots
Niche 5° 15 m long

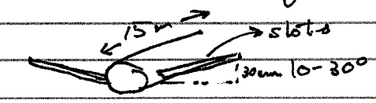

Alcove 8 → niche 3 tests (tracer test

12/1/2000 WI

12/4/2000 Seepage meeting
D. Hughson –
TPA – its shortcomings → highly simplified
– parameter sets
– models

Consider transfer function approach
Multiflo simulation approach!

12/4/2000 WI.

1/2/2001 PTn modeling

Van Genuchten Relationship.

$$S = [1 + (\alpha\psi)^n]^{-m}$$

$$1 + (\alpha\psi)^n = S^{-m}$$
$$(\alpha\psi)^n = S^{-m} - 1$$
$$\alpha\psi = (S^{-m} - 1)^{1/n}$$
$$\psi = \frac{1}{\alpha}(S^{-m} - 1)^{1/n}$$

$1/n = 1 - m$
$m = 1 - 1/n = n/n - 1/n$
$= n - 1/n$

1/2/2001 WI

1/2/2001 PTn modeling

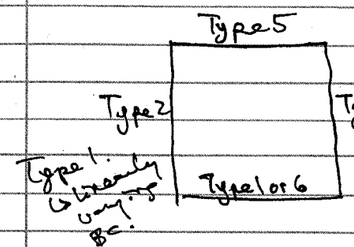

~> how about Type 1? let gas escape

- Richards approach
- Two phase approach?

different results due to entrapped air?

Priorities:

→ Finish 3 layer model
- vary BC
- conduct sensitivity analysis
- heterogeneous model under development

- use statistics from analogue site?
  ALRS
  ↳ do geostatistics?
  Initial file — log Transformed value
  alrs3m2.hd → alrs3m3.hd.

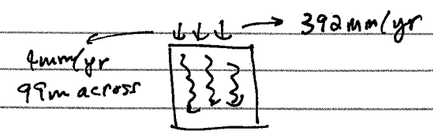

Also think about:

- Total volume of percolation in 2D model.

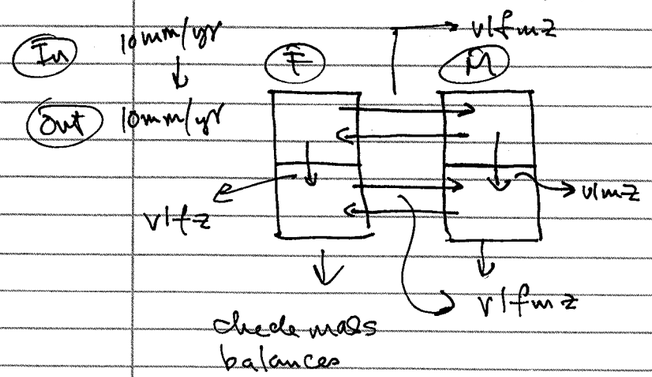

Input: how much goes in fracture divided by volf

Output - Results @ volf

1/2/2001 WI

1/2/2001 WI

Single continuum version of a Metra run

dhughson/multiflo/seep/strucapdir/multi.dat

1/2/2001 WI

1/31/2001

Rerun previous Metra runs

→ Inputs	Subdirectory
srf0831	012901
srf0831-3	013001
srf0831-5	013001

→ plotted $t = 0.1; 1.0; 10.0; 100.0; 1000.0; 10{,}000$

→ plotted spatial vs steady state variations of S_l, f_l for both matrix and fractures; calculated summary statistics for fluxes at $y = 99.5$ observations

Try new set of simulations

			model type
$\lambda_1 = 2$	$\lambda_2 = 2$,	$\lambda_3 = 10$	$\sigma^2 = 1$; spherical
"	"	"	$\sigma^2 = 3$; spherical
"	"	"	$\sigma^2 = 5$; "

Average fracture k $\bar{X} = -10.8$ $\sigma^2 = 1$
$\bar{X} = -10.8$ $\sigma^2 = 3$
$\bar{X} = -10.8$ $\sigma^2 = 5$

$k \sim 10^{-10.8} = 1.58489 \times 10^{-11}$

what I put in (by mistake) 0.00014 cause of discrepancy

$k/\phi = \frac{1.58489 \times 10^{-11}}{1.14 \times 10^{-4}} = 1.39 \times 10^{-7} \sim \ln 1.39 \times 10$
$= -15.79$ WI 1/31/2001

2/1/2001

Started 3 simulations with heterogeneous fracture k.
- $\sigma^2 = 1, 3, 5$
- check to see if generated fracture k distribution is really what we get in terms of σ^2.

2/1/2001 WI.

2/2/2001
- work with another RF generator → bug
- cannot figure out the cause of error in sf3d.
- Instead use program from D. Farrell
  opened directory dh-rg/v1, v3, v5
  started Metra runs – Friday 2/2/2001

WI 2/2/2001

2/05/2001

Anisotropic simulations
$\lambda_x = 2m$
$\lambda_z = 10m$
Exponential model

	sim. no.	dir(sub)	$\bar{x}$	σ^2
Seed 1	482	r1	−11.0420	0.978947
2	382	r2	−11.0712	1.21416
3	101	r3	−11.0374	1.09879
4	553	r4	−10.9815	0.897178
5	401	r5	−11.0018	1.22977
6	253	r6	unknown	unknown
7	227	r7	−10.9421	1.02849
8	184	r8	−10.9512	0.970753
9	185	r9	−11.0191	0.967970
10	203	r10	−11.0187	1.12237

2/5/2001 WI

2/9/2001 PTn modeling

→ completed 10 realizations – model runs
→ conducted early time simulations
$t = 10^{-5}, 10^{-4}, 10^{-3}, 10^{-2}, 10^{-1}$ yrs.

⇒ observed very large fluxes at early time
used uniform saturation in both the matrix and fractures – initially drains because it is spatially variable (geologic medium)

⇒ how long does it take to reach steady-state?
⇒ we are not concerned with time it takes to reach steady state
– drainage occurs for quite a long time before the IC/BC comes into equilibrium

2/9/2001 WI

3/6/2001 USFIC – PTn modeling
Isotropic model; exponential; $\lambda_x = \lambda_z = 2m$ fracture le.
→ Take out coordinates from output file and write .prn file
→ Use Tecbm.f to write fn.phk
→ Condition fn.phk (remove spaces at the top/bottom)
→ Run Metra on each one.... used same seed as aniso case.

	$\bar{x}$	σ^2
r1	−11.0367	0.965823
r2	−11.0293	1.04718
r3	−11.0168	0.985443
r4	−11.0098	0.909356
r5	−11.0103	1.07177
r6	−10.9703	1.01130
r7	−10.9893	1.00891
r8	−10.9723	0.967079
r9	−11.0148	0.934346
r10	−11.0109	1.03139

3/6/2001 WI

3/6/2001 PTn modeling

Objectives: Compare water fluxes/statistics resulting from permeability fields generated using isotropic/anisotropic models

→ obtain basic statistics ($\bar{x}$, σ^2 of fluxes)
→ histogram
→ Volume of water moving through / % volume of rock
→ Amplitude, frequency of water flux at the top and bottom

3/6/2001 WI

3/7/2001 USFIC notes

Some thoughts/questions

→ Flow focusing → heterogeneities in rock properties that cause channeling behavior in water flow
→ local saturation can become greater, causing permeability to be much higher

→ Episodic infiltration – driven by episodic nature of precipitation

→ Random fields ⇒ Is there enough data at YM that allows for the determination of anisotropy in correlation scales? Is the data sufficient to obtain correlation structure? (Model?)

→ Ignoring the role of air under infiltration event.
⇒ Is the solution to the Richard's equation sufficient to the solution of water flux problem (deep percolation) in deep/vadose zones?

3/7/2001 WI

3/8/2001 PTn modeling

⇒ Start new simulations to study fluxes in PTn (single layer)
→ Examine flow paths in PTn prior to running a layered model (3 layers with heterogeneity)

Simulate flow through 99x99 PTn unit — guesses
isotropic case – exponential model $\lambda_1 = 2m$ $\lambda_2 = 2m$
anisotropic case – exponential $\lambda_1 = 6m$ $\lambda_2 = 2m$

→ 1 realization each

→ In tec6m.f we adjusted the volf to be 5.59×10^{-5}
→ Use $k \sim 10^{-13.0}$

$$\frac{k}{\phi} = \frac{1 \times 10^{-13}}{5.59 \times 10^{-5}} = 1.7889 \times 10^{-9}\ m^2$$

$$\ln(1.7889 \times 10^{-9}) = -20.14$$

→ Also adjust params.in file

	Fira Canyon	Paintbrush
i11, i21, j11, j21, k11, k21	1,99,1,1,1,99	1,99,1,1,1,99
gm1	−15.79	−20.14
ist1	2	4
ithrm1	1	2
vb1	1.0	1.0
porf1	1.0	1.0
pormm1	0.103	0.378
permm1	1.62×10^{-17}	2.37×10^{-14}
ist m1		3
ithrmm1		2

need to update this for paper/deliverable

3/8/2001 WI

3/8/2001 PTn modeling (cont.)

Need to make sure that all model parameters are consistent with theory and observations

use of harmonic vs. arithmetic mean to average, for example.

→ use of geostatistical parameters obtained from single hole data at the site

→ dual continuum parameters

In the deliverable → we need to describe how the parameters were obtained → considered the thickness of unit;

Also, we have edited the volfst.dat file for the single layer PTn runs

1, 99, 1, 1, 1, 99	1.14e-4	4.90e-4	1.0	1.0	1.0	TCw
1, 99, 1, 1, 1, 99	5.59e-5	3.10e-1	1.0	1.0	1.0	PTn

tec6m.f run in rptn/iso

		mean	variance
iso	1	−13.0367	0.965823
aniso	2	−13.0625	0.985685

Errors in running Metra.

e.g.
block=1 ist > nst 3 2
block=1 ithrm > nrks 2 1
block=2 ist > nst 4 2
block=2 ithrm > nrks 2 1

	TCw1	PTn			
ist1	2	4	needs to be for a single layer	2	!
ithrm1	1	2		1	.
istm1	1	3		1	
ithrmm1	1	2		1	

3/8/2001 WI

3/9/2001 PTn modeling

UZ PTn modeling

fracture & heterogeneous		
exponential	λ_x,	λ_y
isotropic	2m,	2m
anisotropic	6m,	2m

→ Bulk of flow through the PTn matrix
→ Matrix has dominant effect on flow in the fracture using parameters given by DOE researchers.

→ Concern: Less flux going through the unit ~ 2mm/yr not 4mm/yr.

→ When Debra tries 1-D column with matrix/fracture no interaction → it takes the pulse to go through in 25 years.

→ Fingering in the PTn unit? SPN says so.
- Instability in fluid flow movement
- Memory effect as seeps mostly through the same pathways
- By passing fractures

3/9/2001 WI

3/14/2001 PTn modeling

Isotropic model
- runs for r3-r6 completed
- started for runs r7-r10.
- update scientific notebooks.
- write papers/deliverables on numerical modeling to leave a record of work → justification for additional data collection → important

3/14/2001 WI

3/14/2001 PTn modeling

Ron Smetzley says I'm running too many metra runs

Renice runs

user ID 7812

ps -al | grep 7812 "To check my processes"
renice -n 10 -p 8936 5232 . . . .
process ID

dh runs in r7 15947
r8 15953
r9 15918
r10 15528

3/14/2001 WI

3/16/2001 PTn modeling

→ Metra runs in r7 – r10 have been completed
→ Create subdirectories in ptn/iso/type6
ptn/aniso type6
to test the type6 boundary condition.

→ type command ~spainter/bin/metra15beta

→ Also start simulation for single layer Tiva Canyon unit with areamodf increased by a factor of 10 – created directories job#
~wt7/mam/geostats/df-rg/r1/iso/r1m 19163
" " " " r2m 19225
and started these 2 cases on 3/16 10 AM

renice -n 10 -p 19163 19225

3/16/2001 WI

3/17/2001

Read WRR article by S. Finsterle.

3/17/2001 WI

3/18/2001

PTn modeling. → finished jobs in subdirectories r1m & r2m; both look as if the change in areamodf has not much of an effect; start new jobs in subdirectories r1mm & r2mm → increase areamodf by 10^3 from original level.

water fluxes obtained from 90.5m level from → Due to lightning/thunderstorm, had to restart jobs in ptn/type6 iso & aniso

10 metra runs with 10 realizations of fracture permeability → preliminary examination of data shows that free drainage boundary condition is working...

Isotropic model shows less variation

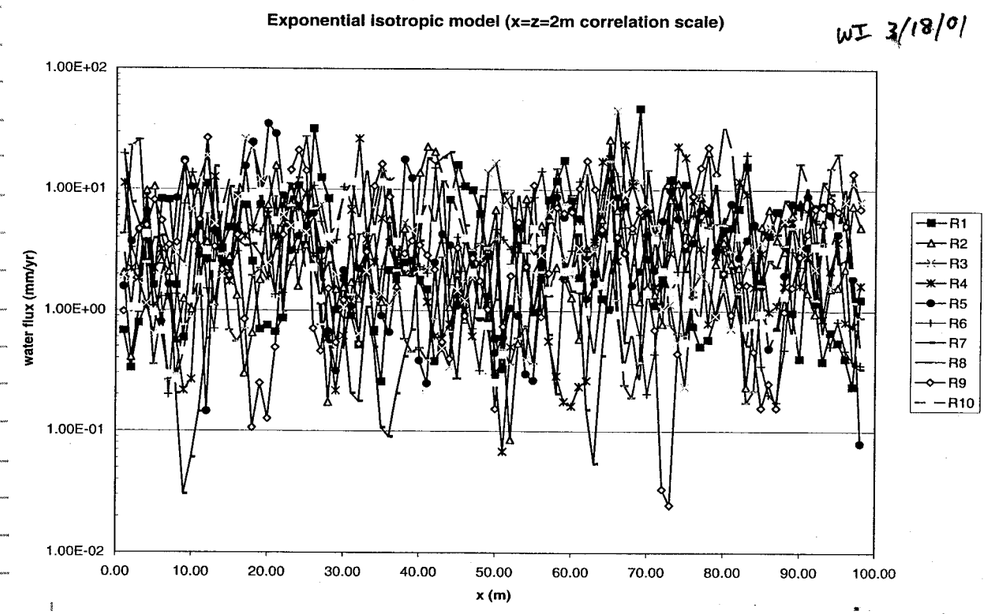

WI 3/18/01

WI 3/18/01

WI 3/18/01

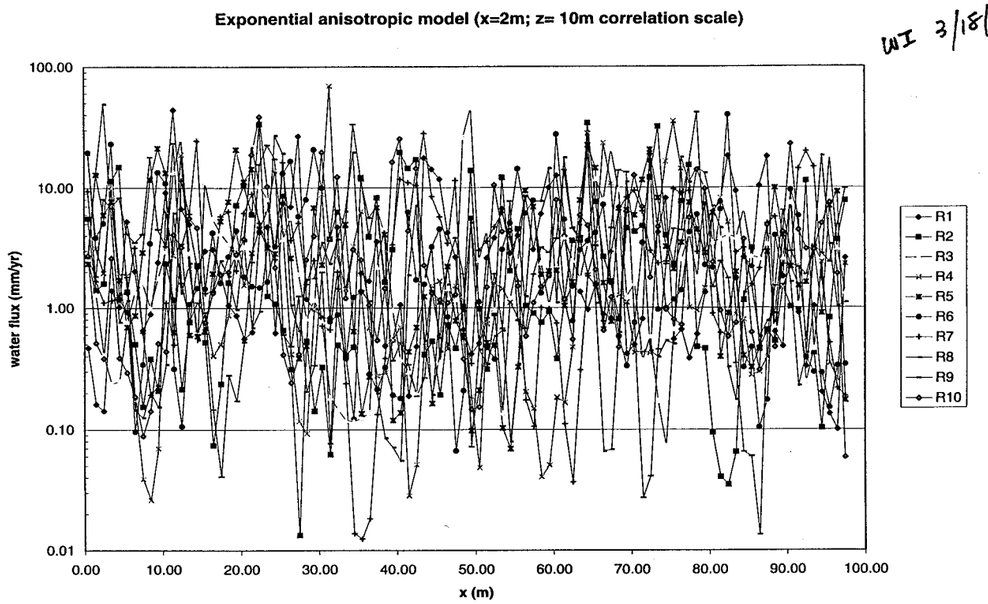

WI 3/18/01

→ Results from 10 metra runs with 10 realizations of fracture permeability; exponential anisotropic model

→ large variability in water fluxes in the fracture

→ For each case, ① plot the histogram
② Calculate the volume of water carried by the preferential flow path (assign a cutoff of 10 mm/yr? or a value of input flux, for this case would be 4 mm/yr)
③ Study the statistics of water fluxes including correlation, mean, variance min., and max values.

3/18/2001 WI.

3/20/01

→ Killed jobs in r1mm, r2mm because it was taking too long for practical use.
→ Metra getting stuck with calculations during early time.

→ Created directories r1LF, r1MF, r1HF
LF = low flux — 1 order of magnitude lower than present mass flux.
MF = medium flux — 1 order of magnitude higher in flux
Started 3/20/01 11:30 AM HF = high flux — 2 orders of " " " "

→ Setting up a batch file
e.g. run.bat — subdirectories r1 r2 r3 ...

Step 1

Contents:
```
cd r1
m dh
cd..
cd r2
m dh
cd..
```
→ give full path if accounting of files is important

Step 2 Change permission/status of file after writing the script
- chmod +x run.bat

Step 3 - run.bat ...

3/20/01

3/21/01 WFIC PTn modeling
⇒ Started new runs in r1MF; r1LF
→ Updated vel-v1.xls spreadsheet with fracture realizations

3/21/01 WI

→ Stopped metra run in r2mm because it was taking too long stopped at step 2573 1.343e+1 (time yrs)

3/21/2001 WSFIC modeling

Examined Permeability statistics for realization 1 (Isotropic case) @ 4mm/yr

Fracture

→ $\bar{x} = -11.04$ Fracture le
$\sigma^2 = 0.97$

→ $\bar{x} = 4.72$ mm/yr Water flux at steady state
$\sigma^2 = 33.15$

LOG10 values $\bar{x} = 0.39$, $\sigma^2 = 0.29$ $10^{0.39} = 2.455$ mm/yr

Matrix

$\bar{x} = 8.27 \times 10^{-3}$ mm/yr
$\sigma^2 = 1.89 \times 10^{-6} \sim 0$

LOG10 values $\bar{x} = -2.391$, $\sigma^2 = 0.02$ $10^{-2.391} = 0.00406$ mm/yr

3/21/2001 WI

3/22/2001

Homogeneous case to test if code is working properly

→ ~willman/geostats/df-rg/v1/iso/homo.
→ homo-t7.lay shows that fluxes (of water) in the fracture ~ 4.0 mm/yr → which is what we put in. We see a very slight decrease in water velocities at the bottom because of the influence of the constant head boundary.
→ slight numerical errors.

→ How can I explain the difference between 4.72 mm/yr and 4.0 mm/yr?

→ Check results from r1HF, r1MF, r1LF, r1 in ~willman/geostats/df-rg/v1/iso/r1

WI 3/22/01

3/22/01

run.txt

```
cd ptniMF
m dh
preplot dhfldf7.xyp
preplot dhfldm7.xyp
cd ..
cd ptniHF
m dh
preplot dhfldf7.xyp
preplot dhfldm7.xyp
cd ..
cd ptnaMF
m dh
preplot dhfldf7.xyp
preplot dhfldm7.xyp
cd ..
cd ptnaHF
m dh
preplot dhfldf7.xyp
preplot dhfldm7.xyp
cd ..
cd r1p
m dh
preplot dhfldf7.xyp
preplot dhfldm7.xyp
cd ..
cd r1pLF
m dh
preplot dhfldf7.xyp
preplot dhfldm7.xyp
cd ..
cd r1pMF
m dh
preplot dhfldf7.xyp
preplot dhfldm7.xyp
cd ..
cd r1pHF
m dh
preplot dhfldf7.xyp
preplot dhfldm7.xyp
cd ..
cd ..
cd r1LF
m dh
preplot dhfldf7.xyp
preplot dhfldm7.xyp
cd ..
cd r1MF
m dh
preplot dhfldf7.xyp
preplot dhfldm7.xyp
cd ..
```

Page 1

3/22/01
WI

↔ Batch file to run in ~willman/geostats/df-rg/v1/iso

ptniMF
isotropic, 40 mm/yr
ptniHF
isotropic 400 mm/yr
ptnaMF
anisotropic 40 mm/yr
ptnaHF
anisotropic 400 mm/yr.

"Variable fluxes; PTn"
~~Recharge at a point not over entire boundary~~
"Point fluxes; isotropic; variable fluxes"

r1p	~~0.4~~ 0.1	4 mm/yr
r1pLF		0.4 mm/yr
r1pMF		40 mm/yr
r1pHF		400 mm/yr

from center node into the fracture.

r1LF, r1MF, r1HF } anisotropic cases TCw
~willman/geostats/df-rg/v1

3/22/01 WI

3/22/01

```
cd r1HF
m dh
preplot dhfldf7.xyp
preplot dhfldm7.xyp
cd ..
cd ..
cd v3
cd r1
m dh
preplot dhfldf7.xyp
preplot dhfldm7.xyp
cd ..
cd r1LF
m dh
preplot dhfldf7.xyp
preplot dhfldm7.xyp
cd ..
cd r1MF
m dh
preplot dhfldf7.xyp
preplot dhfldm7.xyp
cd ..
cd r1HF
m dh
preplot dhfldf7.xyp
preplot dhfldm7.xyp
cd ..
cd ..
cd v5
cd r1
m dh
preplot dhfldf7.xyp
preplot dhfldm7.xyp
cd ..
cd r1LF
m dh
preplot dhfldf7.xyp
preplot dhfldm7.xyp
cd ..
cd r1MF
m dh
preplot dhfldf7.xyp
preplot dhfldm7.xyp
cd ..
cd r1HF
m dh
preplot dhfldf7.xyp
preplot dhfldm7.xyp
cd ..
cd ..
```

run.txt

3/22/01
WI

Page 2

~willman/geostats/df-rg/v3

r1	9mm/yr
r1LF	0.4mm/yr
r1MF	40mm/yr
r1HF	400mm/yr

- High variance case

$\sigma^2 = 3$

$\bar{x} = -11.0636$ ← sample mean

$\sigma^2 = 2.89747$ ← sample variance from the random field generator

~willman/geostats/df-rg/v5

$\sigma^2 = 5$

$\bar{x} = -11.0821$

$\sigma^2 = 4.82912$

Runs in ~willman/geostats/df-rg/v1/iso/r1HF
r1MF
r1LF
are finished. Compare the results when I come back.

3/22/01 WI

3/22/01

work on 3 layer model.

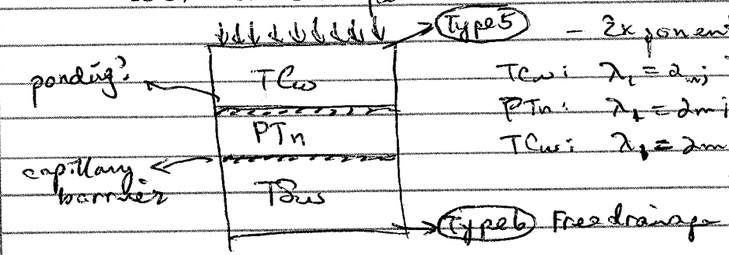

- Exponential model

TCw: $\lambda_1 = 2m$; $\lambda_2 = 10m$

PTn: $\lambda_1 = 2m$; $\lambda_2 = 2m$

TCw: $\lambda_1 = 2m$; $\lambda_2 = 2m$

→ Document parameters that go into this model better.
- less arbitrary — but not a realistic case still because the statistics just do not exist.
- State in paper that model parameters are derived from the literature but do not represent actual conditions at YM.

→ read C. Ho's (1997) paper; Birkholzer / Tsang (1997), Finsterle's (2000) paper.

The issue of flux not matching → input & output fluxes
- Random field generated using 10^{-11}. → try $10^{-10.8}$
-

r1 corr. gen. → on my D: drive
fgen95.exe
r1corr.HXY
r1corr.prn → through MS EXCEL
→ move to willman directory r1corr

subdirectory
~willman/geostats/df-rg/v1/iso/r1corr

→ unix2dos r1corr.prn r1corr.dat
→ use tec6m.f to generate fn.phk
→ Condition/edit fn.phk file

$\bar{x} = -10.8367$ $\sigma^2 = 0.965823$

→ Started Inatra run

Check results when I get back

3/22/01

→ Compare results from r1 HF 400 mm/yr
r1 MF 40 mm/yr
r1 LF 0.4 mm/yr
r1 4 mm/yr

→ Examined homogeneous case once more.
→ results look good

→ Build 3 layer case as soon possible.

→ Average Fluxes coming down at z = 90.5 m are slightly higher

D. Hughson suggests to examine:
1) convergence
2) storage
3) output file / summary BCs. / check mass balance calculations from BC summary

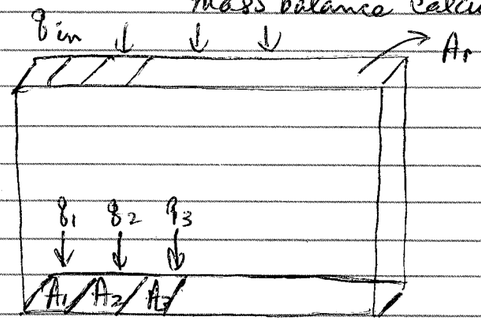

Use Cl-36 data to constrain model?

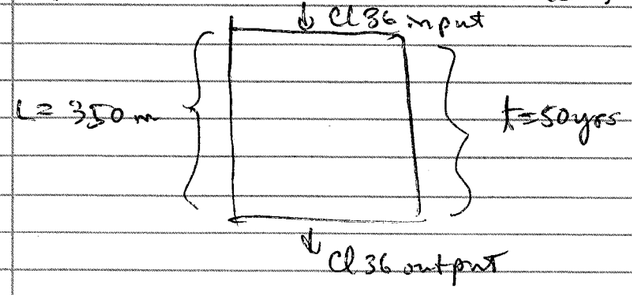

Very simplistic calculation.

$$v = \frac{d}{t} = \frac{350\,m}{50\,yrs} = 7\,m/yr$$
$$= 700\,\frac{mm}{yr}.$$

WI 3/22/2001

4/11/2001 PTn modeling

Checked results from several simulations
- convergence problems → PTn simulations
→ point injection simulations
→ high variance cases - r3
r1 → less flowchannels carrying higher volumes of water
boundary condition may be revised. ↳ data

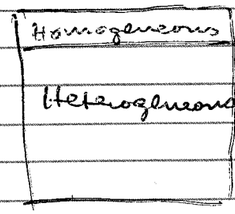

3 2 layers?

D. Hughson

FRITZ HABER / KARL BOSCH - Green Revolution 4/11/2001 WI

4/12 PTn modeling

→ create 3 layer model
→ generate random fields for each layer independently
→ put them together using tec7
→ run single simulation

→ Then work on above model from 4/11/2001.
→ Also think about poster.

4/12/2001

Matrix and Fracture Parameter Sets for the DKM Base Case (Present Infiltration)
DTN: LB971100001254.002

Model Layer	Matrix Perm. k_m [m^2]	Matrix Porosity ϕ_m (-)	Matrix Alpha α_m (Pa^{-1})	Matrix VG m m_m (-)	Matrix Res. Sat. S_{rm} (-)	Matrix Satia.Sat. S_{sm} (-)	Thickness b (m)	b/k
Tcw12	5.37E-18	0.066	1.32E-06	0.236	0.13	1.00	30	5.59E+18
Tcw13	4.90E-17	0.14	6.46E-07	0.427	0.33	1.00	6	1.22E+17
TCw (HM)	9.68E-18	0.090	8.67E-07	0.304	0.19	1.00		
TCw (HM)	6.31E-18							
TCw (AM)	2.72E-17	0.103	9.83E-07	0.332	0.23	1.00		
Ptn21	3.09E-14	0.369	3.80E-05	0.231	0.10	1.00	3	9.71E+13
Ptn22	3.02E-15	0.234	8.71E-06	0.488	0.14	1.00	3	9.93E+14
Ptn23	8.32E-14	0.353	4.57E-05	0.287	0.17	1.00	6	7.21E+13
Ptn24	1.15E-13	0.469	4.27E-05	0.349	0.10	1.00	6	5.22E+13
Ptn25	2.46E-13	0.464	1.95E-04	0.279	0.10	1.00	12	4.88E+13
PTn (HM)	1.29E-14	0.355	2.61E-05	0.307	0.12	1.00		
PTn (HM)	2.37E-14							
PTn (AM)	9.56E-14	0.378	6.60E-05	0.327	0.12	1.00		
Tsw31	4.90E-17	0.042	1.00E-05	0.237	0.11	1.00	3	6.12E+16
Tsw32	2.75E-16	0.146	2.29E-05	0.273	0.04	1.00	30	1.09E+17
TSw (HM)	8.32E-17	0.065	1.39E-05	0.254	0.06	1.00		
TSw (HM)	1.94E-16							
TSw (AM)	1.62E-16	0.094	1.65E-05	0.255	0.08	1.00		

Model Layer	Vertical Fracture Perm. k_f(m^2)	Horizontal Fracture Perm. k_f (m^2)	Fracture Porosity ϕ_f (-)	Fracture Alpha α_f(Pa^{-1})	Fracture VG m m_f (-)	Fracture Res. Sat. S_{rf} (-)	Fracture Satia.Sat. S_{sf} (-)	Fracture Frequency f (m^{-1})	Frac.-mat. Conn. Area Mod. Fac. X_{fm} (-)	Thickness b (m)	Vertical Fracture Perm. b/k	Horizontal Fracture Perm.
Tcw12	1.38E-11	6.03E-12	2.99E-04	2.95E-04	0.492	0.01	1.00	1.83	4.90E-04	30	2.17E+12	4.98E+12
Tcw13	2.82E-12	2.40E-13	7.05E-05	9.12E-05	0.492	0.01	1.00	1.27	4.90E-04	6	2.13E+12	2.50E+13
TCw (HM)	4.68E-12	4.62E-13	1.14E-04	1.39E-04	0.492	0.01	1.00	1.50	4.90E-04			
TCw (HM)	8.37E-12	1.20E-12										
TCw (AM)	8.31E-12	3.14E-12	1.85E-04	1.93E-04	0.492	0.01	1.00	1.55	4.90E-04			
TCw (GM)									4.90E-04			
Ptn21	5.25E-13	5.25E-13	4.84E-05	1.10E-03	0.492	0.01	1.00	0.87	1.10E-01	3	5.71E+12	5.71E+12
Ptn22	1.95E-13	1.95E-13	4.83E-05	1.82E-03	0.492	0.01	1.00	0.29	7.08E-01	3	1.54E+13	1.54E+13
Ptn23	2.57E-13	2.57E-13	1.30E-04	3.39E-03	0.492	0.01	1.00	0.29	6.92E-01	6	2.33E+13	2.33E+13
Ptn24	6.17E-14	6.17E-14	6.94E-05	9.33E-04	0.492	0.01	1.00	0.63	4.79E-01	6	9.72E+13	9.72E+13
Ptn25	7.76E-14	7.76E-14	3.86E-05	1.95E-04	0.279	0.01	1.00	0.65	4.79E-01	12	1.55E+14	1.55E+14
PTn (HM)	1.25E-13	1.25E-13	5.59E-05	6.29E-04	0.427	0.01	1.00	0.45	3.10E-01			
PTn (HM)	1.01E-13	1.01E-13										
PTn (AM)	2.23E-13	2.23E-13	6.69E-05	1.49E-03	0.449	0.01	1.00	0.55	4.94E-01			
PTn (GM)									4.15E-01			
Tsw31	1.07E-11	1.00E-12	8.92E-05	3.98E-05	0.481	0.01	1.00	1.10	5.01E-01	3	2.80E+11	3.00E+12
Tsw32	1.51E-11	7.08E-13	1.29E-04	9.33E-05	0.488	0.01	1.00	1.01	2.88E-05	30	1.99E+12	4.24E+13
TSw (HM)	1.25E-11	8.29E-13	1.05E-04	5.58E-05	0.484	0.01	1.00	1.05	5.76E-05			
TSw (HM)	1.46E-11	7.27E-13										
TSw (AM)	1.29E-11	8.54E-13	1.09E-04	6.66E-05	0.485	0.01	1.00	1.06	2.51E-01			
TSw (GM)									3.80E-03			

Model Layer	Vertical Fracture Perm. k_f(m^2)	Horizontal Fracture Perm. k_f (m^2)	Fracture Porosity ϕ_f (-)	METRA* Vertical Fracture Perm. k_f/ϕ_f(m^2)	METRA* Horizontal Fracture Perm. k_f (m^2)
Tcw12	1.38E-11	6.03E-12	2.99E-04	4.62E-08	2.02E-08
Tcw13	2.82E-12	2.40E-13	7.05E-05	4.00E-08	3.40E-09
TCw (HM)	4.68E-12	4.62E-13	1.14E-04	2.53E-08	2.50E-09
TCw (HM)	8.37E-12	1.20E-12		4.53E-08	6.50E-09
TCw (AM)	8.31E-12	3.14E-12	1.85E-04	4.31E-08	1.18E-08
Ptn21	5.25E-13	5.25E-13	4.84E-05	1.08E-08	1.08E-08
Ptn22	1.95E-13	1.95E-13	4.83E-05	4.04E-09	4.04E-09
Ptn23	2.57E-13	2.57E-13	1.30E-04	1.98E-09	1.98E-09
Ptn24	6.17E-14	6.17E-14	6.94E-05	8.89E-10	8.89E-10
Ptn25	7.76E-14	7.76E-14	3.86E-05	2.01E-09	2.01E-09
PTn (HM)	1.25E-13	1.25E-13	5.59E-05	1.87E-09	1.87E-09
PTn (HM)	1.01E-13	1.01E-13		1.51E-09	1.51E-09
PTn (AM)	2.23E-13	2.23E-13	6.69E-05	3.95E-09	3.95E-09
Tsw31	1.07E-11	1.00E-12	8.92E-05	1.20E-07	1.12E-08
Tsw32	1.51E-11	7.08E-13	1.29E-04	1.17E-07	5.49E-09
TSw (HM)	1.25E-11	8.29E-13	1.05E-04	1.15E-07	7.60E-09
TSw (HM)	1.46E-11	7.27E-13		1.33E-07	6.67E-09
TSw (AM)	1.29E-11	8.54E-13	1.09E-04	1.19E-07	8.35E-09

*-in DCM mode, fracture permeabilities are intrinsic not bulk properties.
Intrinsic permeability is bulk permeability divided by SIGMAF

HM = harmonic mean
GM = geometric mean
AM = arithmetic mean

HM<GM<AM

→ Final parameter sets for the homogeneous 3 layer model in r:\illman/geostats/homog/041201
→ homog.dat file

		$\ell_1 - \ell_2$
LAYER 1	TCw	1 – 36
LAYER 2	PTn	37 – 69
LAYER 3	TSw	70 – 99

4/12/2001 PTn modeling

Previous value of $\frac{\rho \ell_f}{\phi} = 1.11 \times 10^{-3} \frac{kg}{m^2 s}$ $\phi = 1.54 \times 10^{-4}$

$$\rho q = \frac{\rho \ell_f}{\phi} \cdot \phi = 1.2654 \times 10^{-7} \frac{kg}{m^2 s} \qquad \rho = 998 \frac{kg}{m^3}$$

$$q = 1.267936 \times 10^{-10} \frac{m}{s} \cdot \frac{1000\,mm}{1\,m} \times \frac{86400\,s}{1\,day} \times \frac{365\,days}{1\,yr}$$

$\cong$ 4mm/yr.

Now we use ϕ_f for the Tiva Canyon unit to be $\phi_f = 1.85 \times 10^{-4}$ Therefore, we have

$$\frac{\rho q}{\phi} = \frac{1.2654 \times 10^{-7}\ kg/m^2 s}{1.85 \times 10^{-4}} = \boxed{6.84 \times 10^{-4} \frac{kg}{m^2 s}}$$

For the 3 layer model, we will use statistical parameters for the 3 layers with a mean of

from the previous page
TCw $k_v = 4.68 \times 10^{-12} m^2$ $k_H = 4.62 \times 10^{-13} m^2$
PTn $k_v = k_H = 1.25 \times 10^{-13} m^2$
TSw $k_v = 1.25 \times 10^{-11} m^2$ $k_H = 8.29 \times 10^{-13} m^2$

Isotropic simulation → take the geometric mean between k_v, k_H

TCw: $\bar{k} = \sqrt{k_v k_H} = \sqrt{(4.68 \times 10^{-12})(4.62 \times 10^{-13})} = 1.47 \times 10^{-12}$
$\log_{10}(1.470429 \times 10^{-12}) \cong -11.83$

WI 4/12/01

4/12/2001

PTn: $\log_{10}(1.25\times10^{-13}) = -12.90$

TSw: $\bar{k} = \sqrt{(1.25\times10^{-11})(8.29\times10^{-13})} = 3.229084\times10^{-12}\ m^2$

$\log_{10}(8.22\times10^{-12}) \cong -11.49$

Generate random fields for the 3 layers with $\sigma^2 = 1$; isotropic

			seed
Domain 1 (TCw)	99 x 36	WI 4/12/01	482
Domain 2 (PTn)	99 x ~~32~~ 33	WI 4/12/01	323
Domain 3 (TSw)	99 x ~~29~~ 30	WI 4/12/01	255

TCw-r1.gen

```
                                    TCw-r1.gen
 482                                 ISEEDH, ISEEDG first seeds for H and G
128      128     1                   NFULL   nodal dimensions of full field
  99      36     1                   NTRUNC  nodal dimensions of truncated f
ield
 1.0     1.0     0.05                SSTEP   spatial step size (delta X, Y,
Z)
 -11.83                                 HMEAN,GMEAN   mean of H,G
 1.0                                 HVAR,GVAR    variance of H,G
 0.0                                 HNUG,GNUG    nugget of H,G
   2                                 ITYPE   power spectrum type (1=gaussian
, 2=exp. cov)
 2.0    2.0     0.15                HLAMDA  correlation lengths H
 1                     IPSCRN  = 1 -> progress output to screen
 1                     IWSEC   = 1 -> write 3 sections through middle of f
ield
 1                     ISURFER = 1 -> write to surfer format
 2                     I_THIN      -> data thinner
```

WI 4/12/01

Convert Tcw-r1.HXY -> Tcw-r1.prn using MS EXCEL.

4/12/2001
WI

4/12/2001

```
                                    PTn-r1.gen
 323                                 ISEEDH, ISEEDG first seeds for H and G
128      128     1                   NFULL   nodal dimensions of full field
  99      33     1                   NTRUNC  nodal dimensions of truncated f
ield
 1.0     1.0     0.05                SSTEP   spatial step size (delta X, Y,
Z)
 -12.90                                 HMEAN,GMEAN   mean of H,G
 1.0                                 HVAR,GVAR    variance of H,G
 0.0                                 HNUG,GNUG    nugget of H,G
   2                                 ITYPE   power spectrum type (1=gaussian
, 2=exp. cov)
 2.0    2.0     0.15                HLAMDA  correlation lengths H
 1                     IPSCRN  = 1 -> progress output to screen
 1                     IWSEC   = 1 -> write 3 sections through middle of f
ield
 1                     ISURFER = 1 -> write to surfer format
 2                     I_THIN      -> data thinner
```

```
                                    TSw-r1.gen
 255                                 ISEEDH, ISEEDG first seeds for H and G
128      128     1                   NFULL   nodal dimensions of full field
  99      30     1                   NTRUNC  nodal dimensions of truncated f
ield
 1.0     1.0     0.05                SSTEP   spatial step size (delta X, Y,
Z)
 -11.49                                 HMEAN,GMEAN   mean of H,G
 1.0                                 HVAR,GVAR    variance of H,G
 0.0                                 HNUG,GNUG    nugget of H,G
   2                                 ITYPE   power spectrum type (1=gaussian
, 2=exp. cov)
 2.0    2.0     0.15                HLAMDA  correlation lengths H
 1                     IPSCRN  = 1 -> progress output to screen
 1                     IWSEC   = 1 -> write 3 sections through middle of f
ield
 1                     ISURFER = 1 -> write to surfer format
 2                     I_THIN      -> data thinner
```

→ Started run in ~wittman/geostats/dif-rg/v1/3L/r1
→ Computations for 3 layer model finished relatively fast (several hours) for this realization of fracture k.
→ I am having problems computing velocities for late time (t=6, t=7) in the fractures.
→ checked/finalized parameter values. 4/12/2001 WI.

4/13/2001
→ Began runs (medium/high flux cases) in
~wittman ..... /3L/r1/r1MF q = 40mm/yr
/3L/r1/r1HF q = 400 mm/yr
→ created tect.f for 3 layer models
WI 4/13/2001

4/20/2001 PTn modeling

⇒ Began homogeneous fracture permeability flow thru 3 layer simulations

homog.dat (Bottom BC ; type 1)
homog2.dat (Bottom BC ; type 6)

in the directory ~wilman/geostats/homog to obtain results from homogeneous case to compare against heterogeneous case.

4/20/2001

4/23/2001 PTn modeling.

→ Killed job in ~3L/r1/r1HF because it ran for over 10 days and did not converge. reason? flux imposed at the top could have been too high?

→ Examine results from homog.dat
homog2.dat.
The results look good → plotted vectors

→ print results from homog1 & homog2
compare again 3L-r1-iso-t5.lay in D:drive

→ plot results from ~3L/r1/r1LF
~3L/r1/r1MF
printed results; added vectors to show flow directions

→ Start simulations hbc1.dat
hbc2.dat
→ get zero flux in the fracture for 4mm/yr.

→ Use hbc1 as base file for 3L-r1 simulation in subdirectory 042301
Started simulation with q = 8mm/yr instead of q = 4mm/yr

WI 4/23/2001

4/23/2001 PTn modeling

Added stream traces to velocity plots in fracture and matrix for 3L-r1MF-t75t.lay

	beginning	ending
x	0.5	97.5
y	0.5	97.5

→ varied by increments of 5

3L-r1-iso-t5st.ps → stream traces stop at top of PTn/TCw contact in the matrix.
3L-r1MF-t75t.ps

Redo calculations in { hbc1.dat using 8mm/yr
hbc2.dat

$$\frac{\rho g}{\phi} = 8.84\times10^{-4}\ \frac{kg}{m^2 s} \quad \text{for 4mm/yr}$$

$$\frac{\rho g}{\phi} = 1.368\times10^{-3}\ \frac{kg}{m^2 s} \quad \text{for 8mm/yr}$$

$$q = 2.5358\times10^{-10}\ \frac{m}{s}\times\frac{1000\ mm}{1\ m}\times\frac{86400\ s}{1\ day}\times\frac{365\ days}{1\ yr}$$

$$\approx 8\ mm/yr.$$

4/23/01 TECPLOT
- check streamtraces in fracture/matrix plots
- removed contour lines → red color ⇒ multicolor.

WI 4/23/01

5/17/2001

Generation of random fields for 3L PTn model

Exponential
Isotropic model
Random numbers for the generator.

realization#	TCw	PTn	TSw
1	482	323	255
2	382	660	834
3	101	954	628
4	553	270	525
5	401	172	366
6	253	969	169
7	227	733	806
8	184	506	330
9	195	197	871
10	203	245	746

TCw $\bar{x} = -11.83$, $\sigma^2 = 1.0$
PTn $\bar{x} = -12.90$, $\sigma^2 = 1.0$
TSw $\bar{x} = -11.49$, $\sigma^2 = 1.0$

- generated fields with $\sigma^2 = 1$ today
- also generate field with $\sigma^2 = 0.5, 2$ factor of 4 difference

Statistics		$\bar{x}$	σ^2
R2.	layer 1	-11.8059	1.11104
	2	-12.9257	0.876080
	3	-11.3297	0.887787
R3	1	-11.9808	0.948875
	2	-12.8309	0.963389
	3	-11.3206	1.02850
R4	1	-11.8320	0.844026
	2	-12.6666	1.01703
	3	-11.4010	0.984288

5/17/2001
WI

5/18/2001

		$\bar{x}$	σ^2
R5	layer 1	-11.7500	1.19371
	2	-12.9857	0.986437
	3	-11.5166	1.08799
R6	1	-11.7458	0.912415
	2	-12.7822	0.923694
	3	-11.4095	0.959564
R7	1	-11.7827	1.01187
	2	-12.8014	0.927790
	3	-11.4522	0.949865
R8	1	-11.7452	0.897914
	2	-12.9128	1.04086
	3	-11.5671	0.867342
R9	1	-11.8932	0.910772
	2	-12.9675	0.916713
	3	-11.4862	0.904194
R10	1	-11.9226	1.01333
	2	-12.9179	0.943864
	3	-11.4746	0.951508

→ Run the 10 cases, sequentially and prepare Isotropic model simulations for $\sigma^2 = 0.5$ and $\sigma^2 = 2.0$

→ Prepare 1 case each (99x 99x 33 simulation)

5/18/2001
WI

5/24/2001

Prepared input file fn.plt for the 3D code

layer	mean	variance
1	-11.8081	0.849257
2	-12.8843	0.797202
3	-11.5137	0.846755

Bigmetra
nbmx=50,000
mf10/02.3/bigmetra
parmetrs.h
5/24/2001 WI

6/15/2001 PTn modeling – preparation for 3D model (heterogeneous)

Size: 99x10x99

Statistics of generated field

	$\bar{x}$	σ^2
layer 1 (TCw)	−11.7919	0.857330
2 (PTn)	−12.8779	0.880032
3 (TSw)	−11.4299	0.832504

6/15/2001 WI

6/19/2001

→ Big metra – with larger dimensions to run larger simulations

~/spainter/multiflo/mflo1.2.3/bigmetra/metra1

→ run started 3D simulation

→ Ron J. came by to talk to me about renicing jobs.

top → command to get into screen with job status.

renice ␣ -n ␣ 5 ␣ 22098.

space

→ renice 2nd/3rd, ... jobs.

WI 6/19/2001

6/20/2001 Testing of Metra on large, 3D problems

99x10x99 = 98010 nodes

→ run on bigmetra – vulcan; unsuccessful

– requires larger array dimensions (large matrix)

– Scott thinks that executable is too big to fit onto vulcan RAM.

→ Test metra run on PC → with Windows NT, 2000 (seems to run well) → 3 layer, stochastic model r5

WI 6/20/2001

6/20/2001

→ Jose asked me several questions via email about my metra use: size of problem, job control, need, time frame for completion

→ continue simulation (2D) for now and strive to analyze those results first.

WI 6/20/2001

6/22/2001 PTn modeling

→ Mflo1.2.3 not Mflo1.5

dh.dat in

→ Runs on PC, laptop finished very quickly (r5)

→ began bigmetra run (5)

pid → 17107 (reniced run 14:30 Friday)

→ batch file run → pid 28984

→ Plan is to finish existing simulations (UNIX)

→ summarize results and plan for new ones

→ Right now, we are not interested in transient results (with monitoring points) but eventually, when we test the DOE steady state assumption, we will need to monitor Pc, Saturation, etc at the following:

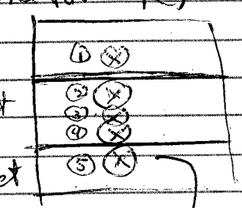

1) Point above the PTn/TCw contact in the center.

2) Point below the PTn/TSw contact

3) Central part of PTn unit

4) Point above the PTn/TSw contact

5) Point below the PTn/TSw contact

→ try to monitor in a flowing channel

→ examine the memory effect in flow paths

→ establish monitoring lines depending on steady state results

6/20/2001 WI

6/22/2001

Results from Metra runs

version #	Steady state reached @ (yrs)	H_2O Bal	Air Bal	Inrg bal	
metra1.2.3	53689.2 (CNWRA 2592)	0.910771	1.007831	0.911235	laptop
"	53689.2 (CNWRA 2545)	"	"	"	PC
metra15 beta	40877.8	0.974746	0.999554	0.974703	UNIX

Plot → q Mersus (vs) x
→ Frequency vs. q
→ Statistics of q?
→ Volume of water vs x
→ Capillary pressure at certain monitoring points
→ Saturation at certain monitoring points.

Generate random fields $\sigma^2 = 2.0$ (and then 0.5)

→ adjusted all input files: TCw − r1 → r10
PTn − r1 → r10
TSw − r1 → r10

→ Build just one for now: TCw − r1, PTn − r1, TSw − r1 } $\sigma^2 = 2.0$

Realization 1 $\sigma^2 = 2.0$ → run on laptop (CNWRA 2592) Dell Inspiron 5000 w/ windows 2000

start simulation 17:00

	$\bar{x}$	σ^2
layer 1	−11.9212	1.94254
layer 2	−13.0176	2.03487
layer 3	−11.6284	1.81781

Realization $\sigma^2 = 0.5$ → run on PC CNWRA (2545)

start simulation 17:00

	$\bar{x}$	σ^2
layer 1	−11.8756	0.485638
layer 2	−12.9588	0.508717
layer 3	−11.5592	0.454451

6/22/2001 WI

→ 6/26/2001

Realization 2 $\sigma^2 = 2.0$

	$\bar{x}$	σ^2
L1	−11.7959890	2.22209191
L2	−12.9363003	1.75215662
L3	−11.2632303	1.77557230

stored in a directory on NT workstation

Realization 3 $\sigma^2 = 2.0$ WI

L1	−12.04	~~1.89~~	1.90
L2	−12.80	1.93	
L3	−11.25	2.06	

from here on will provide numbers to 2 significant figures

R4 $\sigma^2 = 2.0$

L1	−11.83	1.69
L2	−12.57	2.03
L3	−11.36	1.97

R5 $\sigma^2 = 2.0$

L1	−11.72	2.39
L2	−13.02	1.97
L3	−11.53	2.18

R6 $\sigma^2 = 2.0$

L1	−11.71	1.82
L2	−12.73	1.85
L3	−11.38	1.92

R7 $\sigma^2 = 2.0$

L1	−11.76	2.02
L2	−12.76	1.86
L3	−11.44	1.90

R8 $\sigma^2 = 2.0$

L1	−11.71	1.80
L2	−12.92	2.08
L3	−11.60	1.73

6/26/2001 WI

R9	$\sigma^2 = 2.0$	
	$\bar{x}$	σ^2
L1	-11.92	1.82
L2	-13.00	1.83
L3	-11.48	1.81

R10	$\sigma^2 = 2.0$	
	$\bar{x}$	σ^2
L1	-11.96	2.07
L2	-12.93	1.89
L3	-11.47	1.90

Started simulations in batch mode real2 – real0

FINAL Entry:

I have reviewed this scientific notebook and find it in agreement with QAP-001. There is sufficient information regarding methods used for conducting tests, acquiring and analyzing data so that another qualified individual could repeat the activity.

E. C. Pearcy
July 27, 2001